

## Stimulating cartilage development of chondroprogenitor cells via GDF-2 supplementation in combination with melt electrowriting microfiber meshes

F Abinzano<sup>1</sup>, M de Ruijter<sup>1</sup>, A Mensinga<sup>1</sup>, M Castilho<sup>1</sup>, IM Khan<sup>2</sup>, R Levato<sup>1</sup>, J Malda<sup>1,3</sup>

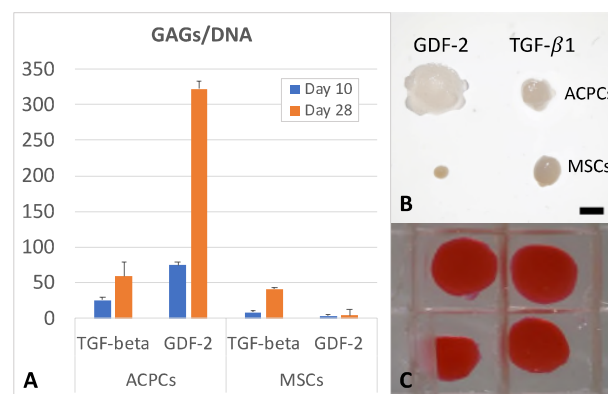
<sup>1</sup> Department of Orthopedics, University Medical Center Utrecht, Utrecht, The Netherlands.

<sup>2</sup> Centre for NanoHealth, Swansea University Medical School, Swansea, UK. <sup>3</sup> Department of Equine Sciences, Faculty of Veterinary Medicine, Utrecht University, Utrecht, The Netherlands.

**INTRODUCTION:** Articular cartilage-derived progenitor cells (ACPCs), are a promising cell source for cartilage regeneration, as they can be expanded in culture, achieving clinically relevant numbers without losing differentiation capacity<sup>1</sup>. However, culture protocols for ACPCs are not optimized and are based on media used for expansion and differentiation of mesenchymal stromal cells (MSCs). The aim of this study is to i) maximize 3D cartilage production by aggregated ACPCs compared to MSCs via an optimized growth factor supplementation and ii) to incorporate these enhanced aggregates within 3D meshes of organized microfibers to guide the growth and eventual condensation of these cells into a durable, organized cartilage construct.

**METHODS:** Adult ACPCs and MSCs were cultured in pellets of 250.000 cells for 4 weeks, supplementing the media with 100 ng/ml of growth differentiation factor 2 (GDF-2) or the standard dose of 10 ng/ml of TGF-beta1. To test if an initial boost of GDF-2 was sufficient for differentiation, switching from GDF-2 to TGF-beta1 after the first week was also tested. Matrix production was evaluated with histology and GAG/DNA quantification. Next, GDF-2 grown chondrogenic pellets were combined with polycaprolactone meshes, fabricated via melt electrowriting. Microfibers (20µm) were printed to form a boxed structure (0-90° laydown, fiber spacing 700µm). Pellets were individually housed into each printed box.

**RESULTS:** After 1 week, the ACPC pellets showed 84% more GAGs/DNA than the MSCs growing in TGF-beta1 after 28 days. After 4 weeks, the GDF-2 ACPCs pellets presented 8x higher GAG production compared to the MSCs grown in TGF-beta1 and 5x higher than the ACPCs with TGF-beta1 ( $p < 0.0001$ ) (Fig. A-B). Switching stopped the growth but stimulated high GAG production. Histology showed GAG and collagen II-rich matrix for ACPCs stimulated with both growth factors, but only with the standard TGF-beta1 protocol in the MSCs group.



GDF-2 stimulates GAG deposition (Fig. A) and growth of ACPC aggregates (Fig. B). A microfiber mesh can help guide their maturation (Fig. C).

**DISCUSSION & CONCLUSIONS:** GDF-2 has been reported as potent factor for chondrogenic differentiation of immature ACPCs<sup>1</sup>. In this experiment, GDF-2 supplementation significantly improved and hastened cartilage-like matrix deposition of mature ACPC aggregates compared to MSCs and the standard TGF-beta1 protocol. PCL microfiber meshes have been shown to have a reinforcing effect on gels<sup>2</sup>. Incorporating the pellet into the box structure (Fig. C) can guide its growth and condensation into a larger tissue construct, enhanced through the addition of GDF-2. Overall, the combination of an optimized culture condition based on GDF-2 grown ACPCs with the physical support given by the microfibrillar scaffold, provides a promising platform for developing a long-term and durable solution for implantation of cartilage tissue.

**REFERENCES:** <sup>1</sup> I.M. Khan et al. (2017) *BMP9 is a potent chondrogenic factor for articular cartilage-derived chondroprogenitors*, TERMIS EU. <sup>2</sup> J. Visser et al. (2015) *Reinforcement of hydrogels using three-dimensionally printed microfibres*. Nature communications **6**, p.6933.

**ACKNOWLEDGEMENTS:** Research funded by EU grants 309962 (HydroZONES)/647426 (3D-JOINT); Reumafonds (LLP-12, LLP-22 and CO-14-1-001); and UK grants (MR/L02280X/1) and 20864.

## Effects of mechanical stimulation combined with FGF18 on bovine chondrocytes embedded in a novel Fibrin:HA hydrogel

BP Antunes<sup>1,2</sup>, ML Vainieri<sup>3</sup>, E Monsonogo-Ornan<sup>2</sup>, M Alini<sup>3</sup>, S Grad<sup>3</sup>, A Yayon<sup>1</sup>

<sup>1</sup> Procure Bio med, Ltd., Ness Ziona, Israel <sup>2</sup> Institute of Biochemistry, Food Science and Nutrition, The Hebrew University of Jerusalem, Rehovot, Israel <sup>3</sup> AO Research Institute, AO Foundation, Davos, Switzerland.

**INTRODUCTION:** Current treatments for cartilage lesions such as microfracture, osteochondral graft and autologous cell implantation are often associated with fibrocartilage formation, donor site morbidity and further osteoarthritic progression [1]. Hence, there is an interest in the development of new approaches for cartilage repair, such as the use of hydrogels as cell carrier platforms and the controlled delivery of bioactives that promote matrix production and tissue healing [1]. Herein, we describe the use of a novel Fibrin:Hyaluronic Acid (Fibrin:HA) chemical conjugate-based hydrogel as a 3D environment for the mechanical stimulation of embedded bovine chondrocytes. The combined effect of mechanical stimulation with an FGFR3 specific variant of Fibroblast Growth Factor 18 (FGF-18v), was also studied.

**METHODS:** Bovine chondrocytes, isolated from fetlock joints, were embedded in HA:Fibrin hydrogels and subject to compression and shear forces for 14 days, in a bioreactor simulating natural joint movements. Compression displacement was set between 0.4-0.45 mm (upon contact with the hydrogel), while shear as set to  $\pm 25^\circ$ , at a frequency of 0.5 Hz. The effect of FGF-18 variant (10 ng/mL and 100 ng/mL, with continuous and non-continuous exposure) was also tested, in combination with mechanical stimulation.

After 14 days, samples were analysed for Glycosaminoglycans (GAGs) content (DMMB assay) and for the gene expression of aggrecan, cartilage oligomeric matrix protein (COMP) and proteoglycan 4 (PRG4).

**RESULTS:** Loaded samples, accumulated more GAGs and overexpressed COMP and PRG4 when compared to unloaded controls. There was no further increase in GAG content upon the addition of FGF18 (Fig. 1). FGF-18 however, increased aggrecan, and PRG4 expression, as well as COMP when applied without or with mechanical loading respectively (Fig 2).

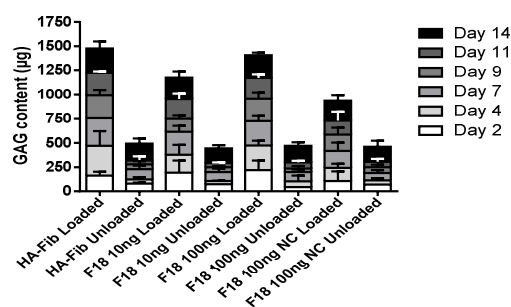


Fig. 1: GAG content accumulated in the culture medium over 14 days. NC – non-continuous.

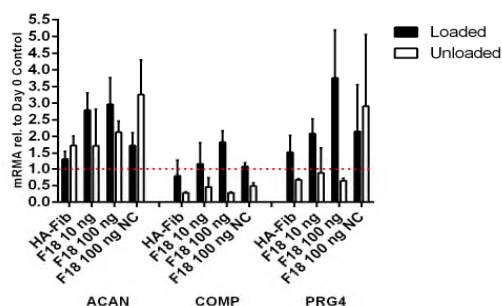


Fig. 2: Gene expression of Aggrecan (ACAN), Cartilage Oligomeric Protein (COMP) and Proteoglycan 4 (PRG4; Lubricin) after mechanical loading of bovine articular chondrocytes and treatment with FGF-18.

**DISCUSSION & CONCLUSIONS:** Mechanical stimulation of primary bovine chondrocytes embedded in a conjugated Fibrin-HA hydrogel leads to increased production of GAGs and expression of cartilage differentiation markers, ACAN, COMP and PRG4, some of which are further enhanced by the presence of FGF-18 in a concentration dependent manner.

**REFERENCES:** <sup>1</sup> K.L. Spiller et al. (2011) *Hydrogels for the Repair of Articular Cartilage Defects*, Tissue Engineering Part B: Reviews

**ACKNOWLEDGEMENTS:** This project has received funding from the European Union's Horizon 2020 research and innovation programme under Marie Skłodowska-Curie grant agreement No 642414.

## Deformation of chondrocytes and collagen structure in healthy and osteoarthritic articular cartilage by polarized light microscopy

F Badar<sup>1</sup>, A Tetmeyer<sup>1</sup>, A Thomas<sup>1</sup>, Y Xia<sup>1</sup>

<sup>1</sup> Department of Physics and Center of Biomedical Research, Oakland University, Rochester, MI, United States

**INTRODUCTION:** Polarized light microscopy (PLM) is a quantitative tool used in a variety of biological and material science studies [1]. Articular cartilage is heterogeneous with three histological zones (superficial SZ, transitional TZ, radial RZ) based on the orientation of collagen fibers. This work aims to quantify the depth dependent orientations of the collagen fibers and the chondrocytes in healthy and OA cartilage when it was loaded in an unconfined manner.

**METHODS:** Cartilage-bone specimens were harvested from 11 knee joints (5 healthy, 3 contralateral, 3 OA), which were studied in an extensive OA study by  $\mu$ MRI at 20 $\mu$ m pixel resolution [2]. The imaging specimens were fixated in 10% formalin for 7 hours and snap-frozen in ice-blocks using liquid nitrogen. 6- $\mu$ m slices were obtained with a cryostat microtome and placed on glass slides. The slices were then imaged using a quantitative PLM system at 5x for collagen orientation ( $^\circ$ ) and retardation (nm). Subsequently, the slices were imaged at polarized light at 20x or 40x magnification to quantify the morphology of cells. ImageJ (ver. 1.51u) was used to collect data on the elliptical shaped chondrocytes: the area, the major and minor axes, and the angle of orientation. Data of individual cells were tabled in a depth-dependent order from surface (0) to tidemark (1) in a relative scale. Equation (1) was used to fit the depth-dependent angle data

$$\vartheta(r) = a(\tanh[(r-r_0)/b] + c) \quad (1)$$

where  $a$  is half of the fiber (cell) orientational difference between the SZ and RZ;  $r_0$  is the center location of TZ;  $b$  is half the relative length of TZ and  $c$  is the orientation baseline factor.

**RESULTS:** Figure 1 showed the retardation and azimuth maps of the whole-thickness cartilage where the orientation of collagen changes from articular surface to the subchondral bone, where the red ellipses are the chondrocytes. Using Equation 1, the relative histological zone thickness was calculated for all tissue slices using the collagen matrix and the cell orientations. The cell area and aspect ratio were also averaged across each zone to show the cell changes per zone,

disease and strain (%). With an applied load of 10%, Figure 2 showed the orientational changes of collagen and cell due to the external loading. These changes are studied across different strains and disease stages, showing the linear relationships between strain and relative zone thickness.

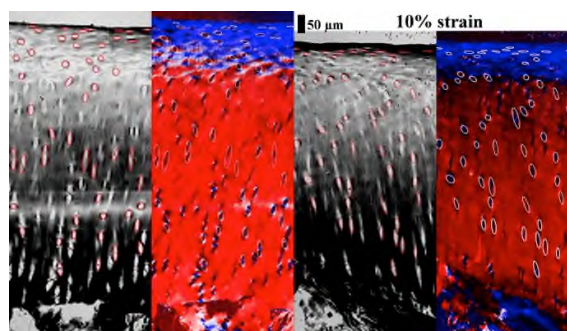


Fig. 1: Retardation (grayscale) and Azimuth (color) maps of unloaded (left) and loaded (right) cartilage samples with the chondrocytes in red ellipses. (Each image is from 2 20x mag images.)

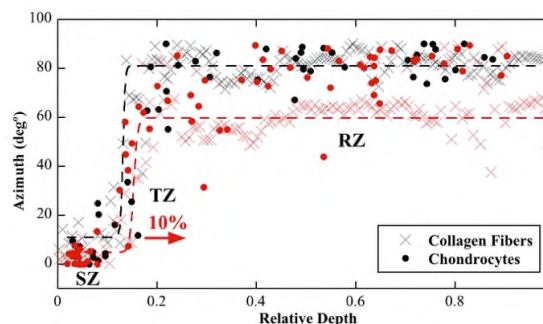


Fig. 2: Depth-dependent azimuth ( $^\circ$ ) profiles of unloaded (black) and loaded (10% strain, red) cartilage. Azimuth profiles of collagen matrix ( $\square$ ) and chondrocytes ( $\bullet$ ) were fitted using equation 1.

**DISCUSSION & CONCLUSIONS:** Quantitative measurement of collagen and chondrocyte morphology at 0.5  $\mu$ m pixel resolution showed changes in cartilage from healthy to OA, and under different external loading.

**REFERENCES:** <sup>1</sup>Y. Xia, J. B. Moody, N. Burton-Wurster, et al (2001) *Osteoarthritis and Cartilage* **9**:393-406. <sup>2</sup>J.H. Lee, F. Badar, D. Kahn, et al (2015) *J Biomech* **48**:3625-33.

**ACKNOWLEDGEMENTS:** The authors thank NIH for the R01 grants (AR52353 and AR69047).



## Highly tunable di-tyramine hyaluronan hydrogel enables mechanical stimulation of encapsulated mesenchymal stromal cells towards chondrogenesis

P. Behrendt<sup>1,2</sup>, Y. Ladner<sup>1</sup>, M.J. Stoddart<sup>1</sup>, S Lippross<sup>2</sup>, M. Alini<sup>1</sup>, D. Eglin<sup>1</sup>, A.R. Armiento<sup>1</sup>

<sup>1</sup> AO Research Institute Davos, Davos Platz, Switzerland. <sup>2</sup> Department of Orthopedic and Trauma Surgery, University Medical Center Schleswig-Holstein, Kiel, Germany

**INTRODUCTION:** The aim of this project was to develop a mechano-responsive hydrogel based on tyramine-modified hyaluronic acid (HA-Tyr) to allow for mechano-induced chondrogenesis of embedded mesenchymal stromal cells (MSCs). We defined a cytocompatible range of HRP and H<sub>2</sub>O<sub>2</sub> concentrations for MSCs encapsulation within HA-Tyr and then assessed the influence of the embedded cells on the biomechanical properties of the hydrogel and the adhesive properties of HA-Tyr to native cartilage. Lastly, we examined the chondrogenic response of cell-laden HA-Tyr upon joint-mimicking loading in a custom-made bioreactor [1].

**METHODS:** MSCs were isolated from bone marrow of human vertebral bodies, expanded in monolayer, and encapsulated at passage 3 in HA-Tyr hydrogels (20x 10<sup>6</sup> MSC/ml). Crosslinking was initiated by addition of 1 U/ml HRP and various dosages of H<sub>2</sub>O<sub>2</sub> (0.05 – 2.0 mM). Cytocompatibility and biomechanical properties were analysed by Live/Dead staining, rheology and unconfined compression test (Young's modulus), respectively. For multiaxial loading, cell-laden hydrogels were subjected to 10% compression superimposed on a 0.5 N pre-load and shear loading ( $\pm 25^\circ$ ) at 1 Hz for 1 h a day and five days per week for 4 weeks. Samples were compared to non-loaded sample equivalents. Culture media was collected three times a week. TGF- $\beta$ 1 production and activation was measured by ELISA and sulphated glycosaminoglycans (sGAG) by modified DMMB assay. Adhesion to native cartilage was assessed by push-out test.

**RESULTS:** The combination of 1 U/ml HRP and 2 mM H<sub>2</sub>O<sub>2</sub> was found as the optimal concentration in order to achieve sufficient biomechanical properties ( $G' 1120 \pm 96.39$  Pa) and maintain high cell viability for up to 28 days (80.2% viable cells). Push-out test demonstrated a bonding strength to native cartilage significantly higher ( $24.7 \pm 9.36$  kPa,  $p = 0.0013$ ) than agarose ( $8.94 \pm 5.54$  kPa). Interestingly, HA-Tyr had a bond strength comparable to the clinically used fibrin glue ( $24.2 \pm 15.8$  kPa). The optimised HA-Tyr hydrogel was used for further bioreactor analysis.

Multiaxial loading stimulated the activation of TGF- $\beta$ 1 to a higher extent when compared to unloaded samples (Fig.1). This was paralleled by increased sGAG release in the loaded samples indicating increased GAG biosynthesis.

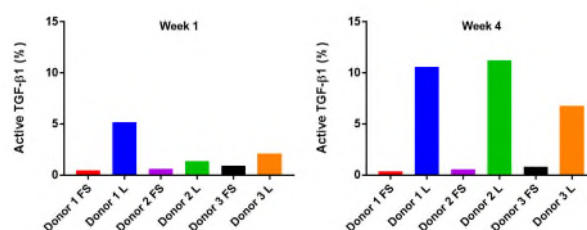


Fig. 1: Mechanical loading of cellularised HA-Tyr induced TGF- $\beta$ 1 activation over a period of four weeks. Colors indicate different donors; FS= free swelling, L= loaded.

**DISCUSSION & CONCLUSIONS:** HA-Tyr was optimised for high-density cell encapsulation concomitant to sufficient biomechanical properties to allow for adhesion to native cartilage and mechanical loading. Joint mimicking loading induced the production and activation of TGF- $\beta$ 1, a key pathway in mechano-transduced chondrogenesis.

**REFERENCES:** 1. Wimmer MA, Grad S, et al. (2004) Tribology approach to the engineering and study of articular cartilage. *Tissue Eng* 2004; 10: 1436-1445.

**ACKNOWLEDGEMENTS:** The authors would like to thank Dieter Wahl, Flavio Linardi and Dr. Peter Varga for their excellent technical support.

**FUNDING:** This work was supported by the AO Foundation. P.B. is a recipient of a research fellowship funded by the German Research Foundation (DFG; BE 6097/1-1/2).



## **Production and evaluation of decellularized hydrogel derived from ovine cartilage for cartilage regeneration**

S Bordbar<sup>1,2</sup>, MR Baghaban Eslami Nejad<sup>1</sup>, FA Sayahpour<sup>1</sup>

<sup>1</sup>Department of Stem Cells and Developmental Biology, Cell Science Research Center, Royan Institute for Stem Cell Biology and Technology, ACECR, Tehran, Iran.

<sup>2</sup>Tehran University of Medical Sciences, Department of Tissue Engineering.

**INTRODUCTION:** Cartilage damages through accident, trauma, tumor or disease in the term of “degenerative joint disease” are one of the most challenging issues in regenerative medicine and tissue engineering. For example, the prevalent nature of osteoarthritis, a cartilage degenerative disease that results in the attrition of joint surfaces and loss of mobility, emphasizes the importance of developing well-designed articular cartilage constructs. To treat damaged cartilage, current pre-clinical trials include the use of natural and acellular extracellular matrix (ECM) preparations in the form of hydrogels, that are competitive with solid scaffolds. These materials can also play the roles as natural ECM replacements.

**METHODS:** As a first step, acellular cartilage was made from sheep knee by decellularization with SDS and snap-freezing. Decellularization was evaluated with DNA assay and histological staining. After preparation of powder in the nano and micro scale size and evaluation by DLS analysis, hydrogel from acellular cartilage powder was made by digestion in acetic acid and pepsin. ECM content of the hydrogel was evaluated by GAG and Collagen content.

Human bone marrow derived mesenchymal stem cells (MSCs) were encapsulated in the hydrogel and cultured for 3 weeks. For cytotoxicity, live/dead assay with Calcein staining and MTT assay was performed. In addition, scanning electron microscopy (SEM), H&E and Alcian blue staining were used to detect proliferation and matrix production of the MSCs in the gel. For testing the chondrogenic induction of this hydrogel, chondrogenic gene expression, such as SOX9, COL2, Acan (aggrecan), Col1 and COL10, was analysed by Real Time PCR. Moreover, rheological analysis evaluated the temperature

and the time of gelation of the decellularized hydrogel.

**RESULTS:** DNA content and histological studies confirmed successful decellularization. ECM content showed no significant difference between natural, acellular and hydrogel in GAG and Collagen assays. Nano and micro scale powder of decellular cartilage was made at the range of 700-800 nm. MTT assay showed that mesenchymal stem cells remained viable after mixing with both acellular cartilage and hydrogel. Calcein staining confirmed these results. H&E and Alcian blue staining showed live and proliferating cells. In addition, SEM indicated that cells were proliferating on the surface of the hydrogel and intact collagen fibers were present in the hydrogel. Decellular hydrogel could induce chondrogenic differentiation, which was confirmed with Real Time PCR by SOX9, COL2, Acan (aggrecan), Col1 and COL10 gene expression. Rheological analysis revealed the temperature and time of gelation was at 37°C and 5-7 minutes, respectively.

**DISCUSSION & CONCLUSIONS:** It has been concluded that the hydrogel from acellular cartilage produced in this project is a promising material for cartilage tissue engineering and can be applied in cartilage repair.

## Nucleus Pulposus age-associated matrisome profiles unravel the ideal pro-regenerative microenvironment

J Caldeira<sup>1,2,3</sup>, M Fiordalisi<sup>1,3,4</sup>, AJ Silva<sup>1,3</sup>, C Santa<sup>5,6</sup>, H Osório<sup>2,3</sup>, M Molinos<sup>1,3,4</sup>, B Manadas<sup>5</sup>, R Gonçalves<sup>1,3</sup>, M Barbosa<sup>1,3,4</sup>

<sup>1</sup> Instituto de Engenharia Biomédica (INEB), University of Porto, Portugal. <sup>2</sup> Institute of Molecular Pathology and Immunology of the University of Porto (IPATIMUP), Portugal. <sup>3</sup> Instituto de Inovação em Saúde, University of Porto, Portugal. <sup>4</sup> Instituto de Ciências Biomédicas Abel Salazar (ICBAS), Porto, Portugal. <sup>5</sup> Center for Neuroscience and Cell Biology, University of Coimbra, Portugal. <sup>6</sup> III – Institute for Interdisciplinary Research, University of Coimbra, Portugal

**INTRODUCTION:** Low back pain, for which existing therapies are inadequate, is often caused by intervertebral disc (IVD) degeneration, which occurs with age and is accompanied by extracellular matrix (ECM) depletion.<sup>1,2</sup> Novel therapeutic solutions to modulate the disc microenvironment have been under study and among them, decellularization of young healthy IVDs seems to be a promising strategy.<sup>3,4</sup> However, a thorough study regarding the effect of NP natural scaffolds with varying age and developmental stage is needed to engineer the next-generation biomaterials for IVD regeneration.

**METHODS:** As so, iTRAQ LC-MS/MS profiling and structural characterization by Scanning Electron Microscopy (SEM) were performed on healthy bovine Nucleus Pulposus (NPs) from foetus, young and old animals. Next, different decellularization protocols were tested consisting in different time and treatment solutions, in order to establish an NP decellularization process that would be effective independently of the age groups under study. Histological and DNA quantification analysis were performed to evaluate the decellularization efficiency. The effect of the distinct decellularized microenvironments on human mesenchymal stem cell (MSC) behaviour is currently being explored.

**RESULTS:** In total, 161 bovine proteins were identified. Of these, 77 molecules were common to the three different age groups, of which 36 defined the NP matrisome. An enrichment of Collagen XII and XIV in foetal NP natural scaffolds, Collagen XI in younger tissues and Fibronectin and Prolargin in old ones was observed and independently validated.

We have identified 36 proteins that define the NP matrisome and demonstrated how this profile shifts during development and ageing. Both biochemical and structural cues identified provide

a starting point to design state-of-the-art biomaterials for IVD regeneration, recapitulating early developmental stage microenvironments (rich in Collagen XI, XII and XIV but poor in Fibronectin and Prolargin) – Figure 1.

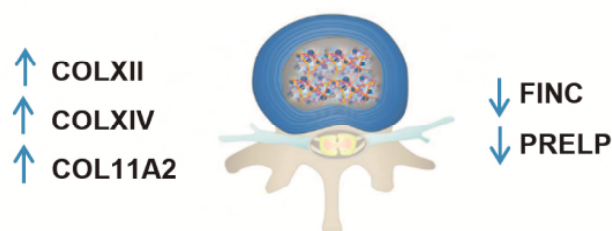


Fig. 1: Ideal microenvironment for IVD regeneration. Concerning the decellularization of distinct microenvironments, we have optimized an SDS-based protocol that is effective at removing cells from different aged NPs, but still preserves most glycosaminoglycans and collagen content

**DISCUSSION & CONCLUSIONS:** We report the first matrisome database of healthy NPs scaffolds with varying age and developmental stage, which is key to unveil the molecular cues that should be integrated or avoided when developing the next-generation biomaterials, aiming to recover tissue homeostasis by recapitulating early developmental stage microenvironments. In addition, the original study that aims to compare the performance of decellularized NPs from different aged donors will provide essential insights for the establishment of a pioneer treatment with potential to improve the already promising stem cell based therapies.

**REFERENCES:** <sup>1</sup> M.A Adams & P.J Roughley (2006) *Spine* **31**: 2151-61. <sup>2</sup> P. Colombier et al (2014) *Joint Bone Spine* **8**: 125-9. <sup>3</sup> R.A Wachs et al (2017) *Spine J* **17**: 435-44. <sup>4</sup> C. Fernandez et al (2016) *J Biomed Mater Res A* **104**: 3093-106.

## Influence of mechanical unloading on articular chondrocyte dedifferentiation

Martina Calì<sup>1,2</sup>, Simon L. Wuest<sup>1,2</sup>, Timon Wernas<sup>1</sup>, Samuel Tanner<sup>1</sup>, Christina Giger-Lange<sup>1</sup>, Fabienne Wyss<sup>1</sup>, Fabian Ille<sup>1</sup>, Benjamin Gantenbein<sup>2</sup>, Marcel Egli<sup>1</sup>

<sup>1</sup>*Institute of Medical Engineering, Lucerne University of Applied Sciences and Arts, School of Engineering and Architecture, Hergiswil, Switzerland*

<sup>2</sup>*Institute for Surgical Technology and Biomechanics, Tissue and Organ Mechanobiology, University of Bern, Switzerland*

**INTRODUCTION:** Due to the limited self-repair capacity of articular cartilage, the surgical restoration of defective cartilage remains a major clinical challenge. [1,2] The cell-based approach, known as autologous chondrocyte transplantation (ACT), has limited success, presumably because the chondrocytes acquire a fibroblast-like phenotype in monolayer culture. This unwanted dedifferentiation process is typically addressed by using three-dimensional scaffolds, pellet culture and/or the application of exogenous factors. Alternative mechanical unloading approaches suggested to be beneficial in preserving the chondrocyte phenotype. In this study, we examined if the random positioning machine (RPM) [3] could be used to expand chondrocytes in vitro such that they maintain their phenotype.

**METHODS:** Bovine chondrocytes were exposed to (a) eight days in static monolayer culture; (b) two days in static monolayer culture, followed by six days of RPM exposure; and (c) eight days of RPM exposure. Furthermore, the experiment was also conducted with the application of 20mM gadolinium, which is a nonspecific ion-channel blocker. Following the harvesting of the different samples, all the conditions were analyzed on an RNA level, to track and assign potential differentiation stages.

**RESULTS:** Visual inspection of the cells revealed that in static culture, chondrocytes adhered to the flask and adapted an elongated and spread-out morphology. In contrast, in RPM-exposed samples, many suspended cell clusters could be observed. The results revealed that the chondrocyte phenotype is preserved when chondrocytes go into suspension and aggregate to cell clusters. Interestingly, the gene expression (mRNA) of mechanosensitive ion channel TRPV4 decreased with progressing dedifferentiation. In contrast, the gene expression (mRNA) of mechanosensitive ion channel TRPC1 was reduced around 5-fold to 10-fold in all conditions. The application of gadolinium had only a minor influence on the results.

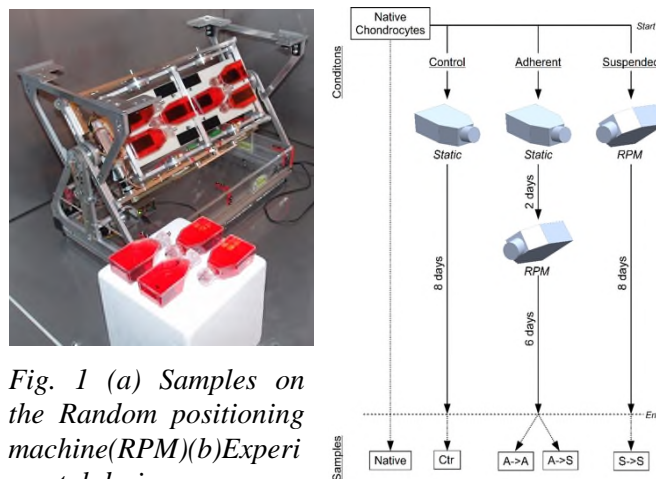


Fig. 1 (a) Samples on the Random positioning machine (RPM) (b) Experimental design.

**DISCUSSION & CONCLUSIONS:** This and previous studies suggest that the chondrocyte phenotype is preserved if cells maintain a round morphology and that ion channel TRPV4 could play a key role in the dedifferentiation process. Further key players are in the process of being analyzed.

**REFERENCES:** <sup>1</sup> Brittberg, M., et al., Articular cartilage engineering with autologous chondrocyte transplantation. A review of recent developments. *J Bone Joint Surg Am*, 2003. 85-Ap. 109-15. <sup>2</sup> Barlič, A., et al., Quantitative analysis of gene expression in human articular chondrocytes assigned for autologous implantation. *Journal of Orthopaedic Research*, 2008. 26(6): p. 847-853. <sup>3</sup> Brungs, S., et al., Facilities for Simulation of Microgravity in the ESA Ground-Based Facility Programme. *Microgravity Science and Technology*, 2016: p. 1-13. <sup>4</sup> Green, J. D., Tollemar, V., Dougherty, M., Yan, Z., Yin, L., Ye, J., et al. Multifaceted signaling regulators of chondrogenesis: Implications in cartilage regeneration and tissue engineering. (2015). *Genes&Diseases*, 2(4), 307-327.

**ACKNOWLEDGEMENTS:** The project has been supported by Metzgerei Stutzer & Flüeler AG, CC Mechanics and CC Electronics within the Lucerne School of Engineering and Architecture, Switzerland.



## TRPV4 in stretch-induced inflammation of intervertebral disc cells

E Cambria<sup>1</sup>, O Krupkova<sup>1</sup>, N Boos<sup>2</sup>, SJ Ferguson<sup>1</sup>, K Wuertz-Kozak<sup>1</sup>

<sup>1</sup> Institute for Biomechanics, ETH Zurich, Zurich, CH. <sup>2</sup> Prodosro Center for Spinal Medicine, Zurich, CH

**INTRODUCTION:** Low back pain (LBP) and painful degenerative disc disease (DDD) profoundly impact the health and economics of our society. Mechanical loading and inflammation interact to induce disc degeneration and pain. In fact, cyclic stretching of intervertebral disc (IVD) cells was shown to influence the expression of anabolic and catabolic mediators [1], and to induce inflammation [2]. However, little is known on the causal link between mechanical loading and inflammation. Calcium channels may constitute such a link [3]. The transient receptor potential vanilloid 4 (TRPV4) channel was shown to regulate stretch-induced inflammation in mouse lung epithelial cells [4]. Nevertheless, its role in human IVDs remains to be fully elucidated. The aim of this study is to test whether stretch-induced inflammation of IVD cells is regulated by TRPV4.

**METHODS:** Primary human IVD cells (n=5 donors) were enzymatically isolated from surgical biopsies and expanded to passage 1-2. Cells were seeded on fibronectin-coated PDMS chambers and cyclically stretched for different durations (1, 2, 4 or 8 hours) at 20% strain and 1 Hz frequency on a commercial bioreactor (STB-140-10 from Strex). Control samples were cultured statically in identical conditions. Gene expression of inflammatory cytokines, anabolic/catabolic genes and TRP channels was analyzed with RT-qPCR. In a preliminary TRPV4 inhibition experiment (n=1), IVD cells were stretched for 8 hours in the presence of either the vehicle (DMSO) or the specific TRPV4 antagonist GSK2193874. Gene and protein expression of IL-6 and IL-8 were analyzed with RT-qPCR and ELISA, respectively. This experiment was repeated with 15 min stretching in order to analyse the activation of MAP kinases (p-38, JNK, ERK) with Western Blot (n=2). Statistical significance was tested with one-way ANOVA with Tukey correction and the significance level was set to p<0.05.

**RESULTS:** On one hand, stretching significantly decreased the gene expression of collagen type II at 1, 2 or 4 hours (up to 0.6-fold) compared to control. On the other hand, MMP1 expression level was significantly higher than controls (2.7-fold) at 8 hours. Moreover, a difference was observed between samples stretched for 1 or 2

hours compared to 8 hours. The expression of the inflammatory cytokines IL-6 and IL-8 significantly increased with stretching duration. Gene expression of TRP channels was unaltered, with a slight, non-significant 1.5-fold increase of TRPV4 compared to control after 8 hours of stretching. A preliminary experiment shows that stretch-induced inflammation is reduced in the presence of the TRPV4 antagonist GSK2193874 (Fig. 1). Analysis of MAP kinases after 15 min of stretching showed higher phosphorylation of p-38, JNK and ERK compared to controls.

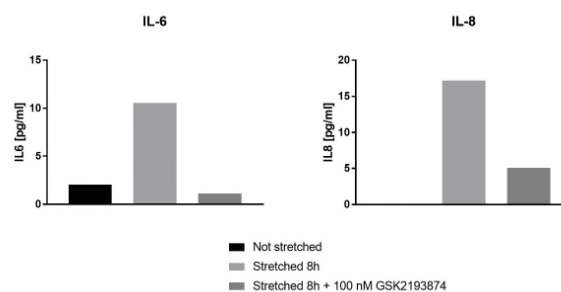


Fig. 1: Protein expression of IL-6 and IL-8 (ELISA) in a preliminary experiment (n=1), where human IVD cells were stretched in the presence or absence of GSK2193874.

**DISCUSSION & CONCLUSIONS:** We recapitulated the findings showing that cyclic stretching induces inflammation and affects the expression of anabolic and catabolic genes. We further show preliminary evidence that pharmacological inhibition of TRPV4 reduces inflammation, thus suggesting that stretch-induced inflammation is mediated at least in part by TRPV4. TRPV4 may constitute a potential therapeutic target to tackle LBP and DDD. Limitations of this work include the small sample size, which is currently increased by ongoing experiments.

**REFERENCES:** <sup>1</sup> G. Sowa and S. Agarwal (2008) *Am J Phys Med Rehabil* **87**:537-544. <sup>2</sup> G.A. Sowa, J.P. Coelho, N.V. Vo, et al (2012) *Am J Phys Med Rehabil* **91**:846-855. <sup>3</sup> T. Kato, N. Ishiguro, H. Iwata, et al (1998) *Biochem Biophys Res Commun* **244**:615-9. <sup>4</sup> P.S. Nayak, Y. Wang, T. Najrana, et al (2015) *Respir Res* **16**:60

## Platelet derivatives reclute nestin-expressing progenitor cells from adult articular cartilage

S Carluccio<sup>1</sup>, D Martinelli<sup>1</sup>, ME Palamà<sup>1</sup>, RC Pereira<sup>1</sup>, C Gentili<sup>1</sup>

<sup>1</sup> Department of Experimental Medicine DIMES, University of Genoa, Italy

**INTRODUCTION:** In the last years the use of platelet-derived products in orthopedics has significantly increased with beneficial outcomes. In our hands, platelet derivatives trigger a strong mitogenic stimulus on articular chondrocytes *in vitro*, allowing the maintenance of their chondrogenic redifferentiation potential. Platelet products have also beneficial effects during the repair process of a damaged cartilage, since they induce a cascade of events leading to cell recruitment, transient activation of inflammation and its subsequent resolution [1]. Here, we report that differentiated chondrocytes can recover some features of stemness when expanded *in vitro* in presence of platelet derivatives. Platelet products can also recruit progenitor cells resident in cartilage [2] that are characterized by the expression of Nestin, marker of proliferating and migrating adult stem cells in several tissue [3].

**METHODS:** Human cartilage biopsies were regularly cut in small pieces and cultured with 10% Fetal Bovine Serum (FBS) or 5% Platelet Lysate (PL). The remaining tissue was subjected to repeated enzymatic digestions, and the released articular chondrocytes (ACs) were cultured as described above. Colony Forming Unit Fibroblast (CFU-F) assay and growth kinetics were performed. Cell phenotype in FBS or PL were characterized by flow cytometry, the expression of Nestin and typical chondrogenic markers were evaluated by real-time PCR analysis and immunofluorescence staining. To test multilineage differentiation capacity, cells were exposed to chondrogenic, osteogenic and adipogenic stimulation *in vitro*. Furthermore, chondrogenesis was investigated also *in vivo* by implantation of cell-seeded scaffold in nude mice. In addition, the conditioned media from ACs treated with PL under physiological or inflammatory conditions (IL1 $\alpha$ ) was used to study the chemotactic activity on CPCs.

**RESULTS:** The treatment of cartilage pieces with PL *in vitro* induces the spontaneous migration of a cell population showing a fibroblastic-like morphology (CPCs), whereas no cells emerge from

tissue cultured in FBS (Fig. 1a, b). This population has a high proliferative rate and shows the capacity to form colonies, as well as mature chondrocytes grown in culture with PL, contrarily to cells cultivated in FBS (Fig. 1c-e). Cells obtained in PL show an up-regulated expression of Nestin, that is undetectable in mature chondrocytes (Fig.1f). CPCs are also capable to give raise to *tri*-lineage differentiation. In particular, they are able to differentiate into good hyaline-like cartilage both *in vitro* and *in vivo* (Fig.1g, h). In addition, CPCs show higher migration under inflammatory conditions and PL enhances this effect.

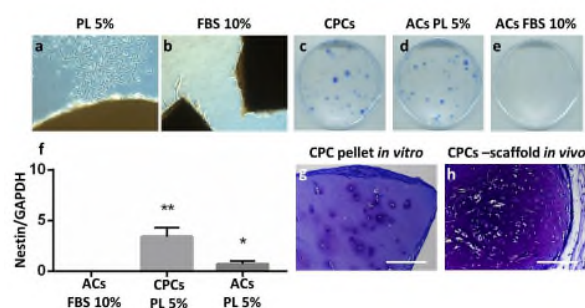


Fig. 1. a,b: CPC exit from cartilage tissue. c-e: CFU-F assay. f: Nestin mRNA levels. g,h: CPC chondrogenic differentiation.

**DISCUSSION & CONCLUSIONS:** PL treatment enriches the AC population with cells showing stemness features. Moreover, PL bring out and activate stem/progenitor cells resident in adult articular cartilage. These cells might be involved in the maintenance of tissue homeostasis and therefore represent a promising tool for reparative strategies of cartilage defects.

**REFERENCES:** <sup>1</sup> R.C. Pereira, M. Scaranari, R. Benelli, et al (2013) *Tissue Eng Part A* **19**:1476-88. <sup>2</sup> G.P. Dowthwaite, J.C. Bishop, S.N. Redman, et al (2004) *J Cell Sci* **117**: 889-97. <sup>3</sup> C. Wiese, A. Rolletschek, G. Kania, et al (2004) *Cell Mol Life Sci* **61**: 2510-22.

**ACKNOWLEDGEMENTS:** This research was supported by Eurostars proposal: Re.Me.Pro.

## Characterization of the stemness potential and the response to inflammatory stimulus of cartilage resident progenitor cells derived from OA patients

P De Luca<sup>1</sup>, M Viganò<sup>1</sup>, D Kouroupis<sup>2</sup>, L de Girolamo<sup>1</sup>, C Perucca Orfei<sup>1</sup>, L Zagra<sup>3</sup>, D Correa<sup>2</sup>, A Colombini<sup>1</sup>.

<sup>1</sup>*Orthopaedic Biotechnology Lab, IRCCS Galeazzi Orthopaedic Institute, Milan, Italy.*

<sup>2</sup>*Department of Orthopaedics, Division of Sports Medicine, Diabetes Research Institute & Cell Transplant Center, University of Miami, Miller School of Medicine, Miami, FL, USA.*

<sup>3</sup>*Hip Department, IRCCS Galeazzi Orthopaedic Institute, Milan, Italy.*

**INTRODUCTION:** Articular cartilage owns a limited self-repairing ability, but, together with terminally differentiated chondrocytes, it contains a subpopulation of progenitor cells [1,2] that may represent the target for treatments aimed to restore tissue homeostasis, the starting point for tissue regeneration. Then, the purpose of the present study is the identification and characterization of cartilage progenitor cells, in terms of stemness potential and response to an inflammatory stimulus. Moreover, donor-matched populations of mesenchymal stem/stromal cells, derived from bone marrow (BMSCs) and adipose tissue (ASCs), were used as comparison.

**METHODS:** ASCs, BMSCs and Cartilage Cells (CCs) were isolated from 8 donors (41-74 years old) undergoing total hip arthroplasty, and then they were cultured until passage 3. The CFU-F ability (CFU-F assay), immunophenotype (cytofluorimetry) and stemness marker expression (Real-Time RT-PCR) of the three different populations were evaluated. After pro-inflammatory induction with 1 ng/ml IL-1 $\beta$ , the production of growth factors and pro/anti-inflammatory cytokine (protein microarrays and ELISA), as well as the gene expression of catabolic and anabolic markers (Real-Time RT-PCR) were analyzed.

**RESULTS:** CCs demonstrated the highest clonogenic ability among the analyzed cell types, whereas the stemness marker expression (*NANOG* and *POU5F1*), as well as the immunophenotype, were similar among the different cell populations. Moreover, CCs showed similar osteo-differentiation potential of BMSCs, while they showed no differentiation toward the adipogenic lineage. ASCs, BMSCs and CCs were able to chondro-differentiate, but CCs showed the higher values in terms of GAG deposition.

For what concern the release of paracrine mediators, CCs produce higher amounts of growth factors at the basal level with respect to MSCs, but while ASCs and BMSCs increase the production of growth factors after inflammation, CCs show unchanged levels. On the contrary, in basal condition CCs demonstrated to release pro/anti-inflammatory cytokines at levels similar to BMSCs and higher than ASCs. After inflammatory stimulation, all cell types enhance the production of cytokines, in particular ASCs. At the same time, in this condition, both CCs and MSCs showed an increased release of the anti-inflammatory mediator IL-1Ra, and higher levels of catabolic enzymes gene expression (*MMP1*, *MMP3* and *MMP13*). For what concern anabolic factors, *TIMP3* gene expression was downregulated in ASCs only.

**DISCUSSION & CONCLUSIONS:** In conclusion, CCs may represent the most suitable cell type for the application of regenerative medicine approaches to cartilage repair, thanks to their stemness features, chondrogenic commitment and basal paracrine activity.

Further investigation aimed to identify feasible procedures to stimulate and exploit this cell population in order to improve cartilage tissue homeostasis and repair are needed in the view of future cell-based therapies for cartilage disorders.

**REFERENCES:** [1] Jiang Y et al., (2016) *Stem Cells Translational Medicine* **5**:733-744.

[2] Oda T et al., (2016) *Biochemical and biophysical research communications* **479**:469-475.



## Stemness potential and paracrine activity in response to inflammation of cells derived from human intervertebral disc

P De Luca<sup>1</sup>, D Kouroupis<sup>2</sup>, L de Girolamo<sup>1</sup>, M Viganò<sup>1</sup>, C Perucca Orfei<sup>1</sup>, M Brayda-Bruno<sup>3</sup>,  
D Correa<sup>2</sup>, A Colombini<sup>1</sup>

<sup>1</sup> *Orthopaedic Biotechnology Lab, IRCCS Galeazzi Orthopaedic Institute, Milan, Italy.*

<sup>2</sup> *Department of Orthopaedics, Division of Sports Medicine, Diabetes Research Institute & Cell Transplant Center, University of Miami, Miller School of Medicine, Miami, FL, USA.*

<sup>3</sup> *Scoliosis Unit, Department of Orthopedics and Traumatology-Spine Surgery III, IRCCS Galeazzi Orthopaedic Institute, Milan, Italy.*

**INTRODUCTION:** Human intervertebral disc (IVD) contains progenitors representing a potential reservoir for tissue homeostasis maintenance and repair [1]. Nevertheless, these cells alone possess a limited ability to counteract IVD degeneration, and they are unable to restore the tissue physiology.

The characterization of the stemness, metabolic and anti-inflammatory potential of cells derived from nucleus pulposus (NP), annulus fibrosus (AF) and cartilaginous endplate (EP) could allow to exploit the specific cell features in regenerative medicine approaches. Thus, the aim of the present study was to analyze the stemness features and the behavior of disc cells after an *in vitro* treatment with an inflammatory stimulus.

**METHODS:** Cells obtained from lumbar NP, AF and EP of 8 patients affected by degenerative disk diseases (56±9 years), freshly isolated or expanded, were characterized for their colony forming unit ability, adipo-osteo-chondro-differentiation potential, *NANOG* and *POU5F1* expression and immunophenotype, in order to define their stemness properties [2].

Furthermore, following pro-inflammatory stimulation with IL-1 $\beta$  (1 ng/ml for 48 h), the expression of *VEGFA*, *TGFB1*, *MMP1*, *MMP3*, *MMP13*, *TIMP1* and *TIMP3* genes and the release of pro/anti-inflammatory cytokines, were evaluated.

**RESULTS:** The results showed that all the disc cells, both freshly isolated or expanded, were able to form colonies, possess osteogenic, but no adipogenic differentiation ability. The chondro-differentiation was observed in all the cell types freshly isolated but only NP cells maintained this ability along the culture. Moreover, *NANOG* and *POU5F1* genes were expressed in all cell types, but their expression decreased in AF and EP cells after expansion.

The three kind of IVD cells shared the same immunophenotype and were negative for CD14, CD34, CD45, CD71, CD146 and positive for CD44, CD73, CD90, CD105, CD151, CD166 surface markers. The presence of the pro-inflammatory stimulus increased the expression of MMPs and *VEGF* in all the cell populations, whereas the expression of the anti-catabolic *TIMP3* and *TGF $\beta$ 1* decreased. Results about the pro/anti-inflammatory cytokine release showed that AF cells were the highest pro-inflammatory population, whereas the EP cells were the most responsive to the inflammatory stimulus, showing the less pro-inflammatory behavior. In all the disc cells an increased secretion of IL-Ra was observed under inflammatory condition.

**DISCUSSION & CONCLUSIONS:** In conclusion, IVD, even when pathological or obtained from adult patients, contains resident progenitor cells exploitable *in situ* as specific targets for tissue repair. These cells alone are not able to counteract efficiently the inflammatory and catabolic processes, thus it would be advisable to reduce the inflammation before stimulating the disc progenitors.

**REFERENCES:** <sup>1</sup> H Brisby, N Papadimitriou, C Brantsing et al (2013) *Stem Cells Dev* **22**:5 804-14.  
<sup>2</sup> M Dominici, K le Blanc, I Mueller et al (2006), *Cytotherapy* **8**:4 315-17.

## Use of autologous chondrocyte-seeded hydrogel to repair osteochondral defect in a non-human primate model

A Dufour<sup>1</sup>, M Verset<sup>2</sup>, A Cohendet<sup>2</sup>, M Buffier<sup>3</sup>, M Rioult<sup>3</sup>, H Contamin<sup>2</sup>, E Perrier-Groult<sup>1</sup>, F Mallein-Gerin<sup>1</sup>

<sup>1</sup> [CNRS-UMR 5305](#), Lyon, France. <sup>2</sup> [Cynbiose](#), Marcy l'Etoile, Lyon, France. <sup>3</sup> [3-D Matrix Europe SAS](#), Caluire, France

**INTRODUCTION:** *In vivo* evaluation of tissue engineered-cartilage is an indispensable step before human application. Most animal models differ in biomechanical functions and/or physiological responses from human, limiting our ability to extrapolate data to clinical practice. The non-human primate (NHP) model overcomes many of these limitations. We have developed a new approach for articular cartilage repair: autologous chondrocytes are amplified and combined with an innovative self-assembling peptide (IEIK13 hydrogel) or a biomaterial already used in other applications than rheumatology (fibrin hydrogel), under the stimulation of chondrogenic factors. We investigated capacity of the cartilage gels to repair osteochondral defects created in knee joint of Cynomolgus monkey.

**METHODS:** Articular chondrocytes were isolated from cartilage biopsies (3.5 mm diameter) sampled from femoral condyles of three adult animals. Cells were amplified for 14 days with FGF-2 and insulin (cocktail FI) and re-differentiated for 21 days in IEIK13 or fibrin in the presence of BMP-2, insulin and triiodothyronine T3 (cocktail BIT). For a given animal, each joint was dedicated to a hydrogel (IEIK13 or fibrin). During a second surgery, cell-loaded or acellular hydrogels were implanted within osteochondral defects originally created at the biopsy zones. Animals were implanted for 3 months. Implant integration is evaluated by micro-computed tomography ( $\mu$ -CT) and immunohistological analyses.

**RESULTS:** NHP articular chondrocytes were responsive to FI/BIT concentrations already used in clinical trial with auricular chondrocytes to treat nasal deformities. Our protocol generated cells in sufficient number to form a hydrogel-based cartilage plug: an average of  $4 \times 10^6$  cells was generated from one biopsy sample, corresponding to 2 ml of regenerated cartilage with  $2 \times 10^6$  cells/ml. *In vitro* analyses (real-time PCR, Western-blotting and immunohistochemistry) revealed that NHP chondrocytes are able to reconstruct a cartilage matrix in IEIK13 and fibrin

hydrogels. Cartilage gels were successfully implanted, all animals showed normal mobility through the study without medical complication or sign of distress. The  $\mu$ -CT analysis allowed the follow-up of the hydrogel-based implants (figure 1A) which appear well integrated into the cartilage defects (figure 1B). Histological analyses are in progress and will determine more precisely the nature/quality of the reconstructed cartilage using IEIK13 or fibrin hydrogel.

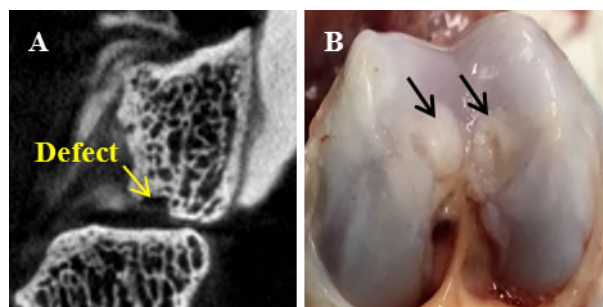


Fig. 1: (A) maintenance of the hydrogel-based implant prevents penetration of the contrast agent within the defect. (B) Macroscopical aspect of implanted defects (arrows) at the end of the study.

**DISCUSSION & CONCLUSION:** Our first results demonstrate the value of a combined approach using autologous chondrocytes, selected soluble factors (available under drug forms) and hydrogel to repair articular cartilage by tissue engineering. Besides, our *in vivo* study shows that NHP is a relevant animal model for challenging articular cartilage tissue engineering protocols.

### ACKNOWLEDGEMENTS:

We thank the AniRA Genetic and Cellular Analysis facilities of SFR BioSciences Gerland-Lyon Sud (UMS 3444 CNRS, US8 Inserm, ENS de Lyon, Lyon 1 University). This research was funded by CNRS, Lyon 1 University and the Fondation de l'Avenir. A Dufour was supported by a fellowship from the Région Auvergne-Rhône-Alpes.

## **Autologous chondrocyte transplantation (ACT): Influence of cell number in an *ex vivo* model**

F Ehlicke<sup>1</sup>, A Schwab<sup>1</sup>, B Schaefer<sup>2</sup>, H Walles<sup>1,3</sup>

<sup>1</sup> Department Tissue Engineering & Regenerative Medicine, University Hospital Wuerzburg, Wuerzburg, Germany. <sup>2</sup> Geistlich Pharma AG, Wolhusen, Switzerland. <sup>3</sup> Fraunhofer-Institute for Silicate Research, Translational Center Regenerative Therapies, Wuerzburg, Germany.

**INTRODUCTION:** Due to the poor intrinsic self-healing capacity of articular cartilage, defects that remain untreated or do not regenerate properly increase the risk to progress to osteoarthritis. Optimal treatment approach, either cell free, cell based or material assisted are yet not known that lead to long-term restoration of functional hyaline cartilage tissue with similar characteristics compared to native cartilage. It is obvious that further research activities are necessary to get a deeper insight to answer questions related to basic biological mechanisms during defect progression but also for clinical relevant applications in cartilage regeneration. Schwab et al. established an *ex vivo* cartilage defect model representing a test system that allows for testing novel biomaterials on formation of repair tissue<sup>1</sup>.

Aim of the study was to mimic ACT procedure in the model and investigate the influence of cell number.

**METHODS:** Porcine osteochondral explants were isolated from medial condyle (diameter: 8 mm, bone height: 3 mm). Full thickness cartilage defects (diameter: 4 mm) were created with biopsy punch. Porcine chondrocytes isolated from lateral condyle were injected on calcified layer at two different cell densities, 1 Mio/cm<sup>2</sup> and 4 Mio/cm<sup>2</sup>. Defect was covered with a collagen type I/III membrane (Geistlich Pharma AG) to keep cells in the defect. Explants were cultured for 28 days with tissue specific media in custom made culture platform under hypoxic conditions (2% O<sub>2</sub>)<sup>1</sup>. No TGF-β was supplemented to cartilage media. Upon harvest (day 0, 14 and 28) live-dead staining and immune-histological analysis followed.

**RESULTS:** Covering the cartilage defect with the membrane induced partial regeneration, which was less pronounced in sham group. The injection of chondrocytes into full thickness cartilage defects improves repair response corresponding with cell amount: The higher the initially injected chondrocyte amount the more cartilaginous matrix (collagen type II, aggrecan, proteoglycans by

means of Safranin-O) was synthesized. No signs of hypertrophy (collagen X, RunX2) were present.

**CONCLUSION:** To conclude, the results showed the predictive properties of the *ex vivo* test system by transferring *in vivo* complexity to an *ex vivo* model. This test system opens the possibility to test effectivity and efficiency of therapeutically approaches by means of cells, scaffolds or drugs for cartilage regeneration.

**REFERENCES:** <sup>1</sup> Schwab A, Meeuwse A, Ehlicke F, et al. (2017) Ex vivo culture platform for assessment of cartilage repair treatment strategies. *Altex*, 34:267-277.



## Time-dependent contribution of BMP, FGF, IGF and HH-signalling to proliferation of mesenchymal stromal cells during chondrogenesis

J Fischer<sup>1</sup>, S Diederichs<sup>1</sup>, N Knoch<sup>1</sup>, T Sims<sup>1</sup>, N Rosshirt<sup>2</sup>, W Richter<sup>1</sup>

<sup>1</sup> Research Center for Experimental Orthopaedics <sup>2</sup> Clinic for Orthopaedics and Trauma Surgery, Heidelberg University Hospital

**INTRODUCTION:** Early loss of up to 50% of cells is common for in vitro chondrogenesis of mesenchymal stromal cells (MSC) in pellet culture, reducing efficacy and tissue yield for cartilage engineering. Enhanced proliferation of MSC during chondrogenesis could compensate for this unwanted effect, but relevant signalling pathways remain largely unknown. Aim of this study was to dissect the contribution of bone morphogenetic protein- (BMP), fibroblast growth factor- (FGF), insulin-like growth factor- (IGF) and hedgehog- (HH) signalling to cell proliferation during chondrogenesis and investigate whether a further mitogenic stimulation is possible and promising.

**METHODS:** Human MSC were subjected to chondrogenesis in the presence or absence of pathway inhibitors or activators up to day 14 or from day 14 to day 28. Subsequently, proliferation was assessed via [3H]-thymidine incorporation, and DNA and proteoglycan contents were quantified.

**RESULTS:** A transient arrest of proliferation was observed on day 3 after which cell division was re-initiated. While BMP signalling was essential for proliferation throughout chondrogenesis, IGF signalling was relevant only up to day 14 (Fig. 1). In contrast, FGF and HH signalling drove proliferation only from day 14 on. Early BMP4, IGF-1 or FGF18-treatment neither prevented early cell loss nor allowed further mitogenic stimulation. However, application of the HH agonist purmorphamine starting at day 14 raised proliferation 1.44-fold ( $p < 0.05$ ) and late BMP4 application enhanced the DNA and proteoglycan content with significant effects on tissue yield.

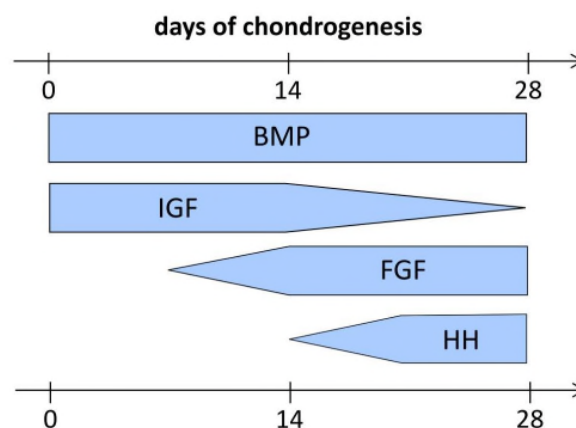


Fig. 1: Time-dependent relevance of signaling pathways for proliferation during chondrogenesis of MSC.

**DISCUSSION & CONCLUSIONS:** A differential and phase-dependent contribution of the four pathways to proliferation was uncovered and HH signalling allowed further stimulation of cell proliferation while BMP4 treatment was promising to enhance tissue yield. This knowledge sheds light on a high similarity of cell growth regulation in MSC chondrogenesis and in the growth plate and is valuable to improve efficacy of chondrocyte formation from MSC for use as in vitro test models and for cartilage regeneration.

## Comparison of two annulus fibrosus injury models investigated in a loaded bovine intervertebral disc organ culture format

DA Frauchiger<sup>1</sup>, SCW Chan<sup>1</sup>, LM Benneker<sup>2</sup>, B Gantenbein<sup>1</sup>

<sup>1</sup> Institute for Surgical Technology and Biomechanics, University of Bern, Bern, CH. <sup>2</sup> Department of Orthopaedic Surgery, Inselspital, Bern University Hospital, University of Bern, Bern, CH

**INTRODUCTION:** Back pain is affecting an increasing number of people. In order to investigate new treatment approaches *in vitro* and organ culture models are required. In this study, we aim to compare annulus fibrosus (AF) injury models that might mimic intervertebral disc (IVD) herniation. These are then tested in a bovine IVD organ culture model under three loading regimes.

**METHODS:** Fresh bovine coccygeal IVDs were isolated under aseptic conditions ~4 hours post-mortem [1]. A circular 2 mm wide and 7 mm deep injury was induced by a 2 mm biopsy punch. The second injury model used a custom-designed cross-incision tool. This fully autoclavable tool creates a 2 mm wide and 7 mm deep cross incision and can be operated single-handed. Both injury models reach the nucleus pulposus in 25% of cases. IVDs (5 per group *i.e.* healthy control, punch injury, cross-incision) were subjected to one of the following three loading profiles over 14 days in HG-DMEM with 5% FCS: 1) no loading, 2) static loading (0.2 MPa for 8 hrs/day), or 3) complex loading (0.2 MPa load and  $0 \pm 2^\circ$  of torsion at 0.2 Hz for 8 hrs/day). Media was changed every 2-3 days. On day 0 and 14 of culture disc height, DNA and glycosaminoglycan (GAG) contents, histology, and qPCR were performed. Additionally, compressional stiffness of complex loaded IVDs was determined from bioreactor reaction force data.

**RESULTS:** Both injury models, 2 mm punch and cross-incision, did not differ from control IVDs for DNA and GAG contents. Further, compressional stiffness did not change between injury models. Histology did not show GAG degradation after 14 days of organ culture (Fig. 1). qPCR of the punch injury, under complex load, induced down-regulation of several anabolic, catabolic and inflammatory genes whereas cross-incision injury did not significantly differ from control discs.

**DISCUSSION & CONCLUSIONS:** Injury models differed mainly in disc height. Here cross-injury model caused a significant height decrease under complex loading. For gene expression, punch injury caused general down-regulation of anabolic, catabolic, and inflammatory genes under complex load, whereas the cross-injury resulted did not differ

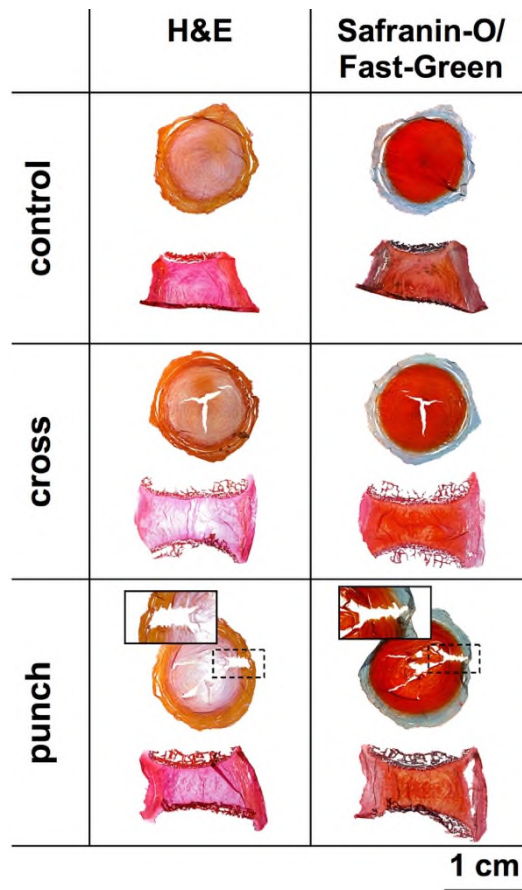


Fig. 1: Histology of healthy control discs (top), cross-incision injured IVDs (middle) and biopsy punch injured IVDs (bottom). Hematoxylin & Eosin (H&E) and Safranin-O/Fast-Green were performed.

from control for catabolic and inflammatory genes and up-regulation of BGN. Finally, we could observe that both sides, injury/repair side and contralateral side) were affected by both injuries regarding mitochondrial activity, GAG, and DNA contents, and gene expression of major catabolic, anabolic, and inflammatory genes.

**REFERENCES:** <sup>1</sup> S.C.W. Chan, B. Gantenbein-Ritter (2012) *J Vis Exp* 60:e3490. <sup>2</sup> R. Gawri, J. Moir, J. Ouellet et al (2014) *PLoS One* 9(7):e101233.

**ACKNOWLEDGEMENTS:** This project was supported by the Gebert R uf Stiftung project #GRS-028/13. We thank Eva Roth for her assistance.

## Annulus fibrosus repair approach – combining genipin-enhanced fibrin hydrogel and engineered silk fleece-membrane composite

DA Frauchiger<sup>1</sup>, RD May<sup>1</sup>, E Bakirci<sup>1</sup>, M Wöltje<sup>2</sup>, LM Benneker<sup>3</sup>, B Gantenbein<sup>1</sup>

<sup>1</sup> Institute for Surgical Technology and Biomechanics, University of Bern, Bern, CH. <sup>2</sup> Institute of Textile Machinery and High Performance Material Technology, TU Dresden, Dresden, DE.

<sup>3</sup> Department of Orthopaedic Surgery, Inselspital, Bern University Hospital, University of Bern, Bern, CH

**INTRODUCTION:** Low back pain (LBP) is affecting an increasing number of people worldwide. Not only the elderly are affected but also the young and active may suffer from LBP mainly caused by intervertebral disc (IVD) herniation. Due to the high number of people affected treatment approaches that reconstitute the IVDs biological function are in high demand. In this study, we aimed to study the feasibility of a genipin cross-linked fibrin hydrogel *in vitro* and *ex vivo* in an organ culture approach.

**METHODS:** Coccygeal bovine IVDs were harvested in aseptic conditions. A 7 mm deep injury was induced by using a 2 mm biopsy punch and removing tissue to create a cavity. The repair was performed by filling the cavity with human-based fibrin hydrogel (Tisseel, Baxter) enhanced with genipin (5.7 mg/mL) [1,2]. A GMP-compliant silk membrane-fleece composite was placed on the hydrogel to form a barrier and prevent IVD herniation (Fig. 1). Subsequently, IVDs (healthy control, injured and repaired) were subjected to *in vitro* organ culture for 14 days using three loading regimes: 1) no-load, 2) static load (0.2 MPa for 8h/day), and 3) complex load (0.2 MPa compression and  $0 \pm 2^\circ$  torsion at 0.2 Hz for 8 h/day). Complex load was applied by using a custom-built two-degree of freedom bioreactor. At the end of culture, the discs were inspected for seal failure and herniation, IVD height, metabolic activity, DNA and glycosaminoglycan (GAG) contents, histology and qPCR of major anabolic, catabolic and inflammatory genes were determined.

Additionally, genipin-enhanced fibrin hydrogel was investigated towards *in vitro* cell cytocompatibility by seeding low-passage human mesenchymal stem cells (N = 6) and donor matched (N = 3) human AF and nucleus pulposus cells on the fleece side of the silk scaffold. Further, compressional stiffness of hydrogels using two different genipin concentrations (5.7 and 11 mg/mL) were compared to bovine nucleus pulposus (bNP) tissue.

**RESULTS:** After 14 days of organ culture no herniation was observed. The repaired unloaded

IVDs lost significantly height. However, metabolic activity, DNA and GAG contents were not negatively affected by this loss and even contained higher DNA concentrations. Gene expression of anabolic, catabolic and inflammatory genes was not significantly different for the repaired and injured IVDs. Although genipin showed strong cytotoxic effects in the 2D *in vitro* culture this was not observed in the organ culture. Further, the 5.7 mg/mL genipin resulted in a fibrin hydrogel with a comparable stiffness to the bNP.

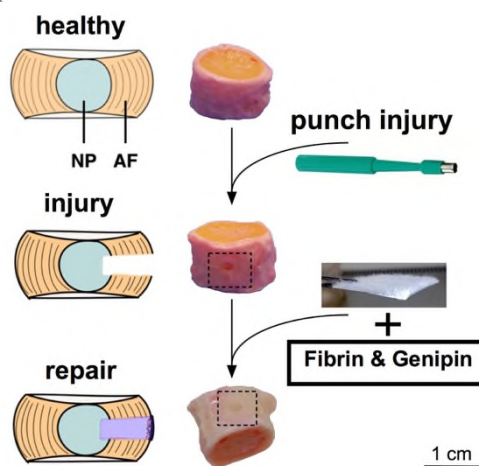


Fig. 1: Overview of experimental groups healthy, injured and repaired IVDs (top to bottom).

**DISCUSSION & CONCLUSIONS:** The investigated repair approach combining genipin-enhanced fibrin hydrogel and silk composite formed a tight herniation-free closure. The repair model was not able to restore disc height, however, the prevention of uncontrolled swelling seemed to have a beneficial effect on IVDs. Despite, superior as filling material, genipin-enhanced fibrin hydrogel is not suitable as cell carrier.

**REFERENCES:** <sup>1</sup> C.C. Guterl, O.M. Torre, D. Purmessur et al. (2014) *Tissue Eng Part A* **20**:2536-45. <sup>2</sup> M. Likhitpanichkul, M. Dreischarf, S. Illien-Junger et al. (2014) *Eur Cell Mater* **28**:25-38.

**ACKNOWLEDGEMENTS:** This project is supported by the Gebert Rűf Stiftung project #GRS-028/13. We thank Eva Roth for her assistance.



## Comparing three cell isolation techniques for “fishing” angiopoietin-1 (Tie 2) positive progenitor cells from the nucleus pulposus

DA Frauchiger<sup>1</sup>, RD May<sup>1</sup>, X Zhang<sup>1</sup>, J Stoyanov<sup>2</sup>, A Bertolo<sup>2</sup>, LM Benneker<sup>3</sup>, D Sakai<sup>4</sup>, S Grad<sup>5</sup>, MA Tryfonidou<sup>6</sup>, B Gantenbein<sup>1</sup>

<sup>1</sup>Institute for Surgical Technology and Biomechanics, University of Bern, Bern, CH. <sup>2</sup>Spinal Injury Research, Swiss Paraplegic Research, Nottwil, CH. <sup>3</sup>Department of Orthopaedic Surgery, Inselspital, Bern University Hospital, University of Bern, Bern, CH. <sup>4</sup>Department for Orthopaedic Surgery, Tokai University School of Medicine, Isehara, Kanagawa, JP. <sup>5</sup>AO Research Institute Davos, Davos, CH <sup>6</sup>Clinical Sciences of Companion Animals, Faculty of Veterinary Medicine, Utrecht University, Utrecht, NL

**INTRODUCTION:** Recently, the presence of a “fifth element” of a cell type has been proposed in the intervertebral disc (IVD), apart from nucleus pulposus, annulus fibrosus, cartilaginous endplate and notochordal cells [1]. Here, to isolate the nucleus pulposus progenitor cells (NPPC), we compared two additional cell sorting methods to the original flow cytometry (FACS) protocol [1, 2], i.e. magnetic associated cell sorting (MACS) and a cell-bead/mesh-based system (pluriSelect). The rationale was to explore alternatives that are independent of FACS-equipment, and to follow the direction of more GMP-relevant and milder sorting procedures, such as pluriSelect, to increase cell survival and possibly cell yields.

**METHODS:** Fresh bovine tails (~one year old animals) were obtained from a local abattoir. For each experiment 6-8 coccygeal IVDs were isolated per tail, and cells from 2-3 tails were pooled, resulting in about 20-25 x 10<sup>6</sup> NP cells after overnight mild digestion protocol prior cell sorting. Cells were then labelled with Tie2 antibody (Bioss, clone bs-1300R; Bioss Antibodies, Woburn, MA, USA), identifying the NPPC. Cells were labelled with secondary antibody tagged with Alexa 488 (Molecular Probes) and sorting was sorted on a FACSaria (BD Biosciences) (N=9); for MACS, secondary magnetic anti-rabbit IgG MicroBeads (Miltenyi Biotec) labelled cells were sorted by a magnetic column (N=7); for mesh-sorting, first a construct of primary antibody against Tie2 coupled to pluriBeads was formed, incubated with NP cells and strained through a 30 µm filter (pluriSelect) (N=5). After sorting, Tie2<sup>+</sup> and Tie2<sup>-</sup> cells were subjected to CFU-assay in MethoCult™ methylcellulose medium (StemCell Technologies, inc.) and to two-lineage-differentiation (adipo- and osteogenesis). Due to limited cell availability chondrogenic differentiation was omitted at this stage and is not shown.

**RESULTS:** Cell yield among isolation methods differed widely; FACS presented the highest cell

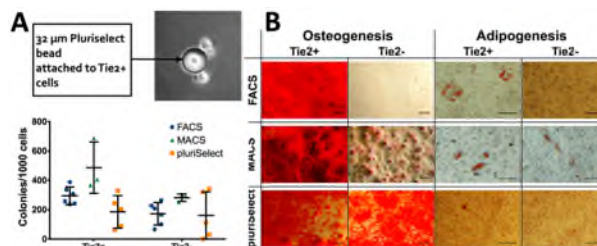


Fig. 1: A. CFU-assay after 7 days of 3D methocult culture. Inlet: Tie2<sup>+</sup> cells attached to pluriSelect bead. B. Osteogenic and adipogenic differentiation of Tie2<sup>+</sup> vs Tie2<sup>-</sup> cells. Scale bar = 100 µm.

yield (mean ± SEM; 5.0 ± 4.0%). Followed by MACS (1.6 ± 2.9%) and pluriSelect (1.1 ± 1.3%). CFU-assay did not show significant changes between the groups. There were more colonies in Tie2<sup>+</sup> than Tie2<sup>-</sup> cells among sorting methods. For FACS (median; Tie2<sup>+</sup> 282.5; Tie2<sup>-</sup> 187.0;  $p < 0.05$ ), MACS (Tie2<sup>+</sup> 527.0; Tie2<sup>-</sup> 296.0,  $p = 0.09$ ) and pluriSelect (Tie2<sup>+</sup> 113.8; Tie2<sup>-</sup> 91.3) were counted (Fig. 1A). Osteogenic and adipogenic differentiation of Tie2<sup>+</sup> and Tie2<sup>-</sup> cells did not result in a clear distinction for MACS and pluriSelect, whereas FACS showed a clear separation between populations (Fig. 1B).

**DISCUSSION & CONCLUSIONS:** Based on the parameters tested, isolation of NPPC is possible with all three methods. However, cell yields differed widely. FACS although most invasive, appears to be the most specific sorting method for these Tie2<sup>+</sup> cells among the tested methods as Tie2<sup>+</sup> cells do not demonstrate osteogenic and adipogenic differentiation. As for cell yield MACS seems to reveal the most, possibly this is due to inclusion of cells expressing Tie2 less strongly.

**REFERENCES:** <sup>1</sup>A. Tekari et al (2016) *Stem Cell Res Ther* 7(1):75. <sup>2</sup>D. Sakai et al (2012) *Nat Commun* 31264.

**ACKNOWLEDGEMENTS:** This project was supported by direct funds from Hansjörg Wyss and HJW medical, US. We thank Eva Roth and Selina Steiner for their assistance.

## **nose to back: compatibility of nasal chondrocytes in a degenerative disc disease environment**

Max H.P. Gay<sup>1,2</sup>, Arne Mehrkens<sup>1</sup>, Michael Rittmann<sup>1</sup>, Andrea Barbero<sup>2</sup>,  
Ivan Martin<sup>2</sup>, Stefan Schaeren<sup>1</sup>

*1. Department of Spinal Surgery, University Hospital Basel, Switzerland*

*2. Department of Biomedicine, University of Basel, University Hospital of Basel, Switzerland*

### **INTRODUCTION:**

Low back pain affects more than 600 million people globally, and intervertebral disc (IVD) degeneration is the most common cause of specific low back pain. Degenerative disc disease is evoked by an imbalance of the anabolic and catabolic processes in resident cells leading to loss of extracellular matrix. Treatments dedicated to restoring IVD homeostasis are greatly in demand, one of which is cell therapy. In recent years, nasal chondrocytes (NCs), have gained a reputation for cartilage tissue regeneration. To assess whether NCs can be considered as an autologous cell source for cell therapy of disc degeneration, we compared the response of NCs to those of mesenchymal stromal cells (MSCs) and articular chondrocytes (ACs), two cells sources presently used in phase two clinical trials for the treatment of DDD.

### **METHODS:**

To implement conditions mimicking the milieu of degenerated IVD in vitro, cells were cultured in low glucose media (1gr/L) in hypoxia (2% O<sub>2</sub>) for 28 days. The media was additionally adjusted to pH 6.8 and/or supplemented with proinflammatory cytokines TNF $\alpha$ , IL1 $\beta$ , and IL6 as is found in the degenerated disc. Furthermore, cells underwent chondrogenic instructional priming due to the addition of TGF $\beta$ 1 for the first seven days of culture.

### **RESULTS:**

Analysis of histology, immunohistochemistry, biochemistry and quantitative rtPCR demonstrated that even though MSCs could be chondrogenically primed, harsh environmental conditions and donor variability play a crucial role in their successful survival and chondrogenesis. ACs were sensitive to priming in that they could accumulate glycosaminoglycans (GAG), however, lack the ability to synthesize Collagen type II (Col2). Commendably, primed NCs produce extra cellular matrix rich in both GAG and Col2 in all nonacidic conditions. Even though an acidic environment reduces GAG accumulation of NCs to the same extent as ACs, the supplementation of the inflammatory cytokines affect the NCs to a lower extent compared to ACs.

### **DISCUSSION & CONCLUSIONS:**

Our data indicate that NCs are more resident to harsher environments than ACs or MSCs upon chondrogenic priming. These findings encourage the assessment that employing NCs in a cell therapy treatment of degenerative disc disease could promote new matrix production in the disc, which could inhibit or delay further disc height loss if not even lead to disc height gain.

## Link N suppresses interleukin-1 $\beta$ induced degradation of human osteoarthritic cartilage by rapidly decreasing NF $\kappa$ B activation

MP Grant<sup>1</sup>, M Alaqeel<sup>1,2</sup>, LM Epure<sup>1</sup>, O L Huk, S Bergeron, J Antoniou<sup>1,2</sup> and F Mwale<sup>1,2</sup>

<sup>1</sup> *Lady Davis Institute for Medical Research, SMBD-Jewish General Hospital, Montreal, QC*

<sup>2</sup> *Department of Surgery, McGill University, Montreal, QC, Canada*

**INTRODUCTION:** Osteoarthritis (OA) is a chronic degenerative joint disorder that affects millions of people. There are currently no therapies that reverse or repair cartilage degradation in OA patients. Link N (DHLSDNVTLTDHRAIH) is a naturally occurring peptide that has been shown to increase both collagen and proteoglycan synthesis in chondrocytes and intervertebral disc cells [1,2]. Recent evidence indicates that Link N activates Smad1/5 signaling in cultured rabbit IVD cells presumably by interacting with the bone morphogenetic protein (BMP) type II receptor [3]; however, whether a similar mechanism exists in chondrocytes remains unknown. In this study we determined whether Link N can stimulate matrix production and reverse degradation of human OA cartilage under inflammatory conditions.

**METHODS:** OA cartilage was obtained from donors undergoing total knee arthroplasty with informed consent. OA cartilage/bone explants and OA chondrocytes were prepared from each donor. Cells were prepared in alginate beads ( $2 \times 10^6$  cells/mL) for gene expression analysis using qPCR. Cells and cartilage explants were exposed to IL-1 $\beta$  (10ng/ml), human Link N (hLN) (1 $\mu$ g/ml) or co-incubated with IL-1 $\beta$ +hLN for 7 and 21 days, respectively. Media was supplemented every three days. Cartilage/bone explants were measured for total glycosaminoglycan (GAG) content (retained and released) using the dimethylmethylene blue (DMMB) assay. Western blotting was performed to determine aggrecan and collagen expression in cartilage tissue. To determine NF $\kappa$ B activation, Western blotting was performed for detection of P-p65 in chondrocytes cultured in 2D following 10 min exposure of IL-1 $\beta$  in the presence of 10, 100, or 1000 ng/mL hLN.

**RESULTS:** Link N significantly decreased in a dose-dependent manner IL-1 $\beta$ -induced NF $\kappa$ B activation in chondrocytes (Fig. 1). Gene expression profiling of matrix proteins indicated that there was a trend towards increased aggrecan and decreased collagen type I expression following hLN and IL-1 $\beta$  co-incubation. HLN significantly

decreased the IL-1 $\beta$ -induced expression of catabolic enzymes MMP3 and MMP13, and the neuronal growth factor NGF ( $p < 0.0001$ ,  $n = 3$ ). In OA cartilage/bone explants, hLN reversed the loss of proteoglycan in cartilage tissue and significantly increased its synthesis whilst in the presence of IL-1 $\beta$ .

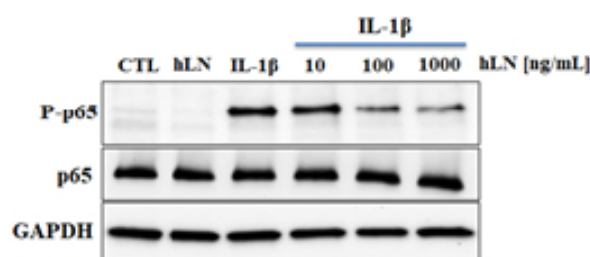


*Fig. 1: Dose-dependent effect of hLN on NF $\kappa$ B activation. Chondrocytes were incubated for 10 min with the indicated concentrations of hLN and IL-1 $\beta$  (10 ng/mL). CTL, DMEM; hLN, 1000 ng/mL. Significance was achieved with 10 ng/mL hLN ( $p < 0.05$ ,  $n = 4$ ) and 100 and 1000 ng/mL hLN ( $p < 0.01$ ,  $n = 4$ ).*

**DISCUSSION & CONCLUSIONS:** Link N stimulated proteoglycan synthesis and decreased MMP expression in OA chondrocytes under inflammatory conditions. One mechanism for Link N in preserving matrix protein synthesis may, in part, be due to its ability in rapidly suppressing IL-1 $\beta$ -induced activation of NF- $\kappa$ B. Further work is needed to determine whether Link N directly inhibits the IL-1 $\beta$  receptor or interferes with NF $\kappa$ B activation through an independent pathway(s).

**REFERENCES:** <sup>1</sup> L.A. McKenna, h. Liu, P.A. Sansom and M.F. Dean (1998) *Arthritis Rheum.* **41**:157-62. <sup>2</sup> F. Mwale, C.N. Demers, A. Petit, P. Roughley, et al. (2003) *J Cell Biochem.* **88**:1202-13. <sup>3</sup> Z. Wang, W.C. Hutton and S.T. Yoon. (2013) *Spine* **38**:1501-7.

**ACKNOWLEDGEMENTS:** This work was supported by the Canadian Institutes of Health Research.

## Establishing a target for annular repair: variations in molecular-level collagen structure of the annulus with circumferential location, radial depth, & disc level

TW Herod<sup>1</sup> & SP Veres<sup>1,2</sup>

<sup>1</sup> [School of Biomedical Engineering, Dalhousie University, Canada.](#) <sup>2</sup> [Division of Engineering, Saint Mary's University, Canada](#)

**INTRODUCTION:** Failure of the lumbar intervertebral disc annulus often occurs preferentially within the posterior region, which contains fewer, thinner lamellae compared to other regions. Beyond these microscopic differences, little is known about the how the annulus' structure varies at the molecular level. In this study we investigated how the thermal stability and crosslinking of collagen molecules in the annulus of lumbar discs changes with circumferential location, radial depth, and disc level.

**METHODS:** Small rectangular bone-annulus-bone samples were cut from the anterior and posterior regions of the lumbar spines of mature ewes. The samples were cut on an oblique sagittal orientation, with their inferior-superior long axis aligned parallel to the collagen fibre orientation at the disc's periphery [1]. Matched-pair anterior-posterior samples were split between two groups: (i) hydrothermal isometric tension (HIT) testing, and (ii) differential scanning calorimetry (DSC). All samples that underwent HIT used a custom apparatus described previously [2]. Briefly, the samples were isometrically mounted longitudinally between a load cell and fixed support, and then submerged in a bath of room temperature distilled, deionized water. A tensile preload of 60 g was applied to each sample. Using a hotplate, the water was then heated to 90°C and maintained at 90°C for 5 hrs. Each sample's denaturation temperature ( $T_d$ ) and half-time of load decay ( $t_{1/2}$ ) were calculated. For samples undergoing DSC, the annulus was first isolated from the sample and then subdivided further to characterize radial depth. Samples were hermetically sealed within DSC pans and tested using a Q200 differential scanning calorimeter. Endotherms were analyzed for onset temperature, peak temperature, full-width at half-maximum, and specific enthalpy of denaturation (based on dry sample weight).

**RESULTS:** Molecular-level collagen structure of the disc annulus varied significantly with circumferential location and radial depth, but not disc level. HIT results revealed that collagen molecules in the posterior annulus showed

significantly greater thermal stability when compared to the anterior (mean  $T_d$  67.3±1.8°C vs. 62.5±1.0°C;  $p<0.0001$ ; Fig 1A). HIT results further indicated that the posterior region contained higher levels of thermally-stable intermolecular collagen crosslinking when compared to the anterior (mean  $t_{1/2}$  34.0±30.8 hrs vs. 9.4±5.8 hrs;  $p=0.0005$ ; Fig 1B). In addition to having greater molecular stability, as shown in HIT, DSC also revealed that collagen molecule stability decreased with increasing radial depth in both the anterior and posterior annulus.

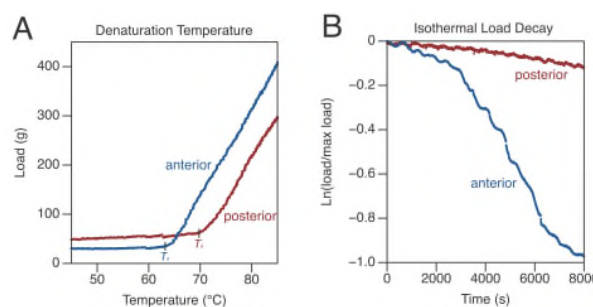


Fig. 1: HIT plots showing load-temperature curves (A) and isothermal load decay-time curves (B) for the anterior and posterior annulus of an L1-2 disc.

**DISCUSSION & CONCLUSIONS:** Significant variations in collagen structure of the lumbar disc annulus exist with both circumferential location and radial depth. Compared to the anterior, the posterior annulus is composed of more robustly structured collagen fibrils. These results have important implications for regenerative therapies designed for annular repair, where there has been recent emphasis in the development of biomaterials that closely mimic the native multi-laminate cross-ply structure of the annulus [3]. Scaffolds that account for the molecular-level variations in collagenous structure may lead to improved regenerative potential.

**REFERENCES:** <sup>1</sup>J.E. Reid et al. (2001) *Clin Biomech* **17**: 312-314. <sup>2</sup>J.M. Lee et al. (1995) *Med Eng Phys* **17(2)**: 115-121. <sup>3</sup>R. McGuire et al. (2016) *J Tis Eng Regen Med* **1**: 1-6.

**ACKNOWLEDGEMENTS:** This work was funded by a grant to SPV from the Nova Scotia Health Research Foundation (NSHRF).



## Functional seated vertical traction for rehydration promotion in lumbar intervertebral discs

ME Johnson<sup>1</sup>, AK Piper<sup>1</sup>, JR Karges<sup>2</sup>

<sup>1</sup>Biomedical Engineering Department, [South Dakota School of Mines & Technology](#), Rapid City, SD, USA <sup>2</sup>Physical Therapy Department, [University of South Dakota](#), Vermillion, SD, USA

**INTRODUCTION:** Prolonged sedentary occupational sitting is ubiquitous due to computer-related work, occupying roughly 80% of an average work day. Little is known about what lumbar intervertebral discs (LIVD) undergo in these long-term compressive forces *in vivo*. In this repetitively prolonged compressed state, LIVD cells may be deprived of vital nutrition, providing avenues for degeneration, priming discs for structural weaknesses.<sup>1</sup> At worst, injured LIVDs can lose pressure and integrity, thus challenged to mechanically perpetuate the nutritional hydration needed for healing. Lying down to recover from gravitational forces permits hydration to resume but is an unacceptable work position. However, reducing gravitational forces typically is one of the few tactics people with low back pain can use to gain relief.<sup>2</sup> Our hypotheses aimed to address LIVD mechanical hydration through a repeat-measures, crossover pilot study to explore functional lumbar vertical traction by: 1) determining LIVD rehydration capabilities (akin to supine lying) by comparing seated spinal height changes (SHC), 2) finding an effective, safe and comfortable dosage of traction, and 3) establishing an individual's functional ability during seated vertical traction application.

**METHODS:** Healthy subjects (n=24, 12 females, 12 males, mean age = 22.6 y,  $\pm 2.9$ ; mean wt = 72.8 kg,  $\pm 12.4$  kg) consented and passed a stadiometer inclusion criterion of 1.3 mm SD over 5 consecutive measurements, out of a maximum of 10, before testing (*Fig 1, Left*). Each of 4 10-min positions were tested with 48 h in between: 1) supine lying (no tasks), 2) 20%, 3) 35%, and 4) 50% body weight removed (BWR) (with computer tasks) via vertical traction apparatus. A custom-built belt with vertical harness pulley system was used to remove body weight (*Fig. 1 Right*). An optional 3-question survey was offered at the end. The overall SHC means were statistically analyzed with a repeat measures ANOVA.

**RESULTS:** Although statistical significance was lacking, 35% BWR dosage was comparable to, and no worse than, the supine lying effectiveness. The

20% and 50% BWR dosages were less favorable to supine. Overall survey results noted subjects felt “very safe”, felt “comfortable” at their upper extremities while working, and “somewhat uncomfortable” around the trunk while in vertical traction.

Table 1. Repeat Measures ANOVA results.

Subjects	Mean SHC (mm)	SD (mm)	P values
Supine	2.979	$\pm 2.992$	-
20% BWR	2.386	$\pm 3.696$	0.439
35% BWR	3.357	$\pm 2.884$	0.300
50% BWR	2.482	$\pm 2.362$	0.552



Fig. 1: Left: Spinal height stadiometry measurement; Right: subject testing in vertical traction harness.

**DISCUSSION & CONCLUSIONS:** The 35% BWR dosage emerged as an interesting equivalent to supine lying in 10 min for disc rehydration, via analysis of SHC. Future analyses in magnetic resonance may elucidate clearer *in vivo* data. Our results provide pathways for future rehabilitation and regenerative exploration to proactively address discogenic issues in prolonged seated occupations.

**REFERENCES:** <sup>1</sup> R. Arun, et al. (2009) *Spine* 34:2324–2337. <sup>2</sup>S.M. Simmerman, et al. (2011) *PM R* 3:447–457.

**ACKNOWLEDGEMENTS:** Midwest Center for Occupational Health & Safety, and CDC/NIOSH Grant #5T42OH008434-12 and sub-award #P005666102

## A method to investigate the glycosignature of the intervertebral disc in health and degeneration

Joyce K<sup>1,2</sup>, Isa ILM<sup>1,2</sup>, Saldova R<sup>3</sup>, Creemers L<sup>4</sup>, Devitt A<sup>5</sup>, Pandit A<sup>2</sup>.

<sup>1</sup>School of Medicine, <sup>2</sup>Centre for Research in Medical Devices, National University of Ireland, Galway. <sup>3</sup>NIBRT GlycoScience group, National Institute for Bioprocessing Research & Training, Dublin. <sup>4</sup>Department of Orthopaedic Surgery, University Medical Centre Utrecht, Netherlands.

<sup>5</sup>Department of Orthopaedic Surgery, Bon Secours Hospital, Galway.

**INTRODUCTION:** Discogenic back pain affects 42% of patients suffering low back pain. Degenerative disc disease is described as failure in cellular response to external stresses leading to physiologic dysfunction and disc destruction. Glycosylation patterns of tissues give insights into the spatially regulated inflammatory/degenerative processes. These glycoconjugates participate in many key biological processes including cell adhesion, molecular trafficking and clearance, receptor activation, signal transduction, and immunomodulation. The glycosylation profile of the intervertebral disc (IVD) has been studied in murine<sup>1</sup>, bovine<sup>2</sup> and ovine<sup>3</sup> models for injury/degeneration. This study aims to develop a method to investigate the changes in glycosylation that occur in degeneration in human IVD (hIVD) tissue to establish a glyco-phenotype for health and disease.

**METHODS:** Glycosylation motifs (Sialylation, GlcNAcylation, mannosylation and fucosylation) in healthy (n=2) and degenerated (n=2) hIVD samples, collected during autopsy at the UMC Utrecht, The Netherlands (Local Medical Ethical Committee [METC] number 12-364, were compared using lectin histochemistry. The N-glycan profile of degenerated hIVD samples has been characterised by UPLC-MS.

**RESULTS:** Healthy and degenerated human discs present distinct glycosylation trends in AF and NP tissue with altered lectin binding. These findings are consistent with previous studies in an injury model of the IVD in murine/bovine tissue and IVD degeneration in an ovine model. Both injured and degenerated IVD express an increase in glycosylation sites versus healthy tissue.

The N-glycan profile of degenerated hIVD is distinct from other cited glycan profiles<sup>4</sup>. The increase in sialylation in lectin histochemistry reflects the hypersialylated glycoprofile of the degenerated hIVD established by UPLC-MS.

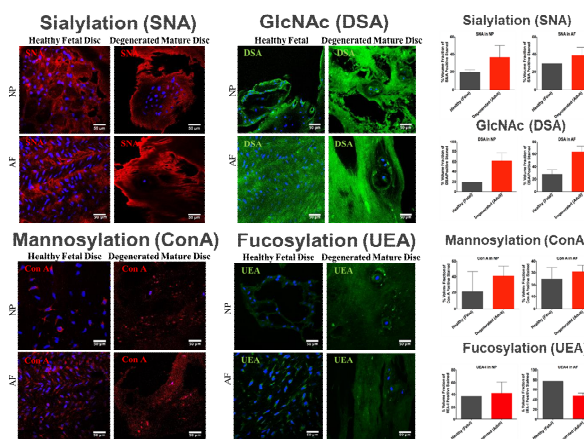


*Fig.1 Glycosylation motifs in healthy and degenerated IVD tissue using lectin histochemistry. Sialylation, GlcNAcylation and mannosylation are increased in degeneration while fucosylation is shown to decrease.*

**DISCUSSION & CONCLUSIONS:** This pilot study is a preliminary validation of previous animal models, demonstrating similar changes in the hIVD glycoprofile. The trends observed in lectin histochemistry can be correlated with the n-glycan profile. This method of glycan analysis using UPLC-MS of hIVD tissue towards maturation and degeneration will establish tissue glyco-phenotype for both healthy and diseased state, creating a glycomic standard when testing the efficacy of regenerative therapies *in vivo*.

**REFERENCES:** <sup>1</sup>I.L.M. Isa *et al.* (2018). *Science Advances* **4**: eaaq0597. <sup>2</sup>Z. Kazezian *et al.* (2017) *Acta Biomaterialia*. **52**: 118-129. <sup>3</sup>E. Collin *et al.* (2016). *Scientific Reports*, **6**(1) <sup>4</sup>R. Saldova *et al.* (2014). *Journal of Proteome Research*, **13**(5):2314-2327.

**ACKNOWLEDGEMENTS:** Funding: Science Foundation Ireland (SFI) and the European Regional Development Fund (Grant Number 13/RC/2073).

## 3D-Plotting of human chondrocytes in alginate-methyl cellulose hydrogels – towards design and fabrication of individualized cartilage substitutes

D Kilian<sup>1</sup>, T Ahlfeld<sup>1</sup>, AR Akkineni<sup>1</sup>, M Gelinsky<sup>1</sup>, A Lode<sup>1</sup>

<sup>1</sup> [Centre for Translational Bone, Joint and Soft Tissue Research](#), Faculty of Medicine Carl Gustav Carus, Technische Universität Dresden, Germany

**INTRODUCTION:** For the individualization of patient-specific substitutes and 3D models, additive manufacturing techniques like 3D plotting offer great potential. Volumetric, multiphasic, cell-laden structures of a designed geometry can be manufactured with a spatially defined distribution of cells. The aim of this study was the additive production of hydrogel scaffolds containing encapsulated functional human chondrocytes (hCh).

**METHODS:** 3D plotting of a cell-laden hydrogel based on 3% sodium alginate and 9% methyl cellulose<sup>1</sup> after encapsulation of primary hCh ( $5.0 \times 10^6/g$ ) was performed using BioScaffolder 3.1 (GeSiM, Großkrummenhain, GER). Cells were cultivated inside volumetric constructs for 28 days, treated with expansion medium (DMEM, 10% FCS) and differentiation medium containing 10 ng/ml TGF- $\beta$ 3, respectively. Cell behaviour of differentiated and non-differentiated cells was analysed regarding cell viability, cytoskeletal morphology, proliferative and chondrogenic potential, via production of sulphated glycosaminoglycans (sGAG) and collagen II, as well as gene expression of respective markers. Co-printing<sup>2,3</sup> of chondrocyte-laden hydrogel and bone interface-mimicking pasty calcium phosphate cement (CPC; INNOTERE, Radebeul, GER) was employed towards an application for multiphasic osteochondral structures.

**RESULTS:** Viability of cells was determined around 60% after the printing process. After cultivation for 21 d, proliferation of cells was detected. In dedifferentiated state, cells tended to aggregate and spread at the strand surface. Maintenance of chondrogenic potential of differentiated cells inside the strands was proven via quantified production of sGAG and collagen II after 21 d of 3D culture. An actual bioprinted multiphasic construct as a model for osteochondral substitutes was designed and realised.

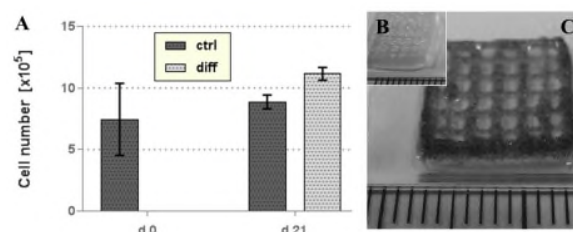


Fig. 1: 3D plotted macroporous scaffolds laden with hCh. A: Cell numbers inside one construct via QuantiFluor® DNA quantification assay ( $n = 3$ ), initially and after 21 days in differentiation (diff) and expansion (ctrl) culture condition. B, C: MTT staining of an empty control scaffold (B) vs. metabolically active differentiated hCh inside a scaffold at day 28 (C); scale in mm.

### DISCUSSION & CONCLUSIONS:

The provided alginate-based hydrogel environment does not offer adhesive properties. However, this characteristic is not required for differentiated chondrocytes to survive and function. The aggregation and adhesion of non-differentiated cells at the strand surface after several weeks of cultivation could be used towards biphasic models for subchondral and osteochondral structures. For both monophasic and biphasic constructs, alginate-methyl cellulose hydrogels provide a promising system for volumetric individualized structures as patient-specific 3D cartilage models.

**REFERENCES:** <sup>1</sup> K. Schütz, A. Placht, B. Paul, S. Brüggemeier, M. Gelinsky, A. Lode (2017) *J Tissue Eng Regen Med* **11**:1574-87. <sup>2</sup> D. Kilian, T. Ahlfeld, A.R. Akkineni, A. Lode and M. Gelinsky (2017) *MRS Bulletin* **42**: 585-592 <sup>3</sup> T. Ahlfeld, A. R. Akkineni, Y. Förster, T. Köhler, S. Knaack, M. Gelinsky, A. Lode (2017), *Ann Biomed Eng* **45**, 224-236

**ACKNOWLEDGEMENTS:** The authors would like to thank the European Social Fund *ESF* and the Free State of Saxony for financial support of this project in the course of the young researchers group *IndivImp* at TU Dresden.



## Synovium-derived stem cells as a potential cell source for cartilage repair – the role of mechanical stimulation

V Korch<sup>1,2</sup>, A Armiento<sup>1</sup>, M Stoddart<sup>1,2</sup>, H Schmal<sup>3</sup>, NP Südkamp<sup>2</sup>, EJ Kubosch<sup>2</sup>

<sup>1</sup>AO Research Institute Davos, AO Foundation, Davos, CH; <sup>2</sup>Department of Orthopedics and Trauma Surgery, Albert-Ludwigs University Medical Center Freiburg, Freiburg, DE; <sup>3</sup>Department of Orthopaedics and Traumatology, Odense University Hospital and Department of Clinical Research, University of Southern Denmark, Odense, DK

**INTRODUCTION:** The progress to find new cell-based therapies for articular cartilage repair is of major interest to orthopaedic research. It has been shown the synovial membrane contains mesenchymal stem cells (MSCs) with high chondrogenic potential [1]. These synovium derived stem cells (SDSCs) “represent a promising cell source for cartilage repair approaches based upon their chondrogenic potential” [1]. Therefore, we investigated if human synovium derived stem cells (hSDSCs) are mechanoresponsive to gain knowledge on the effects of physical stimulation.

**METHODS:** Biopsies of synovial membrane were obtained aseptically from human knee joints (n=3, 23-43 years) during surgery for knee injuries with full ethical approval. hSDSCs were expanded in DMEM, 10% FBS and 1% Penicillin/Streptomycin. Mechanical stimulation was conducted after 5 ng/ml basic fibroblast growth factor (bFGF) priming in monolayer till P2 or P3. Four experimental groups were formed:

- Loading group (1h of load /day, 5 days /week, with compression and shear force at 1 Hz)
- Free swelling static No-TGF-β1 group
- Free swelling static 1ng-TGF-β1 group
- Free swelling static 10ng-TGF-β1 group

5'000'000 hSDSCs into each 3D scaffolds out of fibrin/ polyurethane and 6 scaffolds per group, for 28 days. RT-PCR, GAG/DNA, TGF-β1 and nitric oxide production in the media were all measured, and Histology was performed on day 28.

**RESULTS:** All donors responded to some extent to 10 ng TGF-β1 stimulation as assessed by PCR and GAG quantification. While mechanical stimulation alone increased SOX9 expression, no increases in collagen II or aggrecan were seen. Histological evaluation matched the PCR data. Fig. 1 shows the proteoglycan (in red) and collagen (in green) deposition (donor 114).

Latent and active TGF-β1 quantification shows the same donor-variance as seen in the histology of the samples. However, cells under mechanical load

produce TGF-β1 close to 1ng/ml. Also, nitrite production was increased in the mechanical stimulated group.

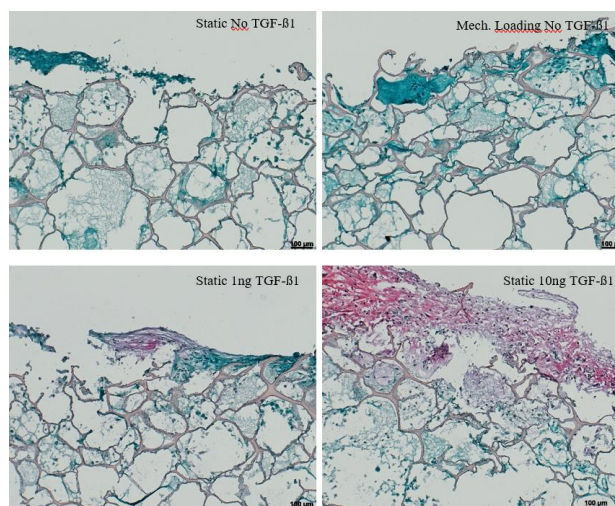


Fig. 1: Images of PU scaffolds, donor 114 after 28 days in static and mechanical load condition. Safranin-O/ Fast Green staining

**DISCUSSION & CONCLUSIONS:** Mechanical stimulation, compression and shear, provides an early stimulation to hSDSCs similarly to that previously seen with bone marrow derived MSCs [2]. Under these conditions, mechanical stimulation alone is not sufficient to trigger upregulation of matrix synthesis, suggesting that further improvements are required. As with bone marrow MSCs, multiaxial load also induces production of nitric oxide and TGF-β1 [3]. These substances could become markers for rehabilitation progress after cartilage damage. However, donor variation is an important subject that should be further investigated.

**REFERENCES:** <sup>1</sup> E.J. Kubosch, G. Lang, D. Fürst, et al., Current Stem Cell Research & Therapy, Vol 12, No. 00 (2017), 1-11. <sup>2</sup> Z. Li, L. Kupcsik, S.J. Yao, et al., Journal of Cellular and Molecular Medicine, Vol 14, No 6A (2010), 1338-1346. <sup>3</sup> O.F. Gardner, N. Fahy, M. Alini, M.J. Stoddart, Eur Cell Mater, Vol 31 (2016) 221-235.



## BMP2 and TGF- $\beta$ differently cooperate during synovial derived stem cell chondrogenesis in a dexamethasone dependant manner

N Kovermann<sup>1,2\*</sup>, V Basoli<sup>1\*</sup>, E Della Bella<sup>1</sup>, M Alini<sup>1</sup>, C Lischer<sup>2</sup>, H Schmal<sup>3</sup>, MJ Stoddart<sup>1,4</sup> and EJ Kubosch<sup>4</sup>

<sup>1</sup> [AO Research Institute](#), AO Foundation, Davos, CH, <sup>2</sup>*Equine Clinic, Free University of Berlin, Berlin, DE*, <sup>3</sup>*Department of Orthopaedics and Traumatology, Odense University Hospital and Department of Clinical Research, University of Southern Denmark Odense, DK*, <sup>4</sup>*Department of Orthopedics and Trauma Surgery, Albert-Ludwigs University Medical Center Freiburg, Freiburg, DE*. \*Equal first author

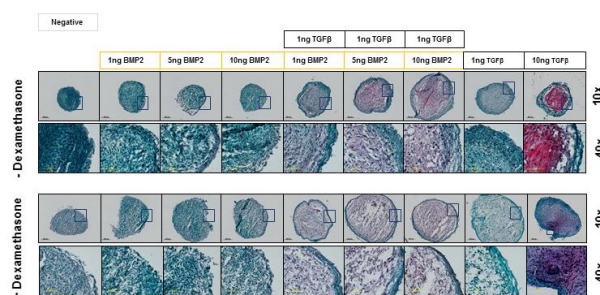
**INTRODUCTION:** Synovium derived stem cells (SDSC) are considered a suitable candidate for the repair of cartilage due to the simplicity of isolation and their chondrogenic potential [1]. However, a differentiation protocol that can guarantee a high commitment for SDSC has not yet been established. Here, we aimed to investigate how SDSCs respond to varying concentrations, and combinations, of BMP2 and TGF- $\beta$ 1. Furthermore, the effect of dexamethasone was investigated.

### METHODS:

Chondrogenic differentiation was induced in SDSC (n= 4, obtained with full ethic consent) using 1 or 10 ng/ml TGF- $\beta$ 1 alone; BMP2 at 1, 5, 10 ng/ml alone or a double combination of 1 ng/ml TGF- $\beta$ 1 plus 1, 5, 10 ng/ml BMP2; all the groups were cultured in the presence (+Dex) or absence (-Dex) of 100nM dexamethasone for 21 days. Gene expression analysis was performed on Col2, ACAN, Col10, MMP13, Sox9, Runx2, SP7 and PPARG, after 21 days. GAG quantification and Histology using Safranin-O and Col2 protein expression by immunohistochemistry were analyzed after 21 Days, as well as Von Kossa staining for calcium deposition.

**RESULTS:** -Dex media upregulated gene expression of Sox9 and Col2 in all groups with 5 and 10 ng/ml BMP2 (alone or in combination) when compared to +Dex. While ACAN expression was upregulated in all -Dex media. However, Col10 expression was higher in +Dex medium containing TGF- $\beta$ 1 (alone or in combination), suggesting that dexamethasone is involved in the modulation of hypertrophy. SP7 (bone) was upregulated in groups containing TGF- $\beta$ 1 but not in BMP2 only groups, while PPARG (adipose) was

downregulated in all TGF- $\beta$ 1 containing groups, an effect strengthened by the absence of Dex. Histological and biochemical evaluation confirmed the increase of GAG production in -Dex medium. Von Kossa staining was not positive for mineralization.



### DISCUSSION & CONCLUSIONS:

Our results suggest that the absence of Dexamethasone promotes the activation of genes involved in chondrogenesis, nevertheless the presence of Dexamethasone modulates genes involved in hypertrophy. Interestingly, we found that the synergistic effect of combination TGF- $\beta$ 1 and BMP2 in dexamethasone free medium positively modulated SDSC chondrogenic commitment with higher Col2 and ACAN expression but lower ColX relative to +Dex, suggesting that this combination can be useful to induce a stable chondrogenic differentiation. The synergistic effect of TGF- $\beta$ 1 and BMP2 has also been seen in adipose derived MSCs. [2]

### REFERENCES:

1. Kubosch, E.J., et al., *The Potential for Synovium-derived Stem Cells in Cartilage Repair*. Current stem cell research & therapy, 2017.13(3):174-184.
2. Mehlhorn, A. T. et al., *Differential effects of BMP2 and TGF $\beta$ 1 on chondrogenic differentiation of adipose derived stem cells*. Cell Prolif. 2007, 40, 809-823

## Bizonal cartilage constructs developing bottom zone–restricted in vivo mineralization

E Kunisch, AK Knauf, E Hesse, F Bothe, S Diederichs, W Richter

Research Centre for Experimental Orthopaedics, Heidelberg University Hospital, Schlierbacher Landstr. 200a, 69118 Heidelberg, Germany

**INTRODUCTION:** Regenerated cartilage tissue lacks the typical zonal structure of healthy cartilage deemed important for proper function. Engineered zonal cartilage constructs with a hyaline-like upper zone and a calcified bottom zone appear promising for improved cartilage regeneration. Objective of the present study was to develop bizonal human cartilage constructs in which in vivo mineralization is self-restricted to the bottom zone.

**METHODS:** For the calcified cartilage zone, a biomaterial-free cell disc was generated by self-assembling of porcine mesenchymal stem cells (MSCs) in transwell culture in the presence of chondrogenic medium over 3 weeks. In vitro mineralization capacity of the pMSC cell discs was assessed in four different mineralization media for up to 8 weeks. For preparation of zonal cartilage constructs, non-mineralized cell discs were overlaid with a chondrocyte-seeded starPEG or fibrin gel to select the best design for upper zone development. Freshly prepared constructs were immediately implanted into subcutaneous pouches of immuno-deficient mice to compare in vivo development. After 6 weeks in vivo, matrix deposition and mineralization were analyzed by  $\mu$ CT and histology (safranin O, collagen II, collagen X, alkaline phosphatase, and alizarin red staining).

**RESULTS:** After 3 weeks of chondrogenic differentiation, pMSCs formed stable non-mineralized cell discs which were rich in proteoglycans and collagen type II. Culture of cell discs with four distinct mineralization media for up to 8 weeks supported calcification when  $\beta$ -glycerophosphate was present. Proteoglycans were retained only in media containing insulin. To test whether in vivo mineralization is restricted to the bottom zone, freshly prepared zonal constructs were subcutaneously implanted into immuno-deficient mice. After 6 weeks in vivo, both construct types were positive for collagen type II

and aggrecan in the upper zone and contained a mineralized bottom zone (Fig. 1A). However, solely for zonal starPEG constructs, tissue volume of the upper zone remained high (Fig. 1B) and alkaline phosphatase, alizarin red, and collagen-type X staining were restricted to the bottom zone.

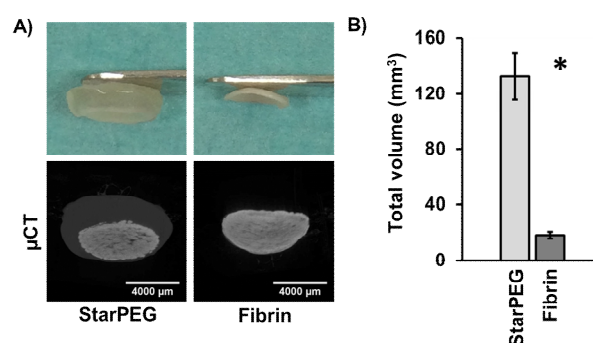


*Fig. 1. Comparison of in vivo outcome of zonal constructs made of a bottom pMSC cell disc and a starPEG or fibrin gel upper zone. A) At 6 weeks in vivo both construct types had a mineralized bottom zone. B) Solely for starPEG constructs, tissue volume of the upper zone remained high (n = 9 from 3 donors; \* p < 0.05 Mann-Whitney-U-test versus starPEG).*

**DISCUSSION & CONCLUSIONS:** Both construct types allowed redifferentiation of chondrocytes and formation of a cartilage-matrix-rich zonal construct with a MSC-derived mineralization zone. However, only zonal constructs made with starPEG showed an ample upper zone and a self-restricted mineralization and hypertrophic marker expression to the bottom zone. Successful generation of bizonal cartilage constructs with a self-restricted mineralization of the bottom zone should now be applied for proper integration and regeneration in an orthotopic cartilage defect model.

## Adrenoceptor expression in the intervertebral disc

J Kupka, A Meurer, K El Bagdadi, I Schaible, F Zaucke, Z Jenei-Lanzl, M Rickert

Dr. Rolf M. Schwiete Research Unit for Osteoarthritis, Orthopaedic University Hospital  
Friedrichsheim gGmbH, Frankfurt/Main, Germany

**INTRODUCTION:** The etiology of IVD degeneration (IVDD) is multifactorial: age, gender, environmental factors or mechanical loading are involved in the pathogenesis [1]. Recent studies revealed that norepinephrine (NE) – a major neurotransmitter of the sympathetic nervous system - plays a role in the insufficient regeneration of articular cartilage tissue [2]. It is known that healthy and degenerating IVDs are innervated by sympathetic nerve fibers [3]. However, adrenoceptor (AR) expression in IVD tissue has never been analyzed systematically. Therefore, the aim of this study was to investigate adrenoceptor expression in degenerated IVD tissue.

**METHODS:** Samples of degenerated IVDs were collected from patients undergoing spondylodesis. The degree of degeneration in anonymized samples was unknown and the ratio of annulus fibrosus and nucleus pulposus was variable. Expression of all known AR subtypes was evaluated by PCR and immunoblot in IVD tissue homogenates and in cells migrated out of the tissue. Collagen IX deficient (Col IX  $-/-$ ) mice develop an early spontaneous disc degeneration [4]. Therefore, we stained spine sections of 10 months old wildtype (WT, C57BL/6N) and Col IX  $-/-$  mice immunohistochemically for ARs to compare healthy and degenerating IVD tissue. DMMB staining was used to visualize proteoglycans and tissue structure.

**RESULTS:** In tissue homogenates,  $\alpha$ 1A,  $\alpha$ 2A,  $\alpha$ 2C,  $\beta$ 1, and  $\beta$ 2 ARs were detected (Fig. 1A), whereas IVD cells after 14 day in culture expressed predominantly  $\alpha$ 1B,  $\alpha$ 2A,  $\alpha$ 2B, and  $\beta$ 2 ARs (Fig. 1B). These results were partly confirmed at the protein level by immunoblot.

In healthy IVDs of WT mice,  $\beta$ 2 AR was detected in the inner and outer annulus tissue, whereas  $\beta$ 2 AR was not detectable in Col IX  $-/-$  discs. In the inner annulus of Col IX  $-/-$ , but not WT IVDs,  $\alpha$ 2a AR was strongly expressed. Moreover, weak  $\alpha$ 2C AR staining was observed in the outer annulus of Col IX  $-/-$  IVDs but not in WT discs (Fig. 1C).

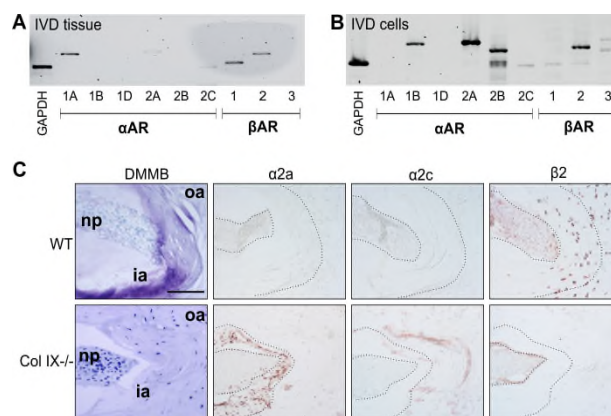


Fig. 1: AR expression profile in human IVD tissue (A) and in isolated IVD cells (B). DMMB and AR stainings in murine IVDs (C). np, nucleus pulposus; ia, inner annulus; oa, outer annulus; bar, 100  $\mu$ m

**DISCUSSION & CONCLUSIONS:** For the first time, the existence of ARs and the differential expression of specific subtypes in healthy and degenerated IVD were demonstrated suggesting that the sympathetic might play a role in IVDD. Further studies will characterize its mechanistic contribution and thereby help to develop novel therapy options IVDD therapy.

**REFERENCES:** <sup>1</sup>Martirosyan NL, Patel AA, Carotenuto A et al. (2016) *Front surg.* 2016;3:59. <sup>2</sup>Grässel S, Straub RH, Jenei-Lanzl Z (2017) *The Sensory and Sympathetic Nervous System in Cartilage Physiology and Pathophysiology in Cartilage: Volume 2: Pathophysiology*, Cham: Springer International Publishing p. 191-227. <sup>3</sup>Tomaszewski KA, Saganiak K, Gladysz T, Walocha JA (2015) *Folia Morphol (Warsz)* 74(2):157-68. <sup>4</sup>Kamper M, Hamann N, Prein C et al. (2016) *Matrix biol* 49:132-43.

**ACKNOWLEDGEMENTS:** This study was supported by the DFG grant JE 642/4-1.

## Validation of anti-inflammatory and regenerative drug therapy in an intervertebral disc organ culture model

G Lang<sup>2</sup>, Y Gehlen<sup>1,2</sup>, F Heizmann<sup>1,2</sup>, D Kubosch<sup>2</sup>, NP Südkamp<sup>2</sup>, M Alini<sup>1</sup>, S Grad<sup>1</sup>, Z. Li<sup>1</sup>

<sup>1</sup> *AO Research Institute Davos, AO Foundation, Davos, CH.* <sup>2</sup> *Department of Orthopedics and Trauma Surgery, University Hospital Medical Center Freiburg, Freiburg, Germany*

**INTRODUCTION:** Disease modifying anti-rheumatic drugs (DMARDs) have demonstrated their potential in the treatment of degenerative disc disease (DDD) by relieving pain. However, the underlying mechanism is not clear yet. The present study investigates the effects of the TNF- $\alpha$  inhibitor Etanercept and the selective JAK3-inhibitor Tofacitinib towards inflammation and degeneration in an *ex vivo* intervertebral disc (IVD) organ culture model.

**METHODS:** Part I: Bovine caudal IVDs were cultured within a bioreactor for 4 or 11 days. The control group (Phy) was cultured under physiological loading (0.02-0.2 MPa; 0.2 Hz; 2h/day) and high glucose (4.5 g/L) medium. In the degenerative group (Deg), detrimental loading (0.32-0.5 MPa; 5 Hz; 2h/day) and low glucose (2 g/L) medium was applied to mimic the condition of abnormal mechanical stress and limited nutrition. TNF- $\alpha$  was injected into the nucleus pulposus (NP) (100 ng/IVD) as proinflammatory trigger. Expression of inflammatory, anabolic and catabolic genes, release of nitric oxide (NO), cytokines and glycosaminoglycan (GAG), and cell viability were assessed.

Part II: Etanercept (3.5 mg/70  $\mu$ L/IVD) or phosphate buffered saline (PBS) (70  $\mu$ L/ IVD) were injected into the IVD cultured under Deg+TNF- $\alpha$  conditions. Tofacitinib citrate (2.5  $\mu$ g/mL) or PBS was added daily into the culture medium to simulate a systemic application of the drug. After 4 days, the effect of Etanercept and Tofacitinib on gene expression and molecule release from IVD cells was analyzed. One-way ANOVA or Kruskal-Wallis tests were used to determine statistical differences (n=6-8).

**RESULTS:** Part I: TNF- $\alpha$  injection combined with detrimental loading and low glucose medium significantly upregulated the expression of interleukin (IL)-1 $\beta$ , IL-6 and IL-8 genes in cells of the organ cultured IVD; moreover, NO and IL-8 release from IVD was increased, indicating a proinflammatory effect (all p<0.05 vs. Phy). The combined initiators also significantly up-regulated matrix metalloproteinase 1 (MMP-1) gene

expression, downregulated gene expression of type I collagen in annulus fibrosus and type II collagen in NP (p<0.05 vs. Phy). Furthermore, the combined treatment induced a degradative reaction, as indicated by markedly higher GAG release into conditioned medium. Deg culture condition with/without TNF- $\alpha$  reduced cell viability to around 40% in AF and 60% in NP after 11 days (p<0.05 vs. Phy).

Part II: Degenerative culture conditions and TNF- $\alpha$  injection upregulated the expression of catabolic enzyme MMP-1, MMP-3, proinflammatory cytokines IL-1 $\beta$ , IL-6, and IL-8, cyclooxygenase-2 (COX-2); whereas Etanercept and Tofacitinib partially reduced these effects. Compared with the Deg+TNF- $\alpha$  group, both drug groups partially reduced the release of GAG. Etanercept partially diminished the release of NO compared with Deg+TNF- $\alpha$  group, whereas Tofacitinib had no effect on NO release.

**DISCUSSION & CONCLUSIONS:** The combination of detrimental dynamic loading, nutrient deficiency and intradiscal TNF- $\alpha$  injection could synergistically simulate the proinflammatory and degenerative condition within a degenerative IVD, demonstrating the potential of our whole IVD organ culture model for testing of anti-inflammatory or regenerative therapies. Etanercept and Tofacitinib showed the ability to slow down the degenerative response and reduce inflammation in the organ culture model, though combined anti-inflammatory and anabolic treatment may be required to completely halt or reverse the degenerative process.

**ACKNOWLEDGEMENTS:** This study is funded by the Foundation for the Promotion of Alternate and Complementary Methods to Reduce Animal Testing (SET).



## A Decellularized Auricular Cartilage Scaffold for Articular Cartilage Repair Recellularized by Removing Elastin Fibres

J. Lehmann<sup>1,2</sup>, C. Schneider<sup>3,4</sup>, R. Narcisi<sup>5</sup>, J.L.M. Koevoet<sup>1</sup>, K. S. Stok<sup>6,7</sup>, S. Wolbank<sup>3,4</sup>, H. Redl<sup>3,4</sup>, D. ten Berge<sup>2</sup>, S. Nürnberger<sup>3,4,7,8,9</sup>, G.J. van Osch<sup>1,5</sup>

<sup>1</sup> Dept. Otorhinolaryngology and Head and Neck Surgery, Erasmus MC, Rotterdam, NL; <sup>2</sup> Dept. Cell Biology, Erasmus MC, Rotterdam, NL; <sup>3</sup> Ludwig Boltzmann Institute, Vienna, AUT; <sup>4</sup> Austrian Cluster for Tissue Regeneration, Vienna, AUT; <sup>5</sup> Dept. Orthopaedics, Erasmus MC, Rotterdam, NL; <sup>6</sup> Institute for Biomechanics, ETH Zurich, Zurich, CH; <sup>7</sup> Dept. Biomedical Engineering, Parkville, Victoria, AUS; <sup>8</sup> Bernhard Gottlieb University Clinic of Dentistry, Vienna, AUT; <sup>9</sup> School of Dentistry Medical University of Vienna, Vienna, AUT

**INTRODUCTION:** Repair of large cartilage defects requires a scaffold that is resistant to biomechanical loading and allows cells to infiltrate. However, there are cues in the cartilage extracellular matrix that are difficult to reproduce in the lab, thought to guide cell behaviour<sup>1</sup>. Hence, many protocols have been developed to generate non-immunogenic scaffolds by decellularizing allogeneic or xenogeneic cartilage matrices. Critically, the dense collagen matrix in cartilage however prohibits recellularization.

**METHODS:** Cartilage was harvested from human and bovine ears, freeze-thawed and treated with porcine pancreatic elastase. The decellularized cartilage was then seeded with human bone marrow derived mesenchymal stem cells or articular chondrocytes. *In vitro*, the seeded cells were chondrogenically differentiated using a chemically defined media mainly consisting in TGF $\beta$ 1, ascorbic acid and dexamethasone. As a model for articular cartilage repair *in vivo*, we used our previously developed system consisting in an empty or seeded scaffolds placed into a 6-mm diameter osteochondral defect<sup>2</sup> generated in bovine metacarpophalangeal joint biopsies that were then transplanted subcutaneously into immunocompromised mice for up to 10 weeks.

**RESULTS:** Treating allogeneic and xenogeneic auricular cartilage with the enzyme elastase permits decellularization and subsequent recellularization of cartilage. Treatment with elastase degraded the elastic fibre bundles traversing auricular cartilage, creating channels. The collagen network remained intact, whereas glycosaminoglycans were mostly removed. Via the generated channels, the elastase-treated cartilage was rapidly invaded by cells (Fig. 1A), which upon differentiation formed new cartilage matrix rich in glycosaminoglycans. Interestingly decellularization and recellularization process did

not compromise the shape of our scaffold. (Fig. 1 A-B). Of note, after restoration of glycosaminoglycans, recellularized cartilage has similar mechanical properties compared to the native tissue. Decellularized scaffolds implants in large osteochondral defects *in vivo*, showed that bone marrow cells and local chondrocytes invaded the elastase-treated cartilage and formed cartilage *de novo* (Fig. 1C), resulting in closure of the defect (Fig. 1D).

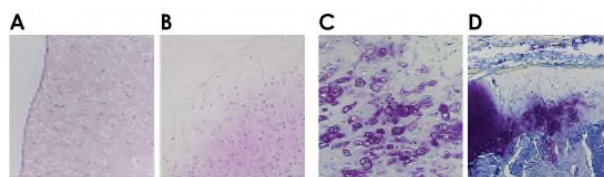


Fig. 1: Elastase-treated bovine auricular cartilage (A) recellularized with human bone marrow derived mesenchymal stem cells 3 days after seeding (H&E staining), (B) after 35 days of differentiation *in vitro* (Thionin staining) or (C,D) 4 weeks after implantation into an osteochondral defect (Thionin staining).

**DISCUSSION & CONCLUSIONS:** This method using elastase allows recellularization of cartilage without destroying its collagen network. This not only enables repair of large cartilage defects, but also permits investigation of chondrogenesis in a near-native architecture.

**REFERENCES:** <sup>1</sup> A.R. Armiento, M.J. Stoddart, M. Alini, D. Eglin. (2018) *Acta Biomater.* 65, 1–20 (2018). <sup>2</sup> M.L. de Vries-van Melle, E.W. Mandl, N. Kops, J.L.M. Koevoet, J.A.N. Verhaar, G.J.V.M. van Osch. (2012) *Tissue Eng. Part C Methods*, 18(1).

**ACKNOWLEDGEMENTS:** This work was supported by the FFG Bridge grant (#842455).

## **SDF-1 mediated-mesenchymal stem cells recruitment: a new perspective for intervertebral disc degeneration treatment**

*C Leite Pereira<sup>1,2</sup>, C Cunha<sup>1,2</sup>, GQ Teixeira<sup>1,2</sup>, M D'Este<sup>4</sup>, D Eglin<sup>4</sup>, M Alini<sup>4</sup>, S Grad<sup>4</sup>, MA Barbosa<sup>1,2,3</sup> & RM Gonçalves<sup>1,2</sup>*

<sup>1</sup>[IBS](#) - Instituto de Investigação e Inovação em Saúde (IBS), UP, Portugal, <sup>2</sup>[INEB](#) - Instituto de Engenharia Biomédica, Universidade do Porto, Portugal, <sup>3</sup>[ICBAS](#) - Instituto de Ciências Biomédicas Abel Salazar, Universidade do Porto, Portugal, <sup>4</sup>[AO Research Institute Davos](#), Switzerland

**INTRODUCTION:** Intervertebral disc (IVD) degeneration is characterized by loss of water content resulting from the degradation of native matrix components and an altered cell function. Repopulation of the IVD with healthy new cells that can replenish the lost matrix would be a major breakthrough in disc degeneration treatment. Simulated-degenerating IVDs were shown to release chemoattractors that can recruit human mesenchymal stem/stromal cells (hMSCs)<sup>1</sup>. *Ex vivo*, hMSCs recruitment from the cartilaginous endplates (CEP) towards IVD was enhanced by the injection of stromal cell derived factor-1 (SDF-1)-hyaluronan-poly(N-isopropylacrylamide) (HAP)-based hydrogel (HAP-SDF)<sup>2</sup>. Here we evaluate the potential of migrating MSCs stimulated by SDF-1-containing hydrogel to repair/regenerate degenerated IVD using two models: 1) an *ex vivo* bovine model of nucleotomized IVD<sup>2</sup>; and 2) an *in vivo* model of IVD caudal lesion in rat<sup>3</sup>.

**METHODS:** *Ex vivo*, human bone marrow-derived MSC (hMSC) were seeded on top of the CEP of bovine IVDs<sup>1,2</sup>. The following groups were compared at distinct time points (7, 14, 21 days): 1) Intact IVDs; 2) Cavity (C) IVDs; 3) C+hMSC; 4) C+HAP-SDF+hMSC and 5) C+HAP-SDF. Metabolic activity, DNA content and ECM were assessed. *In vivo*, IVDs of the rat tail were punctured dorsally. Right after lesion, discs remained empty, or were injected with HAP, or HAP-SDF. 24h after lesion, rat MSCs (P5, 2×10<sup>6</sup> cells) CM-Dil labeled were injected intravenously into the lateral tail vein using a 24-gauge catheter. Six groups: 1) Lesion (L); 2) L+HAP; 3) L+HAP-SDF; 4) L+MSCs; 5) L+HAP+MSCs; 6) L+HAP-SDF+MSCs; were analysed in what concerns to gene expression, cell migration towards the IVD and other organs (e.g.: lungs) and inflammatory response to treatment.

**RESULTS:** *Ex vivo*, CM-Dil labeled hMSC migrated from CEP towards the IVD and remained viable, being detectable even after 21 days in

culture. The presence of HAP-SDF triggered the recruitment of a higher number of hMSCs at earlier time points (7 and 14d). hMSCs-SDF-mediated recruitment was shown to accelerate and increase Col type II expression at early time points (7 and 14d) while aggrecan was increased in the presence of hMSCs, independently of the number of cells recruited and only after 21d. The increase in Col type II seems to be associated with earlier increase of bFGF.

*In vivo*, low numbers of rMSCs were detected in the lungs of the animals, 2 wks after lesion. rMSCs migration towards the degenerated disc, as well as their effect in tissue ECM, is currently being analyzed. rMSCs transplantation increased systemic levels of IL-1 $\beta$ , which were reduced in the presence of HAP. On the other hand, groups containing SDF1 (w/and w/o rMSCs), had higher levels of VEGF. At the gene expression level, the groups containing SDF1 had an upregulation of MMP-3 and CXCR4 was upregulated in animals injected with HAP-SDF1+rMSCs transplantation.

**DISCUSSION & CONCLUSIONS:** This work demonstrates that hMSC migration through CEP can be an alternative route for hMSC-based therapies and suggests that a chemoattractor-delivery system may accelerate ECM remodeling in the IVD. To confirm this hypothesis, the effect of HAP-SDF treatment *in vivo* is being analyzed.

**REFERENCES:** <sup>1</sup>Illien-Junger S, *et al. Spine* 2012; <sup>2</sup>Leite Pereira C, *et al. Biomaterials* 2014; <sup>3</sup>Cunha C, *et al. Stem Cells Transl Med.* 2017

**ACKNOWLEDGEMENTS:** FCT/MEC through National Funds and co-financed by the FEDER via the PT2020 Partnership Agreement under the 4293 Unit I&D and through European Union funds - Projetos Estruturados de I&D&I – POCI-01-0145-FEDER-007274, Portugal; N2020 (Norte-01-0145-FEDER-000012), European TRF, RMG Exploratory Project (IF/00638/2014). CLP, GQT PhD grants SFRH/BD/85779/2012, FRH/BD/88429/2012 and CC Postdoc grant SFRH/BPD/87071/2012.

## Uncovering novel roles of Tenomodulin in intervertebral disk tissue

D Lin<sup>1,2</sup>, D Docheva<sup>3</sup>

<sup>1</sup> [Experimental Surgery and Regenerative Medicine](#), Department of Surgery, Ludwig-Maximilians-University (LMU), Munich, Germany. <sup>2</sup> [Orthopaedic Center of People's Liberation Army](#), Xiamen University Affiliated Southeast Hospital, Zhangzhou, China <sup>3</sup> [Experimental Trauma Surgery](#), Department of Trauma Surgery, University Regensburg Medical Centre, Regensburg, Germany

**INTRODUCTION:** Tenomodulin (Tnmd) is the best known mature gene for tendon and ligament tissues with reported important regulatory roles. In addition, Tnmd C-terminal cysteine-rich domain has been described to exert anti-angiogenic functions in in vitro angiogenic assays as well as in vivo models of tendon injury and age-associated cardiac valve diseases [1]. Interestingly, Tnmd expression in the intervertebral disc (IVD), which is normally avascular tissue, has been already suggested, however so far no functional assessment has been carried out. Thus, the purpose of this study was first, to map the exact expression pattern of Tnmd during IVD postnatal development and aging and second, by implementing Tnmd-knockout mouse model to examine if Tnmd plays a role in IVD homeostasis.

**METHODS:** Lumbar IVDs of Tnmd knockout and wild type mice (n=3-5) were first investigated by immunohistology for Tnmd expression in seven different postnatal stages. For detection of degenerative tissue changes, histological scoring and various stainings, namely hematoxylin/eosin (HE), Safranin O (SO), CD31 (endothelium), TUNEL (apoptosis) and type X collagen and Runx2 (hypertrophy markers) were carried out. Statistical testing by two-tailed non-parametric Mann-Whitney test was performed with the quantitative data on histological scoring, blood vessels and apoptotic cell count.

**RESULTS:** Immunofluorescence staining of Tnmd protein in developing (newborn, day 15, 1 and 2 months), adult (6 and 12 months) and aged (18 months) IVDs of WT mice showed that Tnmd is mainly expressed in the outer annulus fibrosus (AF) and nucleus pulposus (NP) throughout development as well as retained in the adult and aged stages. However, a marked downregulation in Tnmd expression

was observed at 12 and 18 months of age. HE and SO stainings revealed clear degenerative changes such as lower IVD high, loose and disarranged fibers in the outer AF and presence of chondrocyte-like cells in the inner AF and NP of Tnmd<sup>-/-</sup> IVDs. Histological scoring at 6 and 12 months confirmed significant degeneration grade (p<0.01 and p<0.001, respectively). Immunofluorescence analysis for CD31-labelled vessels revealed significantly increased vessel count in the OAF of Tnmd<sup>-/-</sup> than WT mice (p<0.05). TUNEL staining demonstrated also increased number of apoptotic cells in the OAF of Tnmd<sup>-/-</sup> compared to WT mice (p<0.05). Last, immunofluorescence analysis of Col X and Runx2 protein expression suggested upregulation of both hypertrophic markers in the NP of Tnmd<sup>-/-</sup> mice to that of WT.

**DISCUSSION & CONCLUSIONS:** The above findings provide the first evidence the Tnmd is an important factor in prevention of IVD degeneration. The exact effect of Tnmd on endothelial cells is still controversial. Interestingly in tendon development Tnmd loss-of-function does not cause vascular phenotype, however such has been observed in cardiac valve aging [1] as well as in the early healing phase after tendon rupture [3] In IVD tissue, Tnmd-deficiency resulted in significantly augmented vessel count suggesting that the anti-angiogenic role of Tnmd is site-specific or that when the tissue is not challenged there are sufficient compensatory programs.

**REFERENCES:** <sup>1</sup> S. Dex et al (2016) *Gene* **587**:1-17. <sup>2</sup> B.M. Minogue et al. (2010). *Arthritis Res Ther* **12**:R22. <sup>3</sup> D. Lin et al. (2017). *Cell Death Dis.* **8**(10):e3116.

## Specific differentiation of Adipose-derived mesenchymal stem cells in a structured scaffold

A. Mas-Vinyals<sup>1</sup>, L. Figueras-Esteve<sup>1</sup>, S. Borrós<sup>1</sup>

<sup>1</sup> Grup d'Enginyeria de Materials (GEMAT), Institut Químic de Sarrià, Universitat Ramon Llull, Via Augusta 390, 08017 Barcelona, Spain

**INTRODUCTION:** One of the great challenges of osteochondral repair is mimicking cartilage anisotropy. We have designed a scaffold for osteochondral repair that mimics the entire joint structure, from the subchondral bone to articular cartilage. The bilayered scaffold (Figure 1), presents an intimate contact between the two parts, and its design helps in the creation of the stiffness gradient present in joints.

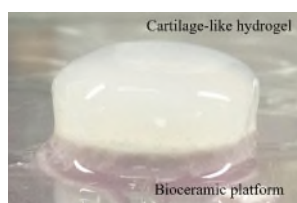


Fig. 1: Proprietary scaffold (patent pending)

**METHODS:** Adipose-derived human mesenchymal stem cells (ADMSCs) were encapsulated into the hydrogel formulation by mixing them with gelling solution. It is composed of a mixture of biopolymers. Real-time PCR (qPCR) was used to evaluate both chondrogenic and osteogenic induction potential of the formulation. The scaffold was prepared preparing a hydrogel onto the bone-like platform.

**RESULTS:** qPCR results show how the hydrogel formulation induces both the chondrogenic (Figure 2) and osteogenic (Figure 3) differentiation of ADMSCs. Gene expression was analysed for both control (collagen gels) and the developed formulation. Expression of chondrogenic markers was generally higher when cultured in chondrogenic medium, however, they were also expressed without induction. The expression of osteogenic markers is more sustained between the different culture media. Osteocalcin, a bone-specific protein has its peak of expression at day 14 and is overexpressed when cultured in induction medium in our formulation, showing its positive effect over the induction of bone formation.

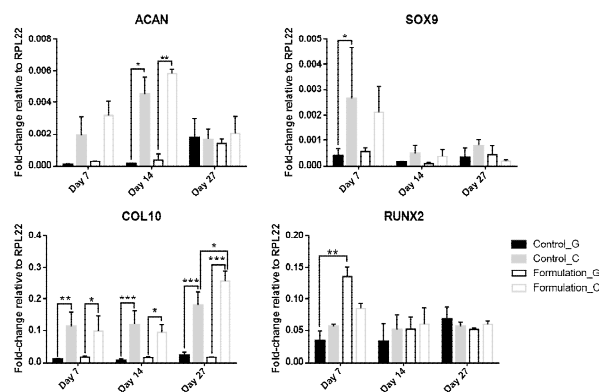


Fig. 2: qPCR results for chondrogenic markers for both control hydrogel and our formulation, in growth (G) and chondroinductive medium (C)

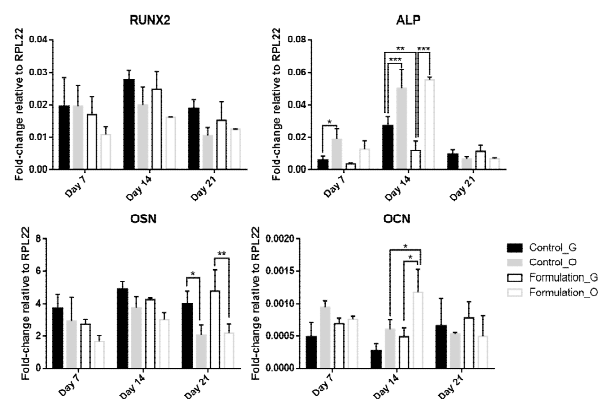


Fig. 3: qPCR results for osteogenic markers for both control hydrogel and our formulation, in growth (G) and osteoinductive medium (O)

**DISCUSSION & CONCLUSIONS:** A methodology to obtain the osteochondral scaffold has been developed, and both the chondrogenic and osteogenic potential of the hydrogel formulation has been demonstrated. Further evaluation of cell behaviour in the whole construct is being carried out, and the effect of calcium and phosphate ions diffusion through the hydrogel structure is being evaluated.

**ACKNOWLEDGEMENTS:** We thank the Secretaria d'Universitats i Recerca of the Dept. d'Economia i Coneixement, Generalitat de Catalunya and European Social Fund for the predoctoral fellowship 2016FI\_B00255 to A.M.-V.



## Osteoinductive stimulation of intervertebral disc cells with bone morphogenetic protein 2 or osteogenic medium

RD May<sup>1</sup>, ES Rodrigues<sup>1</sup>, DA Frauchiger<sup>1</sup>, CE Albers<sup>2</sup>, LM Benneker<sup>2</sup> & B Gantenbein<sup>1</sup>

<sup>1</sup> Tissue and Organ Mechanobiology, Institute for Surgical Technology and Biomechanics, University of Bern, Bern, CH. <sup>2</sup> Department of Orthopaedic Surgery, Inselspital, Bern University Hospital, University of Bern, Bern, CH

**INTRODUCTION:** Today's gold standard to treat a degenerated or traumatic disc is discectomy followed by spinal fusion. However, different treatment strategies to regenerate the intervertebral disc (IVD) are under investigation, like the application of growth factors. Such factors as, bone morphogenetic proteins (BMP) are involved in bone, cartilage and bone formation. The Bone Morphogenetic Protein 2 (BMP-2) is one of the best-studied cytokines from the TGF $\beta$  family. Particularly in clinics, BMP-2 was applied for the support during spinal fusion. Besides several *in vivo* studies for spinal fusion, it was also tested in several *ex vivo* and *in vivo* IVD models and showed promising potential for IVD regeneration [1,2]. The anabolic effect of BMP-2 could be shown in an *ex vivo* rat model by up-regulation of *aggrecan* (ACAN), *collagen type 2* and *type 1* (COL1, 2) in annulus fibrosus [1]. The aim of this study was the investigation of BMP-2 on different cell types of the human IVD in 3D alginate beads, particularly whether they possess even the plasticity to undergo bone formation.

**METHODS:** IVDs were obtained from two patients undergoing spinal surgery (approved by the Ethics Committee of the Canton of Bern, CH). IVD cells were isolated from their native extracellular matrix by gentle digestion protocol of the tissue with pronase for one hour and subsequent overnight collagenase II digestion. Nucleus pulposus (NPC), annulus fibrosus (AFC) and cartilaginous endplate cells (CEPC) were each encapsulated in 1.2% alginate at a density of 4 Mio/mL by using a 22G syringe. NPC, AFC, and CEPC beads were then cultured in  $\alpha$ -MEM supplemented with 10% FBS and 100 ng/mL BMP-2 for seven days. After four days, medium supplemented with cytokines was refreshed. Beads were then snap frozen with liquid nitrogen and then lysed in TRI reagent for total RNA extraction. Gene expression of *COL1* and 2, *SRY Box 9* (*SOX9*) and *ACAN* was performed.

**RESULTS:** Gene expression of IVD cells stimulated with 100 ng/ml BMP-2 showed a trend of *ACAN* (10-fold) and *COL2* (50-fold) up-regulation compared to day 0 beads (Fig. 1). *COL1* remained unaffected for all groups (N=2 donors).

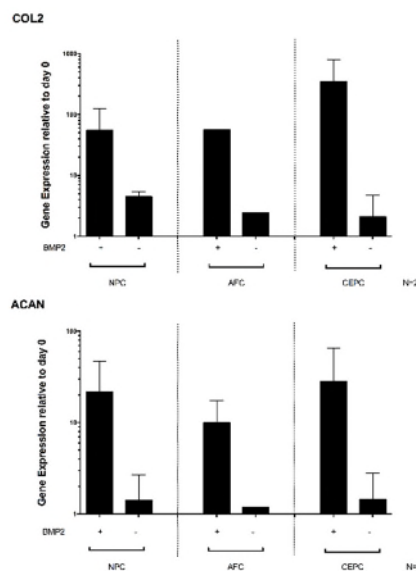


Fig. 1: Gene expression of collagen type 2 (COL2) and aggrecan (ACAN) of nucleus pulposus (NPC), annulus fibrosus (AFC) and cartilaginous endplate cells (CEPC) stimulated with 100 ng/mL BMP-2.

**DISCUSSION & CONCLUSIONS:** In this study, we investigated the effect of osteogenic stimulation by BMP2 application on IVD cells in a 3D model. Recent studies confirmed the anabolic effect from BMP-2 on IVD *in vivo* or in monolayer IVD cells. Thus, we showed the trend of an increase *ACAN* and *COL2* gene expression in stimulated cells. Similar to previous studies collagen type 1 (*COL1*) expression in stimulated IVD cells was unaffected. These results so far point towards a more chondrogenic or a “nucleopulpogenic” stimulation and no signs for ossification could be observed so far [3].

**REFERENCES:** <sup>1</sup> D. Haschtmann, S.J. Ferguson, J.V. Stoyanov (2012) *Eur Spine J* 21(9):1724-1733. <sup>2</sup> S.J. Brown, S.A. Turner, B.S. Balain, et al (2018) *Cartilage*: 1947603518754628. <sup>3</sup> I. Z. Li et al (2017) *J Orthop Res* 35(1):51-60 doi: 10.1002/jor.23351

**ACKNOWLEDGEMENTS:** The project was supported by direct funds from Hansjörg Wyss, the Hansjörg Wyss Medical, US, foundation. C.E.A. was supported by a grant of the Swiss Society of Orthopaedics and Traumatology.

## Biphasic Bioabsorbable Osteochondral Scaffold

Xiangbo Meng<sup>1</sup>, Long Li<sup>1</sup>, Yuxiao Lai<sup>1</sup>, Sibylle Grad<sup>2</sup>, Mauro Alini<sup>2</sup>, Ling Qin<sup>1,3</sup>, Xinluan Wang<sup>1,3,\*</sup>

<sup>1</sup> Translational Medicine R&D Center, Institute of Biomedical and Health Engineering, Shenzhen Institutes of Advanced Technology, Chinese Academy of Sciences, Shenzhen, China. <sup>2</sup> AO Research Institute Davos, Switzerland. <sup>3</sup> Musculoskeletal Research Laboratory, Department of Orthopaedics & Traumatology, The Chinese University of Hong Kong, Hong Kong SAR, China

**INTRODUCTION:** Osteochondral injury commonly results in the development of osteoarthritis. In this study, biphasic bioactive bioresorbable scaffolds were developed, which would be used to treat osteochondral defects by reproducing the different biological and functional requirements and guiding the growth of both bone and cartilage.

**METHODS:** Low temperature 3D printing technology was used to fabricate hierarchical scaffolds. The upper layer was composed of poly lactic-co-glycolic acid (PLGA) for cartilage repair, and the lower layer of a composite of poly lactic-co-glycolic acid and tricalcium phosphate (PT) for subchondral bone repair (Figure 1). The morphologies and porosity of the biphasic scaffolds were observed by scanning electron microscopy (SEM) and micro-CT, respectively. The mechanical properties were tested on an electronic universal mechanical tester.

**RESULTS:** Three-dimensional images of scaffolds reconstructed by micro CT clearly showed two phases due to the different densities, and the clear boundary between two layers was also demonstrated in the SEM images (Figure 2). Micro CT data showed that the porosities of PLGA and PT layers were 43% and 48%, respectively. The pore sizes of the macro-pores in PLGA and PT layers were 420-480  $\mu\text{m}$  and 450-550  $\mu\text{m}$  respectively, measured by micro CT, while SEM images demonstrated that the micropores in PLGA were larger than those in the PT layer (Figure 3). Mechanical test results (Figure 4) showed that the compressive modulus and compressive strength of the PLGA and PT layers were 2.5 MPa and 7.25 MPa, respectively.

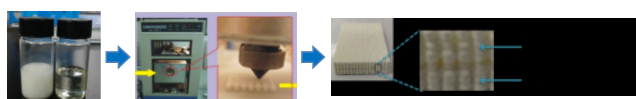


Fig. 1: Fabrication of biphasic scaffolds

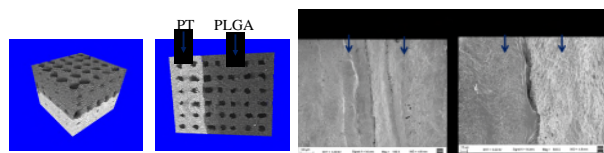


Fig.2: Boundaries of biphasic scaffolds using Micro CT and SEM

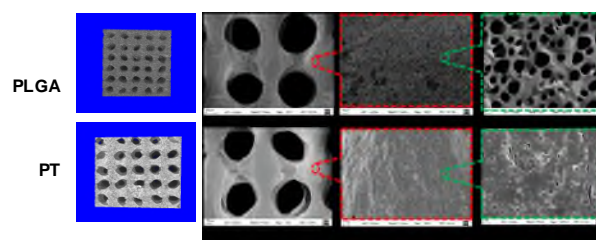


Fig.3: Porosity of scaffolds using Micro CT and SEM

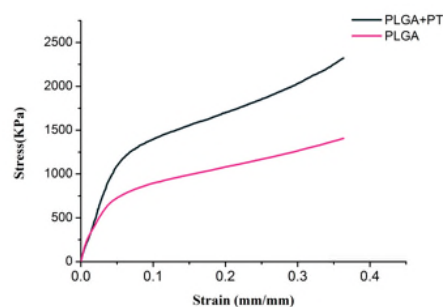


Fig.4: Stress-Strain Curves of PLGA and PT layers

**DISCUSSION & CONCLUSIONS:** A biomimetic osteochondral scaffold with bi-layer architecture including articular cartilage layer to subchondral bone layer was fabricated using a low-temperature 3D printing technology. The bi-layer scaffold featured favorable porosity and mechanical properties. It may also be used as a delivery system carrying bioactive factors to promote bone and cartilage regeneration.

**ACKNOWLEDGEMENTS:** This work was supported by Sino-Swiss collaborative project from Ministry of Science and Technology (2015DFG32200) and the Swiss National Science Foundation under the SSSTC program (156362).

## Hydrostatic pressure has the potential to stabilize accumulated extracellular matrix produced by nucleus pulposus cells

Shuichi Mizuno, Hayato Mizuno, Saori Wada, James D. Kang

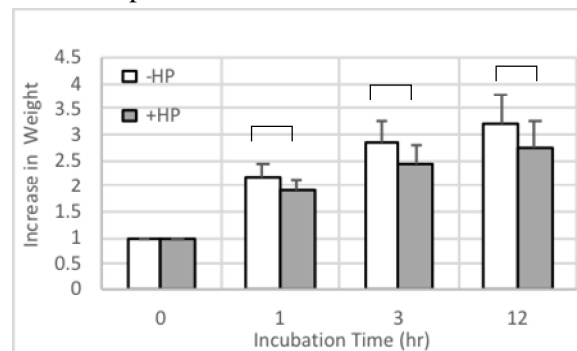
Orthopedic Surgery, Brigham and Women's Hospital, Harvard Medical School, Boston, MA, USA

**INTRODUCTION:** Nucleus pulposus (NP) cells are exposed to high hydrostatic pressure (HP) due to weight bearing and spinal motion and to high osmotic pressure (OP) due to highly negatively charged extracellular matrix (ECM) within the tissue. Our latest study indicates that combined high-HP and high-OP stimulates the gene expression of ECM molecules, but the accumulated ECM had empty spaces at high-OP. We thought that both cellular metabolism and ECM accumulation need to be optimized to promote the regeneration of NP. For our study, we hypothesized that HP prevents NP tissue from swelling, thus, mimicking the spine at rest. We incubated NP tissues with/without HP and compared the weight of the tissues to clarify the material characteristics of NP ECM. We also incubated the NP cells/clusters with HP at constant 0.2 MPa with high (450 mOsm) or low OP (320 mOsm) to identify cellular responses. We evaluated RNA expression levels and ECM morphology.

**METHODS:** We harvested bovine caudal IVD and removed the NPs. The NP explants were incubated at 320, 450, 600, and 750 mOsm with/without HP at 0.5 MPa, 0.5Hz. We measured the weight of the NPs at 0, 1, 3, and 12 hours after incubation to determine swelling. We isolated NP cells/clusters enzymatically from the IVDs and seeded the cells/clusters onto agarose-coated plates and injected them into semi-permeable membrane pouches. We incubated them with 1) no-HP/LOP and 2) HP/LOP as controls, and 3) HP/OP and HP/HOP. After one week of culture, we evaluated the mRNA expression of ECM molecules [aggrecan (ACAN) and collagen type-I and -II (COL-1 and -2)] in NP cells and the immunohistology stained with anti-keratan sulfate (KS) and collagen type-II antibodies.

**RESULTS:** NP tissues at all levels of OP swelled to three times their original size. The increase in weight was significantly larger without HP after 12 hours. This indicates that HP suppressed the increase in NP weight after 12 hours ( $P < 0.05$ ) (Fig.1). High HP/low-OP stimulated ACAN and

COL-2 expression more than the no-HP/low-OP



control and HP/high-OP. (Fig.2)

Fig. 1: Increased ratio of NP weight with and without HP at 750 mOsm. ( $P < 0.05$ ,  $n = 15$ )

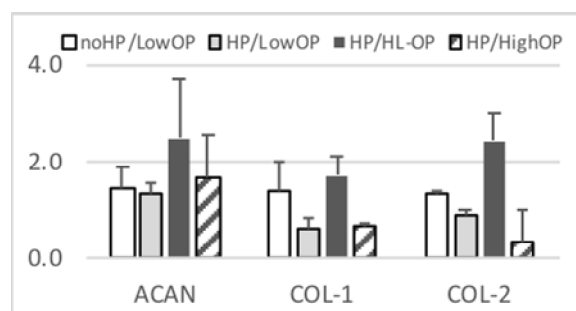
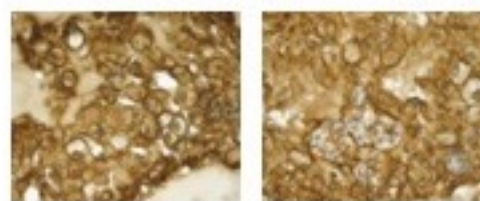


Fig. 2: Gene expression of ECM by NP cells in response to HP/OP (Mean, SD,  $n = 3$ )

Denser accumulation of KS was seen among NP clusters treated with HP/low-OP. (Fig.3)



No-HP/low-OP      HP/High-OP

Fig. 3: Accumulation of keratan sulfate produced by NP cells with HP/low-OP

**DISCUSSION & CONCLUSIONS:** HP has the potential to work as a counterstress against swelling within NP tissue. Furthermore, continuous HP has the potential to contribute to the compaction of ECM at low-OP. The manipulation of HP and OP is a promising method for optimizing the production/condition of desired cells for cell-based therapy.



## Stem cell-based implant fed with hyaluronan chondrogenic media to mimic synovial fluid behaviour of the human knee joint microenvironment

G Monaco<sup>1,2</sup>, M Alini<sup>1</sup>, M J Stoddart<sup>1,2</sup>

<sup>1</sup>[AO Research Institute, AO Foundation, Davos, CH.](#) <sup>2</sup>[Institute for Science & Technology in Medicine, Keele University, UK](#)

**INTRODUCTION:** High molecular weight hyaluronan (hMwHA) of healthy synovial fluid (HSF) is bioactive whilst also effecting osmolality<sup>1</sup>. In this study, we hypothesize that a hMwHA chondrogenic medium may better recapitulate the rheological and biological features of the HSF present in the patients' intra-articular joints. Thus, our aim is to investigate the effect of physiological level of hMwHA supplemented into the culture media on the chondrogenesis of human mesenchymal stem cells (hMSCs) that would be present in a traumatic defect after marrow stimulation techniques such as microfracture.

**METHODS:** Cylindrical (8 mm x 4 mm) porous polyurethane (PU) scaffolds were prepared<sup>2</sup>. hMSCs isolated from bone marrow aspirates, at P3 were evenly seeded at a cell density of  $5 \times 10^6$  per scaffold. Control medium was serum free DMEM plus 1% ITS+, 1% Pen/Strep, 1% non-essential amino acid, 50µg/ml ascorbate-2-phosphate, 5µM ε-amino-caproic acid,  $10^{-7}$ M dexamethasone (HA- TGFβ<sup>-</sup>). This media was further supplemented with 10 ng/mL TGFβ1 (HA- TGFβ<sup>+</sup>) or with 0.2% HA (HA+ TGFβ<sup>-</sup>) or both (HA+ TGFβ<sup>+</sup>). 1.800 kDa HA was added to simulate HSF concentration and viscosity (2.3 mg/ml)<sup>3,4</sup>. 1.000kDa HA was also added to the scaffolds of one group at 0.02% (HAS TGFβ<sup>+</sup>). Real time qPCR was done to investigate gene expression. Total DNA, sulphated GAG and Safranin O/Fast Green staining were evaluated.

**RESULTS:** Gene expression among the groups was comparable, with the notable exception of a downregulation of the hypertrophic marker collagen X in the presence of HA (HA+ TGFβ<sup>+</sup>) in the first two weeks of culture compared to (HA-TGFβ<sup>+</sup>). Total GAG synthesized in samples supplemented with HA alone was consistently higher if compared with the control medium (HA-TGFβ<sup>-</sup>). Significant GAG production was observed within the first week in all samples supplemented with HA, both in the presence and absence of active TGFβ. These findings and the general trend of the GAG level released into the media along 28 days of chondrogenic culture were consistent in all three different donors. ECM

deposition was particularly evident in HAS TGFβ<sup>+</sup> histology sections (Fig 1).

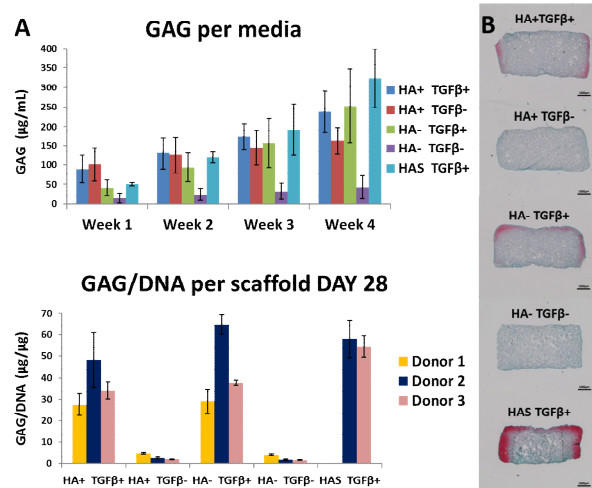


Fig. 1: (A) Total GAG produced by hMSCs (mean ± SD, three donors) and (B) Safranin O/Fast Green staining of 28 days chondrogenic differentiated constructs (scale bar 1000µm).

**DISCUSSION & CONCLUSIONS:** The addition of HA to the culture medium has a positive effect on the intrinsic capacity of hMSCs to produce ECM, especially in the early days of the chondrogenesis. Additionally, exogenous HA may reduce upregulation of the hypertrophic cartilage marker, Collagen X, that is normally induced by active TGFβ. As this work aims to more closely reproduce the intrarticular complexity of the *in-vivo* joint environment, the addition of HA can be also used as a chondrogenic differentiation media model for *in-vitro* or *ex-vivo* studies where hMSCs are involved. Finally, in the current climate of animal welfare and "3Rs", HA media can be helpful to prevent *in-vitro* artefacts and to enable more accurate prescreening of potential cartilage repair therapies.

**REFERENCES:** <sup>1</sup>Avenoso (2017) *Inflammation Research* 1-16, <sup>2</sup>Boissard (2009) *Acta Biomaterialia*, 5(9): 3316-3327. <sup>3</sup>Akmal (2005) *J Bone Joint Surg Br*, 87: 1143-1149. <sup>4</sup>Balazs (1967) *Arthritis Rheum*, 10: 357-376.

**ACKNOWLEDGEMENTS:** Project funded by AO Research Institute, Davos, Switzerland.



## Efficiency of different RNA extraction protocols for chondrocyte -seeded agarose constructs

[AC Ortiz](#)<sup>1</sup>, [A Govaerts](#)<sup>1</sup>, [R Lories](#)<sup>2</sup>, [I Jonkers](#)<sup>1</sup>

<sup>1</sup>[Human Movement Biomechanics Research Group, KU Leuven, Leuven, Belgium.](#) <sup>2</sup>[Skeletal Biology and Tissue Engineering Research Center, KU Leuven, Leuven, Belgium](#)

**INTRODUCTION:** Agarose hydrogels in 3D culture systems are widely used in research. Usage of these systems in chondrocyte research brings the advantage of mimicking the *in vivo* chondrocyte phenotype, whereas in 2D systems chondrocytes loose their phenotype and tend to dedifferentiate. Yet, RNA isolation from agarose gels is known to be difficult as it results in poor RNA yield and purity. Here we compared the efficiency of different RNA extraction methods using chondrocytes cultured on 3% agarose gels.

**METHODS:** Immortalised human chondrocyte (C28/I2) cells were encapsulated at 2 million cells/ml in 3% agarose gels (total volume of 250ul) and cultured for one day with DMEM/F12, 10% FBS media. Hydrogels were snap frozen and stored at -80°C until further manipulation. Total RNA was isolated following different protocol strategies: (1) Trizol (Ambion) as per the manufacturer's instructions; (2) Plant Kit in which RNeasy Plant mini kit (Qiagen) was used as per the manufacturer's instructions; (3) Mio method<sup>2</sup> in which samples are lysated in RLT containing beta mercaptoethanol and 2M Sodium Acetate (pH 5) followed by a RNeasy Plant mini kit (Qiagen) protocol and (4) TZ-Plant method<sup>1</sup> in which samples are lysed in Trizol followed by extraction with RNeasy mini kit (Qiagen) protocol from the ethanol stage. All samples were homogenized in a rotor disruptor (MP) with stainless steel beads and respective lysis buffer to improve lyses and homogenization. RNA clean-up step was performed in some samples for comparison.

**RESULTS:** Although all protocols (table 1) showed good values for the absorbance ratio 260/280 (around 2.0), contamination was still observed in absorbance ratio 260/230 (below 1.8). The RNA elution step using the Trizol method resulted in the formation of a gel like sample that did not dissolve by repeated pipetting. The Plant kit provided low RNA concentration values and high contamination even after RNA clean up (data not shown). Both Mio and TZ-Plant showed good purity values for 260/280 agarose (table 1) and integrity observed when RNA was loaded in gels after RNA clean up (figure 1), however

contamination was still detected in TZ-plant even after the RNA clean up step (table 1 – TZ-Plant\*).

Table 1. RNA measurements for different RNA extraction protocols \* Indicate that RNA clean up was performed. Data are displayed as MEAN ± SD.

Protocol	Concentration (ng/ul)	Absorbance (260/280)	Absorbance (260/230)
Trizol	103.1 ± 15.1	2.0 ± 0.1	1.7 ± 0.3
Plant Kit	122.0 ± 69.9	1.9 ± 0.1	1.4 ± 0.5
Mio	157.1 ± 37.5	2.0 ± 0.0	0.9 ± 0.4
TZ-Plant	348.2 ± 42.3	2.0 ± 0.0	1.0 ± 0.2
Mio*	610.7 ± 280.9	1.9 ± 0.0	2.3 ± 0.0
TZ-Plant*	348.2 ± 42.3	2.0 ± 0.0	1.0 ± 0.2

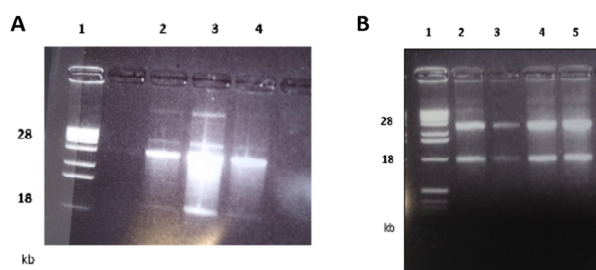


Fig. 1: (A) RNA samples isolated with Mio protocol followed by RNA clean up step on a 1.5% agarose gel. Lane 1: ladder; lane 2-4 samples. (B) RNA samples isolated with TZ plant protocol followed by RNA clean up step on a 1.5% agarose gel. Lane 1: ladder; lane 2-5: samples. Presence of 28S and 18S RNA bands (kb).

**DISCUSSION & CONCLUSIONS:** We suggest that RNA isolation methods using silica membrane kits are the most adequate when working with agarose gel samples. Our protocol of choice uses a motor disruptor with the Mio lysis buffer, followed by the RNeasy Plant Mini kit and a clean-up step. This provides us the best results for both RNA purity and integrity. We considered that this evaluation can provide further insight to those interested in extracting RNA from their 3D agarose culture systems, but also suggest that further improvements can be made.

**REFERENCES:** <sup>1</sup> Ogura, T., et al. (2015). *BMC Res Notes* **8**: 644. <sup>2</sup> Mio, K., et al. (2006). *Anal Biochem* **351**(2): 314-316.

## Application of 3D scaffold-free cartilage transplants (SFCT) to repair damaged articular cartilage in large animals models

I Ponomarev<sup>1</sup>, K Wölfer<sup>1</sup>, T Reuter<sup>2</sup>, D Barnewitz<sup>1</sup>

<sup>1</sup>Research Centre of Medical Technology and Biotechnology, Bad Langensalza, Germany.

<sup>2</sup>ICM - Institut Chemnitzer Maschinen- und Anlagenbau e.V., Chemnitz, Germany.

**INTRODUCTION:** Damaged hyaline cartilage has a limited capability of self-repairing. This is the main cause of arthrosis progress. Therefore, different tissue-engineering methods have been developed to address this particular problem. We focused on the development of a new technology to produce a 3D scaffold-free cartilage transplant (SFCT) by intermittent mechanical stimulation of the chondrocyte pellet cultures. This SFCT-technology was applied successfully in three large animals studies.

**METHODS:** The SFCT were manufactured according to patented technology [1] using chondrocytes of the stifle joint.

Two studies on horses and one study on sheep were conducted. In the first study, three horses were treated successfully (bilateral, six stifle joints). The horses were euthanized after 18 months.

The second study comprised 10 horses (unilateral treatment). Five horses were euthanized after twelve months and another five after 24 months.

In the third study, 30 stifle joints of sheep were treated with SFCT (unilateral). The sheep were euthanized after six and twelve months, respectively (15 sheep each).

Cartilage development in SFCT was documented by macroscopy (Fig.1), immuno-histochemical, histological and biochemical analysis. The scaffold-free constructs were compared with native cartilage of the animals.

**RESULTS:** In all our animal studies, the analyses of the stifle joints revealed the presence of hyaline-like tissue in the scaffold-free transplants. A complete integration into the surrounding native tissue and to the subchondral bone was observed macroscopically. All characteristic matrix components of cartilage, such as type II collagen and glycosaminoglycan (GAG), were detected in histological and immuno-histochemical analyses. Quantitative biochemical analysis showed no significant difference in collagen contents between transplant und native tissue (Tab. 1).

The interspecies comparison revealed wider differences in the GAG contents. In the first study

on horses, the GAG contents in the transplants was 32 % of the native. The second horse study showed 48 % after 24 months. In contrast, the study on sheep yielded a GAG contents of 61 % of the native after six months and 73 % after twelve months, respectively.

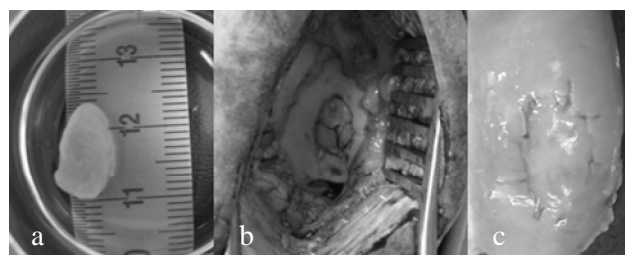


*Fig. 1: Macroscopic view of a 3D scaffold-free cartilage transplant (SFCT) in horse model: before implantation-a, at implantation-b and 24 months after implantation-c.*

*Table 1. Biochemical characterisation of native cartilage and SFCT in horse model.*

Specimens	Collagen	GAG
SFCT	57,7±7,5 µg	60,1±14,2 µg
native	63,3±5,3 µg	125,6±18,1 µg

**DISCUSSION & CONCLUSIONS:** The reason for the differences in GAG contents at interspecies comparison lies in the differing implantation regions within the joint. The implantation site in horses was the throchlea ossis femoris and in sheep the condylus medialis femoris, respectively. The present results demonstrate the effectiveness of SFCT-technology in the treatment of cartilage damage in large animals.

**REFERENCES:** <sup>1</sup>I. Ponomarev, I. Wilke, Manufacturing process of three dimensional tissue structures and structures obtainable thereby, EP 1 550 716 B1, 2004.

**ACKNOWLEDGEMENTS:** This study is part of a research project supported by BMWi Grant IW-060264 and IW-091034.

## Correlation of biochemical and biomechanical parameters from 3D scaffold-free cartilage transplants (SFCT) – First Results

I Ponomarev<sup>1</sup>, T Reuter<sup>2</sup>, K Wölfer<sup>1</sup>, D Barnewitz<sup>1</sup>

<sup>1</sup>Research Centre of Medical Technology and Biotechnology, Bad Langensalza, Germany.

<sup>2</sup>ICM - Institut Chemnitzer Maschinen- und Anlagenbau e.V., Chemnitz, Germany.

**INTRODUCTION:** Articular cartilage and artificial cartilage can be investigated and characterised by biomechanical, biochemical and histological analysis. Correlations between the different methods of analysis can give a better assessment of the maturity level of 3D scaffold-free cartilage transplants (SFCT). Herein, correlations between biomechanical and biochemical parameters are identified and discussed.

**METHODS:** The equine chondrocytes of the stifle joint were used for the production of SFCT. After cultivation and proliferation in monolayer cultures, cells were transferred into a three-dimensional structure without any artificial matrix, growth or differentiation factors. In order to produce SFCT and the extracellular matrix, the samples were manually exposed to undifferentiated mechanical pressure [1].

The SFCT (n = 12) were analysed after 1 – 6 weeks of culturing. Chondrogenesis in SFCT was documented by macroscopic, biochemical, histological and biomechanical analysis. For biomechanical investigations, Young's modulus E, fiber modulus  $\xi$  and permeability k of samples were determined using uniaxial relaxation compression tests and a Finite-Element (FE) parameter identification routine [2]. The relaxation tests of the specimens were executed with a testing velocity of  $v = 0.02$  mm/s, an initial load of  $F = 0.1$  N, a relaxation time of  $t = 3500$  s and a strain of 20 %. For the computational approach, an optimised 3D FE-based method was determined to identify the biomechanical parameters (Fig. 1a). The articular cartilage was modelled as biphasic material with tension-compression nonlinearity. The collagen specific amino acids hydroxyproline (Hypro) and hydroxylysine (Hyls) as well as the matrix shaping substance glycosaminoglycan (GAG) were quantified in biochemical analyses.

**RESULTS:** For the parameter identification of SFCT, the 3D FE-model with an extended biphasic material model yields a  $R^2$  of  $0.941 \pm 0.037$  (Fig. 1b). The linear correlation results clearly demonstrate that the biochemical parameters GAG

and Hyls correlate strongly with the biomechanical parameters E,  $\xi$  and k. However, no or weak correlations exist between Hypro and the biomechanical parameters (Tab. 1). The parameter k indicates negative, the other parameters show positive correlations.

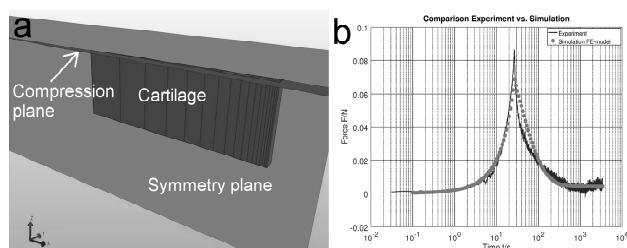


Fig. 1: Optimised FE-model for the parameter identification (a) and fit result (b).

Table 1. Correlation between biomechanical and biochemical parameters (Pearson's r is depicted, \* $p < 0.01$ , \*\* $p < 0.001$ ).

	E	$\xi$	k
GAG	0.82*	0.78*	-0.83**
Hyls	0.77*	0.72*	-0.86**
Hypro	0.35	0.28	0.02

**DISCUSSION & CONCLUSIONS:** These first results show that linear correlations between biomechanical and biochemical parameters exist. The optimised FE-model routine operated robustly. Therefore, it is possible to characterise the maturity level and cultivation state of the SFCT, respectively. Future work will investigate nonlinear correlation functions and increase the number of samples to reach higher accuracy.

**REFERENCES:** <sup>1</sup>I. Ponomarev, L.M. Kochneva and D. Barnewitz (2014) *Bull Exp Biol Med* **156** (4):548-55. <sup>2</sup>T. Reuter (2015) Determination of biomechanical parameters of articular cartilage with the help of FEM using experimental stress relaxation and creep indentation data, *Master thesis*, FSI Beuth University, Berlin.

**ACKNOWLEDGEMENTS:** This study is part of a research project supported by the German Ministry of Economy and Technology: INNO-WATT Reg. Nr.: VF160052

## UNRAVELLING MORPHOLOGICAL PROPERTIES OF CARTILAGE-BONE INTERFACE AT NANO-SCALE

Behdad Pouran<sup>1,3\*</sup>, Amir Raouf<sup>2</sup>, Matthijs de Winter<sup>2</sup>, Vahid Arbabi<sup>1,3</sup>, Ronald Bleys<sup>1</sup>, Jos Malda<sup>1,2</sup>, Amir A. Zadpoor<sup>3</sup>, Harrie Weinans<sup>1,3</sup>

<sup>1</sup>University Medical Center Utrecht, <sup>2</sup>Utrecht University, Utrecht, The Netherlands. <sup>3</sup>TU Delft, The Netherlands

**INTRODUCTION:** Using contrast-enhanced micro-computed tomography (CECT) (1), fluorescent microscopy (2), evidence of transport of small molecules across the osteochondral interface of human, equine and mouse samples has been suggested. Nevertheless, the exact pathways that drives the solute transport has not been fully clarified. In the current work, using advanced focused-ion-beam scanning electron microscopy (FIB-SEM), nano-features of the interface calcified cartilage and subchondral bone plate are highlighted. Feeding the FIB-SEM tomography data to advanced pore-scale computational model allows quantifying the marked transport properties, namely diffusion and permeability in calcified cartilage and subchondral bone plate.

**METHODS:** Osteochondral plugs (diameter = 8.5 mm) were harvested from human cadaveric human femoral condyles (n = 4) using a diamond tip drill bit. Sections (10 µm thick) of the frozen embedded plugs were collected using an Ultra-cryotome. Sections were first freeze-dried prior to FIB-SEM scanning. A region perpendicular to the osteochondral interface containing non-calcified cartilage, calcified cartilage and subchondral bone plate (500 µm) was milled and was then exposed to electron beam. Images at a resolution of 7 nm were taken at several locations. Once each region was identified, a 3D stack of calcified cartilage and subchondral bone plate was obtained. Diffusion and fluid flow simulations were then performed to determine transport properties (3).

**RESULTS:** We found that the pore features were distinct in the calcified cartilage region and the subchondral bone plate (Figure 1); the average pore diameter in calcified cartilage was  $10.7 \pm 6.5$  nm whereas it was  $39.1 \pm 26.2$  nm in subchondral bone plate. Moreover, the connectivity of the pores was compromised in calcified cartilage compared to that in the subchondral bone plate. Within calcified cartilage, the cross-sectional data revealed that pore size increases continuously from the regions near non-calcified cartilage to the regions near the subchondral bone plate where the

maximum difference is approximately two-fold. Our pore-network models showed that hydraulic permeability in subchondral bone was approximately 2000-fold higher than calcified cartilage, whereas diffusivity was 1.5 times higher in subchondral bone plate.

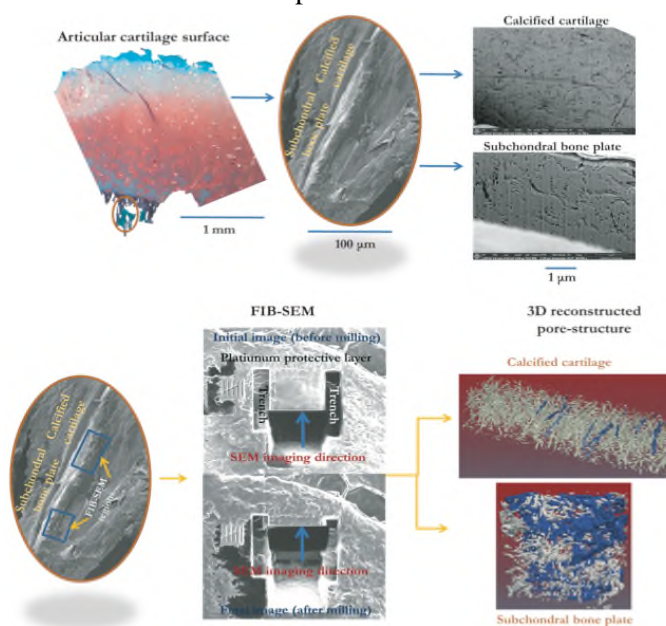


Figure 1: FIB-SEM tomography procedure performed on subchondral bone plate ( $4 \times 4 \times 3 \mu\text{m}^3$ ) and calcified cartilage ( $10 \times 4 \times 2.5 \mu\text{m}^3$ ). Connected pores are displayed in blue.

**DISCUSSION & CONCLUSIONS:** Cross-talk between cartilage and subchondral bone plate for small solutes has been confirmed (1), yet the exact pathways that drive the solute transport has not been clarified. Using FIB-SEM tomography we showed the existence of inter-connected networks in calcified cartilage and to a much larger extent in subchondral bone plate, which resulted in larger fluid and solute conductivity in the subchondral bone plate.

**REFERENCES:** (1) Pouran, B., et al (2017). (2) Pan, J., et al (2009). (3) Raouf, A., et al (2013). (4) Khanarian, N.T., et al (2014). (5) Lyons, T.J., et al (2006).



## **Magnesium alloys and composites as biodegradable biomaterial in orthopaedic: a literature analysis and preliminary report**

AJ Rahyussalim<sup>1</sup>, AF Kamal<sup>1</sup>, S Supriadi<sup>2</sup>, AF Marsetio<sup>1</sup>, PM Pribadi<sup>2</sup>, M Zulhandani<sup>1</sup>

<sup>1</sup> *Department of Orthopaedic and Traumatology, Faculty of Medicine Universitas Indonesia – Cipto Mangunkusumo Hospital, Jakarta, Indonesia.* <sup>2</sup> *Department of Mechanical Engineering, Faculty of Engineering Universitas Indonesia, Depok, Indonesia*

**INTRODUCTION:** Magnesium (Mg) has biomechanical properties close to that of bone, and able to prevent bacterial adhesion while providing a favorable environment for osteoblast growth. Various attempts had been made to improve the biomaterial properties of Mg, for example through alloying, processing, coating or surface modification. Carbonate Apatite (CA) is an inorganic component of bone tissue. Powder form of CA cannot be used directly as bone substitute due to crystal formation from the inflammatory response. It needs to be processed into suitable shapes. The material is known able to bond with bone tissue without formation of fibrotic tissue.

Each of Mg and CA has been found as having stimulatory effect on new bone formation. The stability, biocompatibility and biomechanical properties of composite of these materials have not been known. We did a literature analysis on various studies which attempted to increase the biomaterial properties of Mg. We also report an early result of our study in attempt to synthesize these two materials. Various compositions and methods of processing are on the trial, in order to create a stable composite that is able to be used as a biodegradable biomaterial for orthopaedic application.

**METHODS:** Three specimens to determine the optimal compaction and temperature with dimension of Ø10,5 x 10 mm made of pure magnesium powder were fabricated with the compaction pressure of 265 MPa under 200°C, 250°C, and 300°C compaction temperature, respectively, followed by sintering at 550°C for 1h of holding time and 5°C/min of heat rate. The specimens were then followed by cutting with low speed diamond saw to expose the inner section area. The specimens were grinded with sandpaper progressively, starting from 80-grit up to 2000-grit. The specimens were then polished and observed using optical microscope.

Four more specimens made from pure magnesium, mixture of magnesium and 5wt% of CA, 10wt% of CA, and 15wt% of CA, respectively, with the same

dimension as the previous ones were fabricated with 265 MPa of compaction pressure and 300°C of compaction temperature. The specimens were then followed by sintering under the same parameters as the previous specimens and cut with low speed diamond saw. The inner section of the specimens were analysed by XRD to determine the sintering's effects to the specimens' composition.

**RESULTS:** The result from metallography examination shows that 200°C made the products seemingly more porous than the ones made with the temperature of 250°C and 300°C. After inspecting the XRD results, it is also known that the addition of CA into the mixtures affects its compositions.

**DISCUSSION & CONCLUSIONS:** Higher compaction temperature produces denser product with less porosity. Moreover, adding more CA into the composite material makes it more prone to get burnt and have its composition altered since it is rich with oxygen. Further studies on its properties need to be conducted to determine its compatibility as an orthopaedic implant materials.

**REFERENCES:** <sup>1</sup> Rahyussalim AJ, Marsetio AF, Saleh I, Kurniawati T, Whulanza Y. The Needs of Current Implant Technology in Orthopaedic Prosthesis Biomaterials Application to Reduce Prosthesis Failure Rate. *J Nanomater.* 2016;3:1-9. <sup>2</sup> Li L, Zhang M, Li Y, Zhao J, Qin L, Lai Y. Corrosion and biocompatibility improvement of magnesium-based alloys as bone implant materials: a review. *Regen Biomater.* 2017;4(2):129–137. <sup>3</sup> Radha R, Sreekanth D. Insight of magnesium alloys and composites for orthopedic implant applications: a review. *Journal of Magnesium and Alloys.* 2017;5(3):286-312. <sup>4</sup> Pogorielov M, Husak E, Solodivnik A, Zhdanov S. Magnesium-based biodegradable alloys: Degradation, application, and alloying elements. *Interv Med Appl Sci.* 2017 Mar;9(1):27-38.

**ACKNOWLEDGEMENTS:** This research is supported by grants from Universitas Indonesia and from Ministry of Research, Technology and Higher Education of the Republic of Indonesia.

## Anti tuberculosis drug encapsulated using PLGA and Alginate-PLGA as local treatment of spondylitis TB: an in vitro study

AJ Rahyussalim<sup>1</sup>, M Kamarza<sup>2</sup>, M Setyarani<sup>1</sup>, M Zulhandani<sup>1</sup>

<sup>1</sup> Department of Orthopaedic and Traumatology, Faculty of Medicine, Universitas Indonesia – Cipto Mangunkusumo Hospital, Jakarta, Indonesia. <sup>2</sup> Chemical Engineering, Faculty of Engineering, University of Indonesia. <sup>3</sup> Medical Technology Research Cluster, Indonesia Medical Education and Research Institute, Faculty of Medicine, Universitas Indonesia.

### INTRODUCTION:

Increasing prevalence of musculoskeletal TB is not parallel with its extreme side effects and resistance (MDR TB) of oral drugs. Experimental study regarding slow release local anti tuberculosis drugs (ATD) using PLGA and alginate encapsulation never been performed. It's gelatization ability and non-toxic properties; making it expected to be a solution.

### METHODS:

In vitro study Rifampicin (RIF), Isoniazid (INH), Pyrazinamide (PYR), Etambutol (ETH) encapsulated using PLGA and Alginate. Encapsulated ATD powder plus human plasma was put on dialyzer and baker glass; extracted on day 1,3,5, and 7. ATD amount analyzed using HPLC RP C18e with UV-Vis detector.

### RESULTS:

Alginate and PLGA carrier model for ATD are available. Encapsulated ATD level on dialyzer and baker glass detected on day 3. Encapsulated ATD-dialyzer levels increased until day 7, so did on baker glass, although concentrations in dialyzer were higher. Uncapsulated ATD levels observed on day 1, 3, 5, and 7 at similar concentration of 8300 µg/mL. Significant difference levels of encapsulated and unencapsulated group in RIF ( $p = 0.029$ ), INH ( $p = 0.02$ ), PYR ( $p = 0.02$ ), ETH ( $p = 0.029$ ), and on day 1 ( $p = 0.029$ ), day 3 ( $p = 0,02$ ), day 5 ( $p = 0,026$ ), day 7 ( $p = 0,02$ ).

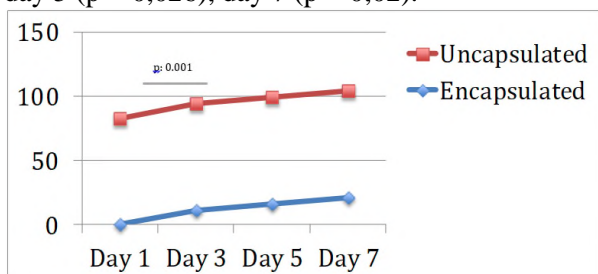


Fig 1. The difference between unencapsulated group and encapsulated group

### DISCUSSION & CONCLUSIONS:

PLGA and Alginate is available for ATD encapsulation.<sup>2</sup> An increase in encapsulated ATD

levels in the dialyzer on days 1 to 7 suggests that ATD with Alginate- PLGA encapsulation has a slow release property can be used as preliminary study of local TB therapy.

### REFERENCES:

- <sup>1</sup>Gulbay GE, Gurkan OU, Yilldiz OA, Onen ZP, Erkekol FO, et al. Side effects due to primary antituberculosis drugs during the initial phase of therapy in 1149 hospitalized patients for tuberculosis. Elsevier. 2006;100:1834-1842
- Ziegler (1991) *Essentials of Writing Biomedical Research Papers*, McGraw-Hill, Inc.
- <sup>2</sup>I.R. Spears, M. Pfeleiderer, E. Schneider, et al (2000) *J Biomech* 33:1471-77.
- <sup>2</sup>Du Toit, Pillay V, Paul M. Tuberculosis chemotherapy: curent drug delivery approaches. Respiratory research. 2006;7(118).
- <sup>3</sup>Ahmad Z, Khuller GK. Alginate-based sustained release drug delivery systems for tuberculosis. Informa UK. 2008; 5(12) : 1323-1334.

## Restoring a healthy human nucleus pulposus cell phenotype: GDF6 as a biologic for intervertebral disc regeneration strategies

[S.M. Richardson](#)<sup>1</sup>, T. Hodgkinson<sup>1</sup>, B. Shen<sup>2</sup>, A. Diwan<sup>2</sup>, [J.A. Hoyland](#)<sup>1</sup>,

<sup>1</sup> *Division of Cell Matrix Biology and Regenerative Medicine, University of Manchester, UK.*

<sup>2</sup> *St. George Clinical School, University of New South Wales, Australia.*

**INTRODUCTION:** Intervertebral disc (IVD) degeneration is a leading cause of low back pain. During degeneration, cell driven imbalances result in significant alterations in extracellular matrix (ECM) composition, which functionally impairs the central nucleus pulposus (NP). Signalling by the growth differentiation factor (GDF) sub-family of the bone morphogenetic protein family is required for correct spine/IVD development and the maintenance of healthy NP cell phenotypes [1, 2, 3]. GDF6 has recently been shown *in vivo* to reduce degenerated IVD-induced pain, attenuate pro-inflammatory molecular changes and increase disc height in the rabbit [4], suggesting it may be a potent biologic for IVD regeneration. However, the effects and mechanism of GDF6 signalling in NP cells are not fully understood. The aim of this study was to investigate GDF6 signalling in adult human NP cells critical to GDF6-mediated phenotypic and functional changes in order to develop more effective regenerative strategies utilising biologics.

**METHODS:** Human NP cells were isolated from IVD tissue obtained with informed written consent and approvals from patients undergoing disc surgery. The BMP receptor expression profile of NP cells was determined at gene and protein level (N=3). Downstream GDF6 signal transduction in NP cells was investigated by analysis of the phosphorylation statuses and blocking of smad1/5/8 and the non-smad pathways p38 MAPK and erk1/2 (specific inhibitors- dorsomorphin, SB20358, U0126 respectively). NP cells were stimulated with 100 ng ml<sup>-1</sup> GDF6. In culture, the effects of GDF6 stimulation and specific pathway inhibition on the expression NP marker genes and matrix remodelling enzymes, glycosaminoglycan (GAG) and total collagen production were assessed.

**RESULTS:** NP cells were found to express all known GDF6 receptor subunits, with highest expression of the type I and II receptor subunits BMPR-1A and BMPR2 at gene and protein level. NP cells responded to GDF6 stimulation by significantly upregulating the expression of NP marker genes (P<0.05). Significantly, ACAN expression was increased >10-fold in comparison to unstimulated controls. GDF6 stimulation had no

significant effect on the expression of catabolic matrix remodelling enzymes. Blocking of smad1/5/8 and erk1/2 signalling significantly decreased expression of all NP marker genes (p<0.05). P38 blocking had decreased comparative effects, in particular on ACAN expression, which was not significantly affected. Total GAG and collagen production were significantly increased following GDF6 stimulation - DMMB assays (p<0.05), Alcian Blue staining (p<0.05) and 3[H]-proline incorporation assays (p<0.05). Inhibition of smad1/5/8 signalling and Erk1/2 pathway significantly decreased GAG production (P<0.01) while inhibition of p38 MAPK did not abrogate GDF6-mediated GAG production. However, both p38 and ERK1/2 inhibition independently decreased total collagen production (p<0.05) to unstimulated control levels.

**DISCUSSION & CONCLUSIONS:** GDF6 has a potential role in NP cell homeostasis through the upregulation of healthy matrix genes/protein expression that are downregulated during IVD degeneration, including aggrecan and type II collagen. For the first time, GDF6-mediated stimulation of GAG and collagen production in NP cells in culture was shown to involve smad-independent signalling, with ERK1/2 essential for stimulation of GAG production and both ERK1/2 and p38 MAPK required for collagen production. This knowledge is important for the effective use of GDF family members as therapeutic molecules and provides insight that facilitates the development of effective small-molecule and cell-based therapies for the treatment of IVD degeneration.

**REFERENCES:** <sup>1</sup> Settle, S.H., et al. *Dev boil*, 2003. 254(1): 116. <sup>2</sup> Wei, A., et al. *J Orthopaed Res*, 2016. 34(2): 279. <sup>3</sup> Le Maitre et al. *Arthrit Res Therap*, 2009. 11(5): R137. <sup>4</sup> Miyazaki, S., et al. *Eur Spine J*, 2018. <https://doi.org/10.1007/s00586-018-5488-1>

**ACKNOWLEDGEMENTS:** This project was funded by UoM awarded MRC CiC, Rosetrees Trust and the Manchester Musculoskeletal Biomedical Research Unit.

## Optimisation of a combined adipose stem cell–GDF6 therapy for intervertebral disc regeneration

[S.M. Richardson](#)<sup>1</sup>, T. Hodgkinson<sup>1</sup>, F. Wignall<sup>1</sup>, L. White<sup>2</sup>, [J.A. Hoyland](#)<sup>1</sup>,

<sup>1</sup> *Division of Cell Matrix Biology and Regenerative Medicine, University of Manchester, UK.*

<sup>2</sup> *Centre for Biomolecular Sciences, School of Pharmacy, Nottingham University, UK.*

**INTRODUCTION:** Low back pain, caused by degeneration of the intervertebral disc (IVD) represents one of the most significant socioeconomic conditions facing Western economies. The poor long-term efficacy demonstrated by current conservative and surgical interventions means novel regenerative therapies are required to restore function and relieve pain.

We have previously shown that stimulation of adipose-derived stem cells (ASCs) with growth differentiation factor 6 (GDF6) promotes differentiation to a phenotype similar to that of nucleus pulposus (NP) cells from the IVD<sup>1</sup> and that it does so better than other commonly used growth factors, namely GDF5 and TGFβ. Thus we propose that a combined ASC-GDF6 therapy offers potential for IVD regeneration and treatment of chronic low back pain. The aims of this study were to (i) elucidate GDF6 cell surface receptor profile and signalling pathways to better understand mechanism of action; and (ii) develop a delivery system to control release of bioactive GDF6 over time whilst ensuring ASC differentiation to NP cells

**METHODS:** GDF6 receptor expression by ASCs (N=6) was profiled through western blot, immunofluorescence (IF) and flow cytometry. Signal transduction was investigated through analysis of Smad1/5/9 phosphorylation and alternative non-smad pathway activation following GDF6 (100 ng ml<sup>-1</sup>) stimulation in culture. Reliance on the type II receptor BMPR2 for signal transduction was investigated by siRNA knockdown. The role of these signalling pathways in the induction of NP-like gene expression in ASCs was investigated through pathway specific blockers (smad1/5/9- dorsomorphin; p38 MAPK – SB20358; ERK1/2 – U0126). GDF6 was then encapsulated in polymer microparticles (MPs) which have previously been demonstrated to control temporal release of bioactive growth factors [2]. Release kinetics of GDF6 from MPs was calculated through BCA protein assays and GDF6 ELISAs. ASC (n=3) differentiation to NP cells in collagen gels with exogenous GDF6 or GDF6 MPs was then assessed by qPCR and DMMB assay.

**RESULTS:** BMPR profiling revealed high BMPR2 expression on ASCs. GDF6 stimulation of ASCs resulted in significant increases in canonical SMAD1/5/8 phosphorylation, along with stimulation of non-canonical ERK phosphorylation, but not p38 phosphorylation. Blocking of SMAD phosphorylation attenuated GDF6-induced upregulation of all NP marker genes, while blocking Erk only partially affected differentiation. Importantly both SMAD and Erk blocking inhibited upregulation of either aggrecan and type II collagen at both gene and protein level.

GDF6 release from MPs was controlled over 14 days *in vitro* and was demonstrated to be equivalent to concentrations added exogenously. SEM and histological analysis confirmed that MPs were distributed throughout gels and that gel formation was not disrupted. In 3D collagen gel cultures, GDF6 release from microspheres elicited equivalent ASC differentiation and NP-like matrix formation compared to that following exogenous delivery of GDF6 to media, indicating activity was not affected by microsphere encapsulation.

**DISCUSSION & CONCLUSIONS:** This study elucidates the signalling mechanisms responsible for GDF6-induced ASC differentiation to NP cells. It further demonstrates the effective encapsulation and controlled delivery of GDF6, which was able to maintain its activity and induce ASC differentiation to NP cells and production of an NP-like ECM. Delivery of GDF6 microspheres in combination with ASCs is a promising strategy for IVD regeneration and treatment of back pain.

**REFERENCES:** <sup>1</sup> Settle, S.H., et al. *Dev Biol*, 2003. 254(1): 116. <sup>2</sup> Wei, A., et al. *J Orthopaed Res*, 2016. 34(2): 279. <sup>3</sup> Le Maitre et al. *Arthrit Res Therap*, 2009. 11(5): R137. <sup>4</sup> Miyazaki, S., et al. *Eur Spine J*, 2018. doi.org/10.1007/s00586-018-5488-1.

**ACKNOWLEDGEMENTS:** This project was funded by UKRMP, Rosetrees Trust, Manchester Biomedical Research Centre and Musculoskeletal Biomedical Research Unit.



## Hyaluronan-hydrogel seeded with autologous nucleus pulposus cell regenerates human intervertebral discs in an ex vivo, physiological culture model.

DH Rosenzweig<sup>1</sup>, R Fairag<sup>1,2</sup>, AP Mathieu<sup>3</sup>, L Li<sup>1</sup>, D Eglin<sup>4</sup>, M D'Este<sup>4</sup>, T Steffen<sup>1</sup>, MH Weber<sup>5</sup>, JA Ouellet<sup>5</sup>, L Haglund<sup>1,5,6</sup>

<sup>1</sup>[Orthopaedic Research Laboratory](#), Division of Orthopedic Surgery, McGill University, Montreal, Canada, <sup>2</sup>[King Abdulaziz University](#), Jeddah, Saudi Arabia, <sup>3</sup>[Brain Imaging Centre](#), The Douglas Mental Health Institute, Montreal, QC, <sup>4</sup>[AO Research Institute Davos](#), Davos, Switzerland, <sup>5</sup>[McGill Scoliosis and Spine Research Group](#), <sup>6</sup>[Shriners Hospital for Children](#), Montreal, Canada.

**INTRODUCTION:** Intervertebral disc (IVD) degeneration has been directly linked to low back pain. Current treatment options for painful IVD degeneration are either physiotherapy and pain management or invasive surgical procedures. We previously developed a whole disc organ culture system for physiological loading of human IVDs and showed feasibility of monitoring cell injection therapy (1). Here we use our unique platform for determining NP cell biocompatibility and matrix production within a hydrogel (2). We also assess human IVD repair under physiological conditions in a bioreactor system.

**METHODS:** Human lumbar IVDs were isolated with institutional ethics approval. NP cells were isolated and expanded for one passage. Cells were first tested for viability and matrix production within hydrogel constructs *in vitro*. The constructs were cultured with or without dynamic loading for 3 weeks and viability and matrix deposition was determined. Intact human IVDs were scanned in sagittal and axial planes using MRI-T1 $\rho$  pulse sequences (3), and then injected with either HA-pNIPAM hydrogel alone or autologous NP cell-seeded HA-pNIPAM ( $2 \times 10^6$  cells/mL). After 5 weeks of dynamic culture, discs underwent follow-up MRI in the same orientation. T1 $\rho$  image quantification was performed using MIPAV software (NIH), and histological tissue sections were assessed for proteoglycan and collagen synthesis within injected regions. Statistical analysis was performed using paired t-tests in Microsoft Excel.

**RESULTS:** NP cells cultured in hydrogel constructs showed > 95% viability in both loaded and unloaded conditions. Loaded constructs displayed significantly more proteoglycan and collagen type II deposition compared to unloaded constructs (*Figure 1*). T1 $\rho$  pretreatment scans provided baseline proteoglycan levels in intact IVDs. After 5 weeks of dynamic loading, imaging analysis revealed significantly increased T1 $\rho$  values compared to pre-treatment scans (*Figure 2A*). Histological analysis showed proteoglycan and collagen type II deposition in samples treated with cell-seeded hydrogel (*Figure 2B*).

Fig.1: NP cell-seeded hydrogel after 3 weeks of unloaded or loaded.

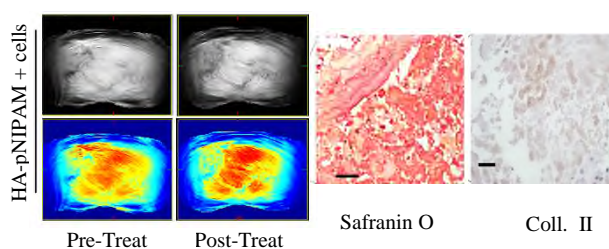
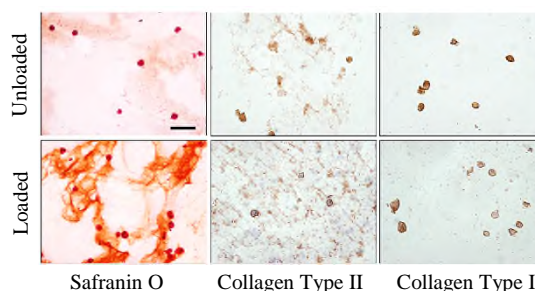


Fig.2: Representative T1 $\rho$  scans, safranin-O and collagen type II staining 5 weeks after dynamic culture.

**DISCUSSION & CONCLUSIONS:** Here, we present a physiological culture platform to assess various hydrogel and cell combinations for tissue regeneration strategies. We focus on autologous NP cell implantation within an injectable hydrogel, which theoretically produces optimal disc matrix proteins. This unique system provides a pre-clinical platform for potentially assessing, O<sub>2</sub> tension, glucose levels, bioactive therapeutics and mechanical properties for human IVDs. Use of T1 $\rho$  MRI allows appropriate quantification of proteoglycan content pre- and post-treatment, which may have clinical significance. Future studies will assess MSC-NP co-culture using this approach.

**REFERENCES:**<sup>1</sup>Rosenzweig et al. *Euro Cells & Mater.*2016;31:26-39.<sup>2</sup>Mortisen et al. *Biomacrom.*2010;11(5):1261-72.<sup>3</sup>Mulligan et al. *Euro Spine J.* 2015;24(11):2395-401.

**ACKNOWLEDGEMENTS:** This work was supported with an AO Spine grant SRN\_2011\_04\_10498 (LH). This template was modified with kind permission from eCM Journal.

## Osteoarthritis and intervertebral disc degeneration: similar but different

CME Rustenburg<sup>1,2</sup>, KS Emanuel<sup>1,2</sup>, M Peeters<sup>1</sup>, WF Lems<sup>3</sup>, PPA Vergroesen<sup>1,4</sup>, TH Smit<sup>2,5</sup>

<sup>1</sup> Department of Orthopaedic Surgery, VUmc, Amsterdam. <sup>2</sup> Department of Orthopaedic Surgery, AMC, Amsterdam. <sup>3</sup> Department of Rheumatology, VUmc, Amsterdam. <sup>4</sup> Department of Orthopaedic Surgery, Noord-West Ziekenhuisgroep, Alkmaar. <sup>5</sup> Department of Medical Biology, AMC, Amsterdam.

Intervertebral disc degeneration is a common cause of low-back pain, the musculoskeletal disorder with the largest socio-economic impact world-wide<sup>1</sup>. The complex disease is radiologically characterized by osteophytes, subchondral sclerosis and loss of joint space, which is remarkably similar to joint osteoarthritis, a condition with also a comparable clinical appearance<sup>2,3</sup>.

Inspired by these similarities, we investigated the analogy between intervertebral discs and articular joints. Although embryonic origin and anatomy suggest substantial differences between disc and articular joint<sup>4,5</sup>, their cell behaviour and extracellular matrix appear much the same; this suggests that the local environment of the cell is more important to its behaviour than embryonic origin. Moreover, great similarities are found in the response to mechanical loading and the matrix-degrading factors involved in the cascade of degeneration in both diseases<sup>6,7</sup>.

Nevertheless, osteoarthritis is regarded as a true disease, while disc degeneration is often considered as a diagnostic detail. Emphasizing the similarity rather than the difference between the two diseases may create more awareness among clinicians and improve diagnostics in disc degeneration. The development of regenerative therapeutics could be accelerated by cross-fertilization between the two relatively separate worlds of disc degeneration and osteoarthritis.

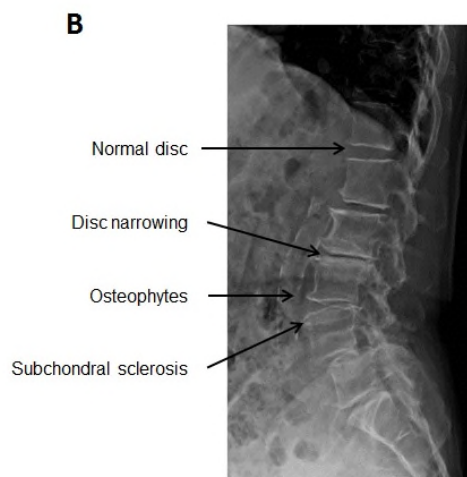
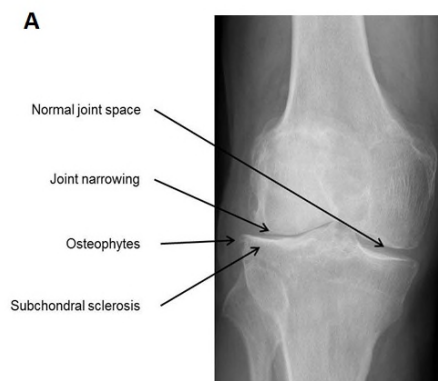


Fig. 1: Radiological examples of the degenerated joint (A) and degenerated intervertebral disc (B).

**REFERENCES:** <sup>1</sup> Hoy D, Bain C, Williams G, et al (2012) A Systematic Review of the Global Prevalence of Low Back Pain. *Arthritis Rheum* **64(6)**:2028–37. <sup>2</sup> Kellgren J, Lawrence J. (1957) Radiological assessment of osteoarthritis *Ann Rheum Dis* **16(4)**:494. <sup>3</sup> de Schepper EI, Damen J, van Meurs JB, et al (2010) The association between lumbar disc degeneration and low back pain: the influence of age, gender, and individual radiographic features. *Spine (Phila Pa 1976)* **35(5)**:531–6. <sup>4</sup> Sivakamasundari V, Lufkin T. (2012) Bridging the Gap: Understanding Embryonic Intervertebral Disc Development. *Cell Dev Biol* **1(2)**:103. <sup>5</sup> Archer CW, Dowthwaite GP, Francis-West P. (2003) Development of synovial joints. *Birth Defects Res Part C - Embryo Today Rev* **69(2)**:144–55. <sup>6</sup> Adams MA, Roughley PJ. (2006) What is Intervertebral Disc Degeneration, and What Causes It? *Spine (Phila Pa 1976)* **31(18)**:2151–61. <sup>7</sup> Carter DR, Wong M. (2003) Modelling cartilage mechanobiology. *Philos Trans R Soc B - Biol Sci* **358(1437)**:1461–71.

## Combined mechanical stress and inflammatory environment contribute to weakening of the annulus fibrosus: insights from a bovine AF organ culture model

T Saggese<sup>1</sup>, GQ Teixeira<sup>1</sup>, L Moll<sup>1</sup>, K Wade<sup>1</sup>, A Weigl<sup>1</sup>, RM Goncalves<sup>2</sup>, A Ignatius<sup>1</sup>, HJ Wilke<sup>1</sup>, C Neidlinger-Wilke<sup>1</sup>

<sup>1</sup> Institute of Orthopaedic Research and Biomechanics, Trauma Research Centre, Ulm University, Germany. <sup>2</sup> Instituto de Investigação e Inovação em Saúde/Instituto de Engenharia Biomédica, University of Porto, Porto, Portugal

**INTRODUCTION:** Annulus fibrosus (AF) disruption often leads to prolapse or herniation of the intervertebral disc (IVD). The trans-lamellar bridging network (TLBN) is a proteoglycan and elastic fibre-rich structure that separates the collagen rich AF lamellae and forms transverse bridges which connect the concentric layers of the AF [1]. Little is known about how mechanobiological factors influence the TLBN and anular wall integrity [1, 2]. We hypothesize that matrix components of the TLBN are altered by mechanical overloading in the presence of inflammatory factors, thereby contributing to tissue weakening. To study this, we established a bovine AF organ culture model (AF-OC) to analysed the influence of defined cyclic strain together with pro-inflammatory stimulus (IL-1 $\beta$ ) on AF matrix composition and mechanical properties.

**METHODS:** AF rings were isolated and prepared from bovine caudal discs. After 7 days of pre-incubation, AF-OCs were exposed to high physiological cyclic tensile strain (CTS) for 5 days (9%, 1 Hz, 3 h/day) in a custom-made device with or without the presence of IL-1 $\beta$  (1 ng/mL). Unstimulated AF-OCs were used as controls. PGE2 released into the supernatant (ELISA) and the production pattern of COX-2, IL-6, and MMP3 in the tissue (immunohistochemistry, IHC) were analysed. The mechanical strength of the TLBN was evaluated using a peel-test. AF segments were dissected into a 'Y' configuration and pulled apart at 0.5 mm/sec in a uniaxial material testing machine. Delamination strength was calculated from the mean force in the plateau region of the force displacement curves [3]. Statistics: ANOVA with Sidak correction.

**RESULTS:** The combination of CTS+IL-1 $\beta$  resulted in a significant 25-fold increase in PGE2 release compared to the controls ( $p < 0.05$ , Fig. 1A). Moreover, IHC evaluations showed that the CTS+IL-1 $\beta$  stimulated group presented higher

production of IL-6 within the TLBN regions compared to the adjacent lamellar matrix. Mechanical testing found a significant decrease in the adhesive peel force of the interlamellar matrix in the CTS+IL1 $\beta$  group compared to the unstimulated Control ( $p = 0.02$ , Fig. 1B).

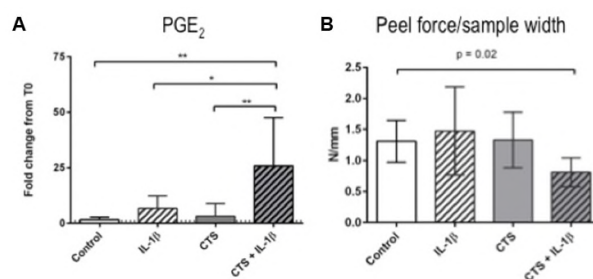


Fig. 1: A) PGE2 release normalised to pre-culture baseline ( $n = 8$ ) and B) delamination peel force normalised to sample width ( $n = 6$ ), for all the conditions tested. \* $p < 0.05$ ; \*\* $p < 0.01$  (ANOVA with Sidak correction).

**DISCUSSION & CONCLUSIONS:** The adhesion of adjacent lamella is an important factor in anular wall integrity. Our loaded bovine AF-OC model enables investigation of the AF and TLBN structure-function relationship. Our findings suggest that the combination of cyclic-strain and IL-1 $\beta$  act synergistically to increase pro-inflammatory and catabolic molecules within the AF, particularly the TLBN matrix, which consequently leads to a weakening of the tissue structure. This approach contributes to a better understanding of the pathomechanism of disc herniation.

**REFERENCES:** <sup>1</sup>M.L. Schollum, P.A. Robertson, and N.D. Broom (2009) *J Anat* **214**: 805-16. <sup>2</sup>S.K. Han, C.W. Chen, J. Wierwille, et al (2015) *J Orthop Res* **33**:304-11. <sup>3</sup>D.E. Gregory, W.C. Bae, R.L. Sah, et al (2012) *Eur Spine J* **21**:1716-23.

**ACKNOWLEDGEMENTS:** Supported by the German Spine Foundation and the Alexander von Humboldt Foundation.



## Comprehensive analysis of microarray data for identification of reliable healthy nucleus pulposus cell markers.

J. Schol<sup>1</sup>, D. Sakai<sup>1</sup>, M. Watanabe<sup>1</sup>

<sup>1</sup> [Tokai University](http://www.tokai.ac.jp), School of Medicine, Isehara, Japan

**INTRODUCTION:** A variety of studies have indicated the benefits of cell therapy for intervertebral disc (IVD) regeneration<sup>1</sup> and as such, researchers have aimed at inducing differentiation toward (healthy) nucleus pulposus cell (NPC). Although some markers, *e.g.* CA12, T, and CD24 have been recognized, the extend of NPC markers remains limited and difficult to discriminate from other chondrogenic or IVD derived cell populations.<sup>2</sup> In order to enhance the range of potential NPCs markers, we reviewed published cDNA microarray data in a systematic fashion to identify new and reliable markers associated with an NPC phenotype.

**METHODS:** A NCBI database search for all publications with the key words “nucleus pulposus”, “annulus fibrosus”, or “intervertebral disc” and “microarray” or “transcriptome” was performed (2018-04-21) with a systematic approach, resulting in 159 publications. All studies presenting mRNA microarray data (including ratio values) of NPCs compared to other cell types or degenerated NP tissue were included, while studies examining the effect of interventions, miRNAs, or non-coding RNAs were excluded.

**RESULTS:** 12 publications were included into the review. In the current abstract only markers independently identified by 2 or more studies are described. This resulted in a total of 31 genes with significantly higher expression by NPCs to be recognized in this review (Table 1).

**DISCUSSION & CONCLUSIONS:** Microarray assessments collectively, identified markers commonly applied as NPC markers; KRT18, KRT19, KRT8, ACAN, CD24, CA12. However, it should be noted that CD24 and ACAN, were only recognized in comparison to annulus fibrosus (AF) cells and degenerated NPC, while CA12 only in comparison to articular cartilage (AC) cells. KRT8, 18, and 19 showed consistent high expression. Additionally, a variety of lesser reported transcription factors were identified; FOXF1, FOXF2, KLF6, and SOX9, which as transcriptional regulators of cell phenotype might pose to important NPC markers.

Table 1. Genes identified as upregulated in NP cells relative to articular cartilage (AC), annulus fibrosus (AF) or degenerated/aged NP

Gene	Species	Compared to	Author	Year	Ref
A2M	Bovine	AC	Minogue	2010-b	6
	Canine	AF	Sakai	2009	8
ABCG1	Human	AC	Power	2011	7
	Human	AC	Minogue	2010-a	5
ACAN	Bovine	AF	Minogue	2010-b	6
	Human	NP (degen)	Gruber	2011	3
	Human	NP (herr/deg)	Zhang	2010	10
ADAMTS10	Human	NP (degen)	Gruber	2011	3
	Canine	AF	Sakai	2009	8
ANXA3	Bovine	AC	Minogue	2010-b	6
	Human	NP (herr/deg)	Zhang	2010	10
	Rat	AC	Lee	2007	4
ANXA4	Bovine	AC	Minogue	2010-b	6
	Canine	AF	Sakai	2009	8
	Rat	AC	Lee	2007	4
BASP1	Bovine	AC	Minogue	2010-b	6
	Rat	AF	Tang	2012	9
CA12	Human	AC	Power	2011	7
CD24	Bovine	AF	Minogue	2010-b	6
	Rat	AF	Tang	2012	9
CDH2	Human	AC	Minogue	2010-b	6
	Rat	NP (aged)	Tang	2012	9
	Rat	AF	Tang	2012	9
COL1A1	Bovine	AC	Minogue	2010-b	6
	Human	AC	Minogue	2010-a	5
DSC2	Human	AC	Minogue	2010-b	6
	Bovine	AC	Minogue	2010-a	5
FOXF1	Canine	AF	Sakai	2009	8
	Bovine	AC	Minogue	2010-b	6
FOXF2	Human	AC	Minogue	2010-a	5
	Human	AC	Minogue	2010-b	6
GPC3	Bovine	AC	Minogue	2010-b	6
	Human	AC	Minogue	2010-a	5
	Rat	AC	Lee	2007	4
IGF1R	Human	AC	Power	2011	7
	Rat	AF	Tang	2012	9
KLF6	Bovine	AC	Minogue	2010-b	6
	Rat	AF	Tang	2012	9
KRT18	Bovine	AC	Minogue	2010-b	6
	Bovine	AF	Minogue	2010-b	6
	Human	AC	Minogue	2010-a	5
KRT19	Bovine	AC	Minogue	2010-b	6
	Bovine	AF	Minogue	2010-b	6
	Human	AC	Minogue	2010-a	5
KRT8	Bovine	AC	Minogue	2010-b	6
	Rat	AF	Lee	2007	4
	Rat	AF	Lee	2007	4
LGAS1	Bovine	AC	Minogue	2010-b	6
	Rat	AF	Tang	2012	9
	Rat	NP (aged)	Tang	2012	9
MT1A	Canine	AF	Sakai	2009	8
	Rat	AF	Lee	2007	4
NCAM1	Bovine	AF	Minogue	2010-b	6
	Bovine	AC	Minogue	2010-b	6
	Human	AC	Minogue	2010-a	5
PTN	Canine	AF	Sakai	2009	8
	Rat	AF	Lee	2007	4
SNAP25	Bovine	AC	Minogue	2010-b	6
	Human	AC	Minogue	2010-a	5
	Human	AC	Minogue	2010-b	6
SOSTDC1	Bovine	AC	Minogue	2010-b	6
	Human	AC	Minogue	2010-a	5
SOX9	Bovine	AF	Minogue	2010-b	6
	Bovine	AC	Minogue	2010-b	6
SPP1	Canine	AF	Sakai	2009	8
	Rat	AC	Lee	2007	4
	Bovine	AC	Minogue	2010-b	6
TNMD	Bovine	AC	Minogue	2010-b	6
	Human	AC	Minogue	2010-a	5
VCAN	Bovine	AF	Minogue	2010-b	6
	Bovine	AC	Minogue	2010-b	6
	Human	AC	Minogue	2010-a	5
VEGF	Bovine	AC	Minogue	2010-b	6
	Canine	AF	Sakai	2009	8

Interestingly, commonly applied markers, such as T, HIF1, EPAS1, COL2A1, GLUT-1, and Shh were not identified in this review.<sup>2</sup> These results suggest, that mRNA expression of commonly applied NPC markers, might not specifically characterize NPCs. On the contrary, KRT18 and KRT19 show high reliability to define NPCs across species. Additionally, CDH2, ANXA3, DSC2, and GPC3 showed reliable expression in NPCs. Further investigation will be required; however, our review suggests selecting the appropriate markers will be crucial to enable the identification and support the differentiation of NPC cells.

**REFERENCES:** <sup>1</sup> Sakai & Schol (2017) J Orthop Transl **23**;8-18. <sup>2</sup> Risbud, Schoepflin, Mwale *et al* (2015) J. Orthop Res **33**;283-93. <sup>3</sup> Gruber, Hoelscher, Ingram *et al* (2011) Exp Mol Pathol **91**;534-9. <sup>4</sup> Lee, Sakai, Nakai *et al* (2007) Eur Spine J **12**;2174-85 <sup>5</sup> Minogue, Richardson, Zeef *et al* (2010) Arthritis Rheum **62**;3695-705. <sup>6</sup> Minogue, Richardson, Zeef *et al* (2010) Arthritis Res Ther **12**. <sup>7</sup> Power, Grad, Rutges *et al* (2011) Arthritis Rheum **62**;3876-86. <sup>8</sup> Sakai, Nakai, Mochida *et al* (2009) SPINE **34**;1448-56 <sup>9</sup> Tang, Jing, Chen *et al* (2012) PLOS ONE **7**. <sup>10</sup> Zhang, Guo, Sun *et al* (2010) J Bone Miner Metab **28**;209-19



## Functioning of mesenchymal stromal cells – need for fast and sensitive assays

J Stoyanov<sup>1</sup>, A Bertolo<sup>1</sup>

<sup>1</sup> Swiss Paraplegic Research, Nottwil, Switzerland

**INTRODUCTION:** Today – with over 900 registered trials involving MSC - translational research with these cells is a major domain. On the contrary, successful MSC-based autologous therapies which are established in the clinical routine are rare. A major challenge to implementation of the MSC in clinical practice is the lengthy, resource-intensive “fit-for-purpose” functional evaluation of an individual sample. Here we review our experience in developing two new methods for characterisation of functioning in MSC. We propose as functional assays the use of motility and autofluorescence of MSC - and outline the next steps which are necessary in order to develop clinically accepted standards.

**METHODS:** We evaluated the in vitro motility of human bone marrow MSCs from different donors and across the in vitro passages were, and the average speed per 24 hours was correlated to their adipogenic, chondrogenic, and osteogenic differentiation potentials and the levels of senescence and cell size. Furthermore MSC, were cultured with or without stimulated PBMC for one week and PBMC proliferation, IgG production and cytokine secretion in MSC and PBMC monocultures and co-cultures were correlated to MSC motility.

We correlated human bone marrow and adipose derived MSC autofluorescence measured with a flow cytometer to senescence by using various senescence-associated assays and expression of senescence markers. Autofluorescence was also correlated to adipogenesis, chondrogenesis and osteogenesis differentiation assays.

**RESULTS:** The average moving cells had better potential for differentiation than both the fast and slow cells. However, the fast moving human MSC were more successful in modulating inflammation compared to the slow ones (Table 1).

Table 1. Functioning of hMSC and their motility

Motility In vitro	Differentiation potential	Immunomodulation potential
High	Medium	High
Average	High	Medium
Low	Low	Low

We demonstrated a significant association between autofluorescence and commonly used markers of senescent cells in vitro ( $p < 0.001$ ) and could negatively associate osteogenic and chondrogenic differentiation potential but not lipogenic potential to autofluorescence (Table 2).

Table 2. Functioning of hMSC and their autofluorescence

Autofluorescence	Differentiation potential	Replicative senescence
High	Low	High
Average	Medium	Average
Low	High	Low

**DISCUSSION & CONCLUSIONS:** The resource intensive task of assessing inter-donor variability and inconsistent cell quality at different stages of manipulation can be reduced by an order of magnitude when MSC motility and autofluorescence are used instead of current assays. However, in order that standard functional assays become reality in clinical practice, standardised MSC reference material has to be produced and accepted by the community. Only then one could confidently define if individual cells should be used for transplantation.

### REFERENCES:

1. Bertolo A, et al. In vitro cell motility as a potential mesenchymal stem cell marker for multipotency. *Stem cells translational medicine*. 2015;4(1):84-90.
2. Bertolo A et al. “Increased motility of mesenchymal stem cells is correlated with inhibition of stimulated peripheral blood mononuclear cells in vitro. *Journal of stem cells & regenerative medicine*. 2017;13(2):62-74.

### ACKNOWLEDGEMENTS:

This research was supported by the Swiss Paraplegic Foundation, and the Swiss National Foundation (Grant number: CR2313\_159744). The authors would like to thank Dr David Pavlicek and Simona Capossela for their contributions.

## Novel ex-vivo osteochondral model for cartilage repair in mechanical stimulated joint bioreactor.

ML Vainieri<sup>1,2</sup>, D Wahl<sup>1</sup>, G Van Osch<sup>2</sup>, M Alini<sup>1</sup>, S Grad<sup>1</sup>

<sup>1</sup>AO Research Institute Davos, Switzerland. <sup>2</sup>Department of Orthopedics and Otorhinolaryngology, Erasmus MC, University Medical Centre, Rotterdam, The Netherlands,

**INTRODUCTION:** Although surgical procedures have been used in clinics to treat articular cartilage lesions, the complete restoration of the hyaline cartilage often fails in term of zonal ECM organization and mechanical behaviour. Post-operative management of joint injuries varies considerably and is poorly understood. For pre-clinical investigations, an *ex-vivo* osteochondral model in a mechanically stimulated environment can be of great value. The aims of this study were 1) to generate osteochondral explants [1] and create reproducible defects, 2) to adapt and validate a custom loading system that recapitulates articulating motion *in-vivo* using a living osteochondral plug-on-ceramic ball articulating interface, and 3) to investigate the specific effect of applied articular motion on the gene expression of chondrocytes seeded in 3D scaffolds, which filled the osteochondral defect.

**METHODS:** Osteochondral plugs (diameter=7.6 mm ± 0.14mm) were harvested from bovine stifle joints and trimmed to obtain a final height of 6.1 mm ± 0.29mm. An adjustable table was designed to guarantee flat plugs and to create defined osteochondral defects with 4.3 mm ± 0.16mm in diameter and a depth ranging from 2.85 mm ± 0.11mm to 3,75mm ±0.3mm. Defects were filled with chondrocytes seeded polyurethane scaffolds and exposed to axial compression by the ceramic ball between 0.4 mm and 0.8 mm displacement, ball oscillation at ±25°, at a frequency of 0.5Hz, 1 hour twice a day for 5 days. Cell viability of the unloaded and loaded explants was assessed after loading by cutting fresh frozen plugs and performing lactate dehydrogenase (LDH)/ ethidium homodimer assay. Safranin O/Fast green staining was performed to visualize proteoglycan and collagen content in the extracellular matrix (ECM). qRT-PCR of chondrocytes in scaffolds was performed for collagen type 2, aggrecan, versican, collagen type 1, matrix metalloproteinase 3 (MMP3), MMP13, cartilage oligomerix protein (COMP) and proteoglycan 4 (PRG4).

**RESULTS:** Five osteochondral plugs were harvested per joint and osteochondral defects were reproducibly created in each plug. Cells within both cartilage and bone regions remained viable throughout the culture period, as assessed by LDH

staining. A zone of cell death was observed in the outermost cell layer at the cut edges of the cartilage and the edges of the defect for all samples. Compression and shear-induction did not wear the cartilage in comparison to the free swelling controls, as assessed by Safranin-O/Fast green staining. Cartilage gene expression profiles increased in loaded groups: mRNA ratios of collagen type II to type I and aggrecan to versican were enhanced by multidirectional articular motion (39 and 5 folds increase), the PRG4 and COMP were markedly increased (20 and 25 folds increase), while MMP3 and MMP13 were relatively stable (Fig.1).

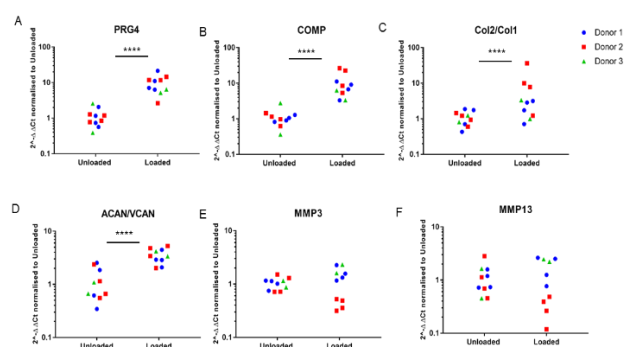


**Fig.1:** mRNA expression of chondrocytes-polyurethane constructs, which filled the osteochondral defect, exposed to dynamic compression/surface motion, normalized to mRNA levels of unloaded constructs (control). Mean±SD, 3 donors; \*p<0.05

**DISCUSSION & CONCLUSIONS:** This study shows that the 3D osteochondral culture model under load provides a stable viable microenvironment. It demonstrates the beneficial effect of articular motion for the preservation of the chondrocytic phenotype. Our system can be employed to screen new biomaterials, regenerative therapies and study cell responses under mechanical stimuli for articular cartilage repair.

**REFERENCES:** <sup>1</sup> de Vries-van Melle *et al.* Tissue. Eng Part A. 2012 ; 18(1) : 45–53.

**ACKNOWLEDGEMENTS:** This project has received funding from the European Union's Horizon 2020 research and innovation programme under Marie Skłodowska-Curie Grant Agreement No 642414.

## Intervertebral disc degeneration from a biomechanical point of view, what do we need to fix?

PPA Vergroesen<sup>1,2,3</sup>, KS Emanuel<sup>2,3</sup>, CME Rustenburg<sup>2,3</sup>, TH Smit<sup>2,3</sup>

<sup>1</sup>NoordWest Ziekenhuisgroep, Alkmaar, the Netherlands <sup>2</sup>Amsterdam Movement Sciences, Amsterdam, the Netherlands <sup>3</sup>Amsterdam Medical Center, Amsterdam, the Netherlands

**INTRODUCTION:** Low back pain has increasingly become one of the main problems in Western society. Low back pain is generally viewed as being multi-factorial, and the mainstay of therapies is physiotherapy and remaining active<sup>1</sup>, *i.e.* biomechanical stimuli. Biomechanics are also important for intervertebral disc homeostasis as they stimulate cells to maintain the extracellular matrix<sup>2</sup>. Due to technical constraints, biomechanical research in the spine has for a long time focussed on bending and torsion studies, although the main loading type is axial. Therefore, we performed a series of *ex-vivo* experiments in a loaded disc culture system to investigate the effects of long-term axial loading on healthy and degenerated intervertebral discs. This in order to provide parameters which regenerative therapies must aspire to restore.

**METHODS:** As a model we used caprine lumbar intervertebral discs in individual *ex vivo* culture chambers where we can culture up to 12 discs simultaneously, for up to 10 days. In the first study, we measured the change in intradiscal pressure due to loading and unloading. In the second study, we used polyethylene glycol (PEG) to increase culture medium osmolality in order to simulate reduced osmotic pressure due to proteoglycan loss. In the third study, we used healthy and degenerated human discs to validate our results from the second study. Finally we performed a fourth study that combined intradiscal pressure measurements with PEG medium to illuminate the discrepancies between modelled degeneration and human degenerated discs.

**RESULTS:** Axial loading has a two-fold effect on intradiscal pressure, initially, pressure rises due to the increased axial stress. Subsequently, due to prolonged loading and water outflow, intradiscal pressure slowly declines, strongly related to disc height. Upon unloading, this process is reversed. PEG reduces poroviscoelastic behavior of the intervertebral disc in a dose-dependent manner, without altering pure elastic deformation. The use of PEG medium closely resembled the changes seen in degenerated human intervertebral discs: disc height, recovery and overall creep where

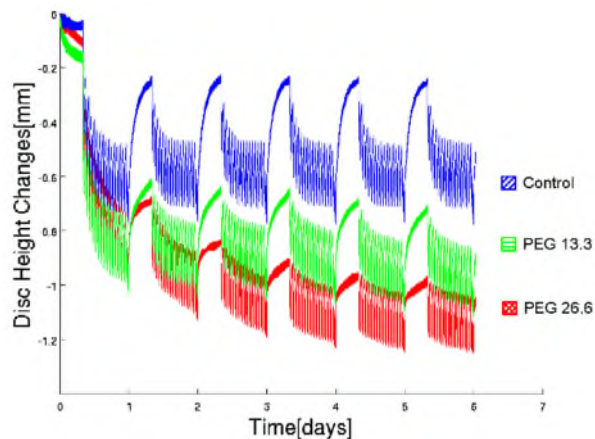


Figure 1: The effect of an impaired osmotic pressure on the axial biomechanics of the intervertebral disc

reduced. However, stiffness was not affected and time-constants increased, in contrast to degenerated human discs. The final experiment showed that changes in axial loading affect disc height, intradiscal pressure and nucleus water content, whereas changes in osmolality only affected disc height and annulus water content.

**DISCUSSION & CONCLUSIONS:** Overall, our series of experiments show that osmotic pressure generated by the discs proteoglycans is largely responsible for normal axial disc biomechanics, and for the changes seen with disc degeneration. Additionally, our work indicates that permeability of the annulus and the nucleus is the second most important parameter. Finally, it is important to note that the intervertebral disc is able to maintain a high hydration of approximately 68% under prolonged loads of around 1.0 MPa<sup>3</sup>. This unique property needs to be well considered in the design of regenerative therapies.

**REFERENCES:** <sup>1</sup>N. Foster (2018) Prevention and treatment of low back pain: evidence, challenges, and promising directions. *Lancet* **6736**:1–16. <sup>2</sup>P.P.A. Vergroesen (2015) Mechanics and biology in intervertebral disc degeneration: A vicious circle. *Osteoarthr. Cartil.* **23**:1057-70. <sup>3</sup>P.P.A. Vergroesen (2018) Are axial intervertebral disc biomechanics determined by osmosis? *J. Biomechanics* **70**:4-9.

## Selecting living human mesenchymal stem cells with an increased proliferation using a *TWIST1* RNA-based probe

C Voskamp<sup>1</sup>, J van de Peppel<sup>2</sup>, S Gasparini<sup>1,3</sup>, P Giannoni<sup>3</sup>, JPTM van Leeuwen<sup>2</sup>, GJVM van Osch<sup>1,4</sup>, R Narcisi<sup>1</sup>

<sup>1</sup> Department of Orthopaedics, Erasmus MC, Rotterdam, NL. <sup>2</sup> Department of Internal Medicine, Erasmus MC, Rotterdam, NL. <sup>3</sup> Department of Experimental Medicine, University of Genova, Genova, IT. <sup>4</sup> Department of Otorhinolaryngology, Erasmus MC, Rotterdam, NL.

**INTRODUCTION:** Bone marrow derived mesenchymal stem cells (BMSCs) are progenitor cells with a high potential in cell-based therapies of bone and cartilage defects. However, the limited proliferation capacity and donor heterogeneity limit their use in clinical applications. We and others showed that *TWIST1* expression correlates with proliferation in BMSCs [1,2]. Therefore, we wanted to evaluate *TWIST1* expression as a marker to select highly proliferative BMSCs. In order to do that, we used a method to detect mRNA in living cells, the SmartFlare technology. SmartFlare was previously used to select a population of BMSCs with an enhanced osteogenic potential [3]. However, a recent study illustrated that the SmartFlare intensity did not correlate with mRNA levels [4]. In this study we aimed to validate SmartFlare technology to detect *TWIST1* in BMSCs and verify whether BMSCs with a high *TWIST1* expression have an enhanced expansion capacity.

**METHODS:** BMSCs were obtained from patients undergoing a total hip replacement (N=8). BMSCs were treated with SmartFlare probes for uptake, scramble, *TWIST1* (cy3 or cy5) or left untreated. Based on signal intensity and specificity, we first determined the optimal probe concentration and incubation time in BMSCs using fluorescence confocal microscopy and FACS. Then, the *TWIST1*-cy3 and Scramble-cy3 probes were used to sort the 15% BMSCs with the lowest (*TWIST1*<sup>low</sup> and scramble<sup>low</sup>) and with the highest (*TWIST1*<sup>high</sup> and scramble<sup>high</sup>) SmartFlare intensity. Post sorting, *TWIST1* gene expression was measured by RT-PCR and the proliferative capacity was evaluated by cell expansion.

**RESULTS:** Confocal time-lapse microscopy and FACS showed that 50 pM of SmartFlare probe and 6 hours incubation are optimal conditions to specifically detect *TWIST1* mRNA in BMSCs. Interestingly, these conditions are different compared to the protocol suggested by the manufacturer. After sorting, *TWIST1*<sup>high</sup> BMSCs had a 6-fold higher *TWIST1* expression compared to *TWIST1*<sup>low</sup> cells, while scramble<sup>high</sup> and scramble<sup>low</sup>

had comparable *TWIST1* levels. Interestingly, we recorded a relatively high difference in uptake between the *TWIST1*<sup>low</sup> and *TWIST1*<sup>high</sup> cells (2.4-fold difference). However, after correction for the uptake capacity, we observed an increased difference in *TWIST1* expression between *TWIST1*<sup>low</sup> and *TWIST1*<sup>high</sup> up to 12.8-fold (Fig 1). Finally, we confirmed that *TWIST1*<sup>high</sup> BMSCs have an enhanced proliferation capacity when re-seeded after sorting (Fig 1).

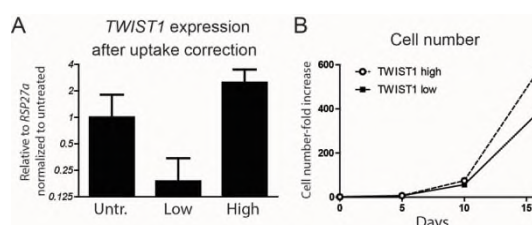


Fig. 1- *TWIST1*<sup>high</sup> BMSCs have an increased proliferation capacity. (A) *TWIST1* RT-PCR results of Untreated, *TWIST1*<sup>low</sup> and *TWIST1*<sup>high</sup> populations, values represent the mean  $\pm$ SD from duplicates. (B) Cell fold increase after 16 days.

**DISCUSSION & CONCLUSIONS:** Our data not only indicate that the SmartFlare technique can be applied as a tool to detect *TWIST1* gene expression in living BMSCs, but it also confirmed that, within one donor, *TWIST1*<sup>high</sup> expressing BMSCs have an increased proliferation capacity. However, differences in concentration, incubation time and cellular uptake can strongly influence the results, highlighting the importance to evaluate the SmartFlare protocol for each specific cell type.

**REFERENCES:** <sup>1</sup>R. Narcisi, M.A. Cleary, P.A. Brama, et al. (2015) *Stem Cell Reports* 4:459-472. <sup>2</sup>S. Isenmann, A. Arthur, A.C. Zannettino, et al. (2009) *Stem Cells* 27:2457-2468. <sup>3</sup>B. Li, U. Menzel, C. Loebel, et al. (2016) *Sci Rep* 6:26014. <sup>4</sup>M. Czarnek, J. Bereta (2017) *Sci Rep* 7:11682.

**ACKNOWLEDGEMENTS:** This work is funded by the Dutch Arthritis Foundation, Mrace Erasmus MC and STW.



## CD146 is a marker for stem cells with increased migration potential towards degenerative intervertebral discs

Sebastian Wangler<sup>1</sup>, Marianna Peroglio<sup>1</sup>, Zhen Li<sup>1</sup>, Ursula Menzel<sup>1</sup>, Lorin M. Benneker<sup>2</sup>, R. Geoff Richards<sup>1</sup>, Mauro Alini<sup>1</sup>, Sibylle Grad<sup>1</sup>

<sup>1</sup>AO Research Institute Davos, Switzerland, <sup>2</sup>Inselspital, University of Bern, Switzerland

**INTRODUCTION:** Homing of mesenchymal stem cells (MSCs) toward degenerative intervertebral discs (IVD) is well described, but little is known about the migrating MSC sub-population.<sup>1</sup> CD146/MCAM is involved in migration of different musculoskeletal tissues.<sup>2</sup>

The aims of this study were to compare:

1. The migration of CD146+ versus CD146- MSCs *in vitro* and in organ culture.
2. The differentiation potential of CD146+ versus CD146- MSCs *in vitro*.

**METHODS:** In-vitro migration: Conditioned medium (CM) was collected from bovine caudal IVDs with endplates after degenerative loading in a bioreactor (high frequency, low glucose) for 7 days. Culture-expanded human MSCs from bone marrow aspirates were separated in CD146+ and CD146- populations through FACS and used for Trans-well migration assays toward CM (n=6 donors). Organ culture migration: CD146+/- sorted MSCs were labelled with PKH26 and PKH67 fluorescent dyes, respectively. Each population was placed on a separate degenerative bovine IVD at a density of  $1 \times 10^6$  cells/disc (MSC: n=3, age  $38.3 \pm 14$ y; discs n=6). After 5 days of migration, IVDs were fixed, cut in sagittal sections, and the number of migrated cells was counted by dual channel fluorescence microscopy. Discogenic differentiation: CD146+/- MSC pellet cultures were performed with GDF-6 supplement<sup>3</sup> (n=5 MSC donors). At day 14, gene expression levels were measured by real-time PCR.

**RESULTS:** Migration: CD146+ MSCs showed significantly higher migration toward CM compared to CD146- MSCs *in vitro* (Fig. 1a:  $22.5 \pm 6.8\%$  versus  $15.7 \pm 6.6\%$  migrated cells). The organ culture experiment confirmed this trend with higher migration of CD146+ MSCs towards induced-degenerative disc tissue (Fig. 1b and 2b,  $179.6 \pm 29.6$  cells/cm<sup>2</sup>) compared to CD146- MSCs (Fig. 1b and 2a:  $99.2 \pm 4.3$  cells/cm<sup>2</sup>). Differentiation by GDF-6: CD146+/- pellets responded with a similar up-regulation of anabolic markers. CD146 expression was maintained over time for CD146- pellets whereas CD146+ pellets responded with a down-regulation of CD146 following 14 days of culture (Fig. 3).

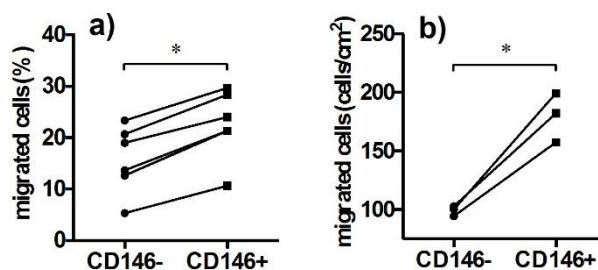


Fig. 1: Migrated cells a) *in vitro* (n=6); b) *in organ culture* (n=3).

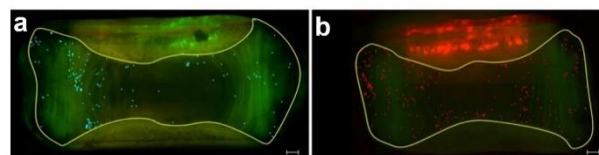


Fig. 2: Combined red and green fluorescent image of migrated MSCs in a sagittal section of bovine IVD: a) CD146- MSCs (blue); b) CD146+ MSCs (red). The IVD region without endplates is marked with a yellow line. Scale bar = 1 mm.

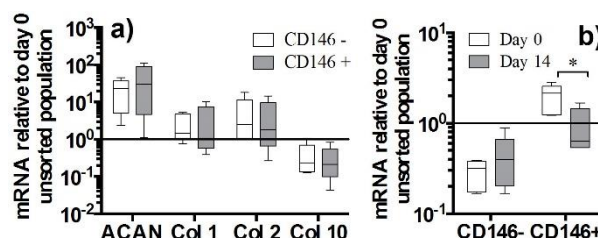


Fig. 3: Gene expression at day 14 relative to day 0 unsorted population: a) anabolic genes; b) CD146.

### DISCUSSION & CONCLUSIONS:

Our data suggest that CD146 characterizes a MSC subpopulation with increased migration potential towards degenerate IVDs. This confirms previous findings that have identified CD146+ MSCs as progenitor cell subpopulation, while CD146- MSCs had a more mature cell phenotype<sup>2</sup>. However, in our study CD146+ and CD146- subpopulations hold a similar discogenic differentiation potential. In conclusion, selection of CD146+ MSCs may represent a new strategy to improve cell recruitment, but further studies are needed to understand their regenerative function in the IVD.

**REFERENCES:** <sup>1</sup>Illien-Jünger et al., Spine 2012. <sup>2</sup>Harkness et al. Stem Cell Res Ther 2016. <sup>3</sup>Clarke et al., Arthritis Research & Therapy 2014.

## Injectable hydrogel versus collagen scaffold: In vitro comparison of two clinically applied biomaterials for autologous chondrocyte implantation (ACI).

JT Weitkamp<sup>1,5</sup>, K Benz<sup>2</sup>, S Lippross<sup>3</sup>, D Eglin<sup>4</sup>, A Armiento<sup>4</sup>, A Seekamp<sup>3</sup>, B Kurz<sup>5</sup>, P Behrendt<sup>3</sup>

<sup>1</sup> *Department of Oral and Maxillofacial Surgery, University Clinic Hamburg-Eppendorf, Hamburg, GER.* <sup>2</sup> *TETEC Tissue Engineering Technologies AG, Reutlingen, GER.* <sup>3</sup> *Department of Orthopaedic and Trauma Surgery, University Clinic Schleswig-Holstein, Kiel, GER.* <sup>4</sup> *AO Research Institute Davos, CH.* <sup>5</sup> *Department of Anatomy, Christian-Albrechts-University, Kiel, GER.*

**INTRODUCTION:** In ACI treatment there is no consensus on biomaterials used with respect to their optimal cell/matrix interactions. The aim of this study was to perform a comparative analysis of two clinically applied biomaterials in terms of: (1) Cytocompatibility; (2) chondrogenic potential; (3) bio-adhesion and (4) lateral integration.

**METHODS:** Monolayer expanded (P2-3) human chondrocytes (n=3) were embedded in a porous type 1/3 collagen scaffold (CS; Novocart 3D ®) and an albumin-hyaluronic acid-based hydrogel (AH; Novocart Inject ®) (both TETEC AG, Reutlingen, Germany). Cells were cultured in chondropermissive medium supplemented with and w/o IL-10 [100pg/ml] and BMP-2 [250ng/ml]. Gene expression of chondrogenic markers (COL1A1, COL2A1, COL10A1, ACAN, SOX9, TGF- $\beta$ 1) was detected via RT-qPCR and TGF- $\beta$ 1 release was quantified by ELISA. Biosynthesis of matrix compounds was analysed histologically (toluidine blue, type 1/2 collagen) and by DMMB assay. Morphological changes (Fig. 1B-C) and cell viability were investigated by confocal laser-microscopy following phalloidin staining and Live/Dead staining, respectively. In addition, cell invasion from surrounding native cartilage and adhesion of the material to adjacent cartilage were recorded by microscopy and a push-out test, respectively.

**RESULTS:** The changes of mRNA expression and GAG production indicated marked chondrogenic re-differentiation in both biomaterials. Shift of COL1/2 ratio towards COL2A1 was more pronounced in AH. In this context, chondrocytes cultured in AH showed a more spherical morphology (Fig 1B) and less microfilament expression compared to CS (Fig 1C). BMP-2 and IL-10 significantly increased COL2A1, SOX9 and ACAN expression, which was paralleled by enhanced staining of GAGs and type 2 collagen in histological sections of CS and AH. None of the biomaterials showed mRNA expression of COL10A1. TGF- $\beta$ 1 was produced in both biomaterials, but there was no activation

detectable. Better interfacial integration and enhanced cell invasion was observed in CS (Fig

1A) compared to the AH. Push-out test showed higher bonding strength to native cartilage for the CS.

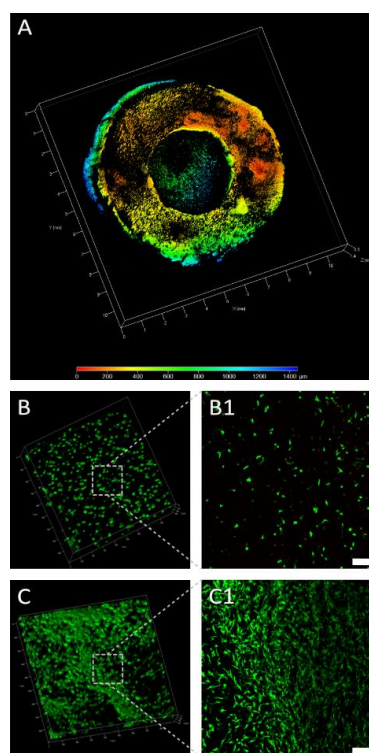


Fig. 1: (A) Cell invasion in a type 1/3 collagen scaffold after 28d of culture (depth coding by colour). (B,C) Morphological differences of articular chondrocytes embedded in AH hydrogel (B) and type 1/3 collagen scaffolds (B1,C1: Bar 100  $\mu$ m).

**DISCUSSION & CONCLUSIONS:** A trend for more chondrocyte-like phenotype was identified in the AH-based hydrogel, while collagen scaffolds showed an advantage in terms of cellular invasion and interfacial adhesion. Both biomaterials demonstrated favorable chondrogenic properties in vitro with no superiority of one compared to the other with a significant increase upon addition of BMP-2 and IL-10.

## Biodegradable scaffolds with a two-step release function for articular cartilage regeneration

Y.-T. Wen<sup>1</sup>, N.-T. Dai<sup>2</sup>, S.-h. Hsu\*<sup>1,3</sup>

<sup>1</sup> [Institute of Polymer Science and Engineering](#), National Taiwan University, Taiwan, R.O.C.

<sup>2</sup> [Department of Plastic Surgery](#), National Defense Medical Center, Taiwan, R.O.C.

<sup>3</sup> [Center of Tissue Engineering and 3D Printing](#), National Taiwan University, Taiwan, R.O.C.

**INTRODUCTION:** Cartilage tissue engineering emerged as an alternative approach for treating osteoarthritic patients because the conventional treatments such as medication, articular cavity injection, and joint replacement surgery have their own disadvantages. In cartilage tissue engineering, the biomaterials scaffolds are often seeded with autologous mesenchymal stem cells (MSCs). The expansion of MSCs in vitro is subjected to the risk of contamination. Here we employed polyurethane (PU) dispersion containing a chemotactic factor (CF) and microspheres embedding Y27632 for printing PU scaffolds with a two-step release function. CF was released first from the scaffolds to promote MSC migration. The drug Y27632 was then released from the microspheres embedded in the scaffolds to provide the chondrogenic induction to the attracted MSCs. Through these efforts, we expected to manufacture a cell-free tissue engineering scaffold, and to provide a potential alternative to cartilage regeneration.

**METHODS:** The biodegradable PU elastomer was synthesized from a water-based process. The soft segment consisted of polycaprolactone diol and polyethylene butylene adipate diol. The hard segment consisted of isophorone diisocyanate. The drug-loaded PU microspheres were fabricated by spray-freezing of the PU NP dispersion containing Y compound. The PU NP dispersion was mixed with poly(ethylene oxide) (PEO) and the Y compound-loaded microspheres as the printing ink. The scaffolds were fabricated from a low-temperature fused deposition manufacturing platform. The ability for chondral regeneration of the scaffolds was evaluated by a rabbit chondral defect model.

**RESULTS:** The scaffolds with a two-step release function for chondral regeneration were printed from the platform. These scaffolds promoted the migration and differentiation of MSCs with timely release of chemokine and bioactive ingredients,

respectively (Fig. 1). Moreover, the rabbit knee implantation supported the potential of the scaffolds in cartilage regeneration (Fig. 2).

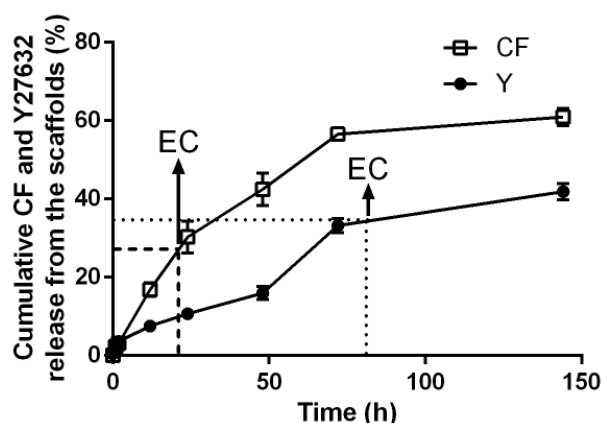


Fig. 1: The cumulative CF and Y release from the scaffolds embedding microspheres in 37°C PBS. “EC” indicates the effective concentration in short.

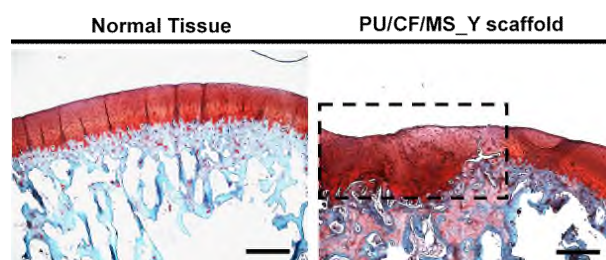


Fig. 2: Histological images of regenerated cartilage stained by safranin O/fast green. The box indicates the repair region. Scale bar: 500 μm.

**DISCUSSION & CONCLUSIONS:** Composite scaffolds were printed from the water-based ink containing PU, chemokine, and bioactive ingredients. The scaffolds were not further seeded with MSCs. The scaffolds repaired the rabbit chondral defects effectively, and may have potential in customized tissue engineering.

## **Anabolic and anti-catabolic effects of small molecules applied in traditional Chinese medicine for treatment of osteoarthritis**

R Ziadlou<sup>1,2</sup>, S Grad<sup>1</sup>, M Stoddart<sup>1</sup>, X Wang<sup>3</sup>, L Qin<sup>3</sup>, A Barbero<sup>2</sup>, I Martin<sup>2</sup>, M Alini<sup>1</sup>

<sup>1</sup>*AO Research Institute Davos, Davos, CH.*

<sup>2</sup>*Department of Biomedicine, University Hospital Basel, University of Basel, Basel, CH.*

<sup>3</sup>*Translational Medicine R&D Center, Shenzhen Institutes of Advanced Technology, Chinese Academy of Sciences.*

**INTRODUCTION:** Osteoarthritis (OA) is the most prevalent degenerative joint disorder and affects millions of patients globally. There is currently no effective cure or preventative treatment available. Pharmacologic therapy for OA shows efficacy in pain relief but is frequently associated with adverse effects, desiring a transition from pharmacological treatment to biotherapies.

**METHODS:** In this study, the anabolic and anti-inflammatory effects of 40 Traditional Chinese Medicine (TCM) compounds were assessed biochemically (GAG/DNA) using 3 donors of human OA chondrocytes in pellet cultures. The most chondrogenically active compounds were then assessed transcriptionally (real-time RT-PCR) and histologically in an inflammatory model. Thereby cartilage pellets were generated in chondrogenic medium followed by 3 days of inflammatory induction with cytokines (IL-1 $\beta$ /TNF- $\alpha$ ). The pellets were exposed to different types and concentrations (1  $\mu$ M, 10  $\mu$ M, 25  $\mu$ M) of TCM compounds after induction of inflammation.

**RESULTS:** After induction of inflammation, the GAG/DNA ratio and anabolic gene expression were significantly decreased, while inflammatory and catabolic markers were up-regulated. To test the anti-catabolic effects of the compounds, they were added either simultaneously with inflammatory cytokines or after induction of inflammation. The result showed that 5-hydroxymethylfurfural in 3 concentrations could inhibit the gene expression of catabolic markers. Also, the expression of the anabolic marker gene COL2A1 was higher in 5-hydroxymethylfurfural treated compared to untreated pellets, while the hypertrophy marker COL10 was completely suppressed. Furthermore, the GAG/DNA ratio was restored by 5-hydroxymethylfurfural treatment.

### **DISCUSSION & CONCLUSIONS:**

In conclusion, 5-hydroxymethylfurfural had anti-catabolic effects, could increase cartilage matrix production of human osteoarthritic chondrocytes towards a healthier phenotype and showed regenerative potential. A local drug delivery system for the bioactive compound is envisioned and optimization of the release mechanisms of the loaded compound(s) and their efficacy in terms of cartilage repair will be tested.

**ACKNOWLEDGEMENTS:** Funded by Swiss National Science Foundation (SNF) under the SSSTC program with grant number 156362.